

BIOENGINEERING OF ADENO-ASSOCIATED VIRUS SEROTYPE 5 FOR INCREASED
LIVER TRANSDUCTION AND RETENTION OF LOW HUMORAL SEROREACTIVITY

Randolph Qian

A dissertation submitted to the faculty at the University of North Carolina at Chapel Hill in
partial fulfillment of the requirements for the degree of Doctor of Philosophy in the Department
of Pharmaceutical Sciences in the Eshelman School of Pharmacy

Chapel Hill
2020

Approved by:

Xiao Xiao

Shawn Hingtgen

Sam Lai

Rihe Liu

Hengming Ke

©2020
Randolph Qian
ALL RIGHTS RESERVED

ABSTRACT

Randolph Qian: Bioengineering of Adeno-Associated Virus Serotype 5 for Increased Liver Transduction and Retention of Low Humoral Seroreactivity
(Under the direction of Dr. Xiao Xiao)

Commonly utilized recombinant adeno-associated virus (rAAV) capsids for delivering therapeutic genes to the human liver have significant seroprevalences in the human population, preventing many potential patients from receiving AAV-based gene therapies. As such, AAV serotype 5 (AAV5) has been commonly utilized in liver gene therapy due to its advantageous minimal humoral seroreactivity compared to other serotypes. However, AAV5 can only be used for diseases where only a small fraction of normal protein expression is required due to AAV5's poor liver infectivity especially when compared with other frequently utilized hepatotropic serotypes. To increase the efficacy of AAV5 based gene therapy for liver diseases, we constructed a random library of AAV5 mutants by error prone PCR and staggered extension protocol (stEP) and screened for variants with increased liver transduction in Huh7 cells. After 7 rounds of selection, two of five selected variants, MV50 and MV53, demonstrated significantly increased transduction efficiency in Huh7 and primary human hepatocytes from donors. Insights into the mechanisms behind the enhancement of infectivity allowed for further rational engineering of these mutants. Swapping the VP1/VP2 common region of AAV8 and AAV9 onto the mutated AAV5 variants further increased their transduction efficiency in primary human hepatocytes. Additionally, results from the VP1/VP2 swapping and the directed evolution

yielded insights into a previously uncharacterized domain in the AAV5 capsid that is important for binding and internalization. All variants also had similar seroreactivity towards pooled human IVIG when compared with wild type AAV5 and significantly less seroreactivity compared to wild type AAV9. These evolved AAV5 capsids have the potential to expand the patient population that can receive AAV-based liver gene therapies

ACKNOWLEDGEMENTS

I would like to thank Dr. Xiao Xiao for serving as my mentor in my doctoral research. His guidance and knowledge were crucial for the successful completion of my dissertation. I am grateful that he gave me the freedom to explore my own ideas to become a self-sufficient scientist. I am also grateful that he introduced me to the field of AAV gene therapy; something I have become extremely passionate and interested in pursuing. I will always remember the conversations we had about the complexities of AAV gene therapy.

I would also like to thank Drs. Shawn Hingtgen, Sam Lai, Rihe Liu, and Hengming Ke for serving as my dissertation committee. Their wealth of knowledge was extremely helpful, and they provided excellent ideas and feedback for my research. It was very enjoyable to talk about my research with this group of esteemed scientists.

Additionally, I would not have been able to complete my dissertation without the help of present and former Xiao lab members. I would particularly like to thank Dr. Juan Li, Dr. Chunping Qiao, and Dr. Bin Xiao for their guidance and teachings. I would also like to thank Dr. Tejash Patel, Dr. Quan Jin, and Jianbin Li for discussing AAV with me and helping me with problems that I would run into.

Finally, I would like to thank my parents, Jim Qian and Xiaoming Wu, for supporting me throughout my life. They were a cornerstone when I most needed help. Without their nurturing I would not have pursued a PhD. I would also like to thank Zoey Tang for her constant support

and companionship. Without her, this dissertation would have been much harder to complete.

Thank you for being there when I needed you.

TABLE OF CONTENTS

LIST OF FIGURES	x
LIST OF TABLES.....	xii
LIST OF ABBREVIATIONS	xiii
CHAPTER 1 INTRODUCTION.....	1
1.1 AAV-Based Gene Therapy	1
1.2 AAV Biology	4
1.3 Structure of AAV	6
1.4 Entry Pathway of AAV.....	8
1.5 Tropism of Naturally Isolated AAV Serotypes 1-9.....	11
1.6 Immunogenicity of AAV	13
1.7 Engineering of AAV for Improved Transduction Properties.....	21
1.8 Significance and Specific Aims	25
CHAPTER 2 DIRECTED EVOLUTION OF AAV5 FOR INCREASED LIVER TRANSDUCTION	35
2.1 Overview.....	35

2.2 Introduction.....	36
2.3 Materials and Methods	38
2.4 Results.....	44
2.5 Discussion.....	50
CHAPTER 3 ANALYSIS OF MUTATIONS IN EVOLVED AAV5 CAPSIDS	64
3.1 Overview.....	64
3.2 Introduction.....	65
3.3 Materials and Methods	66
3.4 Results.....	71
3.5 Discussion	77
CHAPTER 4 RATIONAL ENGINEERING OF EVOLVED AAV5 CAPSIDS FOR FURTHER IMPROVEMENT OF LIVER TRANSDUCTION CAPABILITIES	96
4.1 Overview.....	96
4.2 Introduction.....	98
4.3 Materials and Methods	100
4.4 Results.....	107
4.5 Discussion	114
CHAPTER 5 SUMMARY AND FUTURE DIRECTIONS.....	133

REFERENCES 137

LIST OF FIGURES

Figure 1: Wild-Type AAV Genome	29
Figure 2: AAV VP3, Trimer, and 60mer Structures.....	30
Figure 3: Working Theory of Cellular Response Against AAV Capsids.....	32
Figure 4: AAV Viral Entry Pathway and Prevention of Entry by Neutralizing Antibodies.	33
Figure 5: Diagram Depicting the Main Methods for Directed Evolution of the AAV Capsid	34
Figure 6: Directed Evolution of Adeno-Associated Virus Serotype 5 Capsid by Random Mutagenesis.....	55
Figure 7: Sequential Screening of AAV5 Library in Huh7 Cells	56
Figure 8: Sequencing of AAV5 Variants from 5 th and 7 th Rounds of Selection.....	57
Figure 9: Production and Yield of Five Selected AAV5 Mutants.....	58
Figure 10: Evaluation of Huh7 Transduction for Select AAV5 Mutants	59
Figure 11: Evaluation of HepG2 Transduction for Select AAV5 Mutants.....	60
Figure 12: Evaluation of Primary Human Hepatocyte Transduction for Selected AAV5 Mutants	61
Figure 13: Comparison of Gene Transfer Efficiency in C57/BL6 Mice using a LacZ Vector.....	62
Figure 14: Seroreactivity of AAV5 and MV mutants using an IVIG Based Assay	63
Figure 15: Amino Acid Sequence for Best Performing AAV5 Variants.....	83
Figure 16: Amino Acid Sequence Alignment of AAV5 and MV Mutants.....	85
Figure 17: Alignment of All Mutations found in MV Mutants with Other AAV Serotypes	87
Figure 18: False Color Mapping of Mutations in each MV Variant onto the AAV5 VP3 Structure	90

Figure 19: Sequence and Structural Analysis of Mutant AAV5 Capsids with Increased Human Liver Transduction	91
Figure 20: Comparison of Binding and Internalization between AAV5 and MV Mutants	92
Figure 21: Combination of Mutations from multiple AAV5 Variants	93
Figure 22: Loop1R Mutation in Other AAV Serotypes.....	94
Figure 23: Diagram of Swapping the AAV5 VP1/VP2 unique regions.....	122
Figure 24: Alignment of Phospholipase A2 Domain for AAV Serotypes 1-9.....	123
Figure 25: AAV5 versus 3(5) and 3(5) Loop1R in Huh7 Cells	124
Figure 26: 9(5) Loop1R vs 8(5) Loop1R in Huh7 Cells.....	125
Figure 27: 8(5) Loop1R Primary Human Hepatocyte Transduction.....	126
Figure 28: 9(5) Loop1R Primary Human Hepatocyte Transduction.....	127
Figure 29: Comparison of Gene Transfer Efficiency in C57/BL6 Mice between 8(5) Loop1R and 9(5) Loop1R.....	128
Figure 30: Seroreactivity of 8(5) Loop1R and 9(5) Loop1R	129
Figure 31: Comparison of Binding, Internalization, and Nuclear Localization for AAV5, 9(5) and 9(5) Loop1R.....	130
Figure 32: Effects of Different AAV VP1/VP2 Regions on Binding in Chimeric AAV5 Viruses	131
Figure 33: Probing the VP2/VP3 Junction of 6(5)	132

LIST OF TABLES

Table 1: Approved AAV Gene Therapy Products.....	27
Table 2: Selected Clinical Trials Utilizing AAV-Gene Therapy	28
Table 3: Receptors, Tropism, and Seroprevalence of AAV Serotypes.....	31
Table 4: Mutations of AAV5 Variants with Increased Liver Tropism.....	95

LIST OF ABBREVIATIONS

AAP	Assembly-Associated Protein
AAV	Adeno-Associated Virus
AAVR	Adeno-Associated Virus Receptor
Ad	Adenovirus
ALT	Alanine Aminotransferase
AST	Aspartate Aminotransferase
bp	Base Pair
Cap	Capsid
CB	Chicken Beta
CNS	Central Nervous System
CsCl	Cesium Chloride
DNA	Deoxyribonucleic Acid
DMD	Duchenne Muscular Dystrophy
ds	double-stranded
EDTA	Ethylenediaminetetraacetic Acid
EMA	European Medicines Agency
EPPCR	Error-Prone PCR

FDA	Food and Drug Administration
FGFR	Fibroblast Growth Factor Receptor
HGFR	Hepatocyte Growth Factor Receptor
HEK	Human Embryonic Kidney
hFGFR	Human Fibroblast Growth Factor Receptor
hHGFR	Human Hepatocyte Growth Factor Receptor
HPV	Herpes Papilloma Virus
HSV	Herpes Simplex Virus
ITR	Inverted Terminal Repeat
INF	Interferon
IV	Intravenous
LacZ	B-galactosidase
LamR	Laminin Receptor
MAAP	Membrane-Associated Accessory Protein
MOI	Multiplicity of Infection
mRNA	Messenger Ribonucleic Acid
MyD88	Myeloid Differentiation Primary Response Gene 88
nAb	Neutralizing Antibody

nls	nuclear localization signal
nt	nucleotide
PBMC	Peripheral Blood Mononuclear Cells
PBS	Phosphate Buffered Saline
PCR	Polymerase Chain Reaction
PDGFR	Platelet Derived Growth Factor Receptor
rAAV	Recombinant Adeno-Associated Virus
RBE	Rep Binding Element
RNA	Ribonucleic Acid
RPE	Retinal Pigmented Epithelium
RT	Room Temperature
RTPCR	Real-Time Polymerase Chain Reaction
sc	self-complementary
SDS	Sodium Dodecyl Sulfate
stEP	Staggered Extension Protocol
ss	single-stranded
TGN	Trans-Golgi Network
TLR	Toll-like Receptors

Tris-HCL	Tris(hydroxymethyl)aminomethane hydrochloride
Trs	Terminal Resolution Site
vg	Vector Genome
VP1	Viral Protein 1
VP1u	VP1 Unique Region
VP2	Viral Protein 2
VP3	Viral Protein 2
VR	Variable Region
wt-AAV	Wild Type Adeno-Associated Virus
wt-Ad	Wild Type Adenovirus

CHAPTER 1

INTRODUCTION

1.1 AAV-Based Gene Therapy

Gene therapy, or the treatment of diseases using therapeutic genes or gene editing, as long been thought to be more fantasy than reality. While the idea sounded plausible when first proposed in the early 1990s, there were many hurdles that had to be overcome in order to realize gene therapy in its current state.¹ The main challenge was developing suitable delivery systems that could deliver therapeutic genes safely and efficiently within the human body. It was not until researchers realized that viruses could be repurposed to deliver therapeutic genes that gene therapy became reality.² Viruses are natural vectors that have evolved over time to evade host immune responses and target specific cells to efficiently deliver their nucleic acid cargo.³ Removal of viral replication genes and subsequent replacement with therapeutic genes Non-viral vectors are also utilized for gene therapy, but do not show the same efficiency in transducing target cells when compared to viral vectors.^{4, 5}

Initial attempts at gene therapy involved delivering genes via replication-defective retroviruses and adenoviruses, but concerns over genome integration and immunogenicity substantially hindered the progress of these approaches.^{6, 7} The introduction of Adeno-Associated Virus(AAV) as a safe and non-immunogenic vector immediately re-established interest in utilizing viral vectors for gene therapy. Since its characterization as a potent gene delivery vector, AAV has been the vector of choice for many gene therapy applications due to its ability

to package transgenes and efficiently deliver DNA to target organs.^{8,9} The first AAV serotype, AAV2, was initially discovered as a contaminant in an Adenovirus preparation in 1965.¹⁰ Since then, numerous serotypes of AAV have been isolated from monkeys and humans that all have unique tropisms and serological profiles. AAV currently has no known pathogenicity, and the immune response towards the AAV capsid is mild and manageable.¹¹ Additionally, AAV can efficiently transduce many different organs, such as the heart, muscle, liver, lungs, and brain, to achieve sustained transgene expression over long periods of time.¹² As such, AAV vectors boast many advantages over other commonly used viral vectors that result in its status as the vector of choice for gene therapy applications. Typically, an AAV-based therapeutic consists of a transgene that is packaged into an AAV capsid, which is then subsequently delivered into a human. The AAV capsid will target a specific tissue or organ, transduce the target cells, and introduce a copy of the transgene that exists in an episomal form that confers long lasting gene expression.

As of 2017, AAV was utilized in 183 clinical trials treating a wide range of diseases.¹³ Much progress has been made in the treatment of ocular, liver, muscular, neuromuscular, and neurological diseases culminating in three approved AAV-based therapies, ZolgensmaTM, LuxturnaTM, and GlyberaTM (Table 1).¹⁴ GlyberaTM was the first EMA-approved AAV-based therapy that utilized AAV1 to deliver a copy of lipoprotein lipase to treat patients with lipoprotein lipase deficiency.¹⁵ GlyberaTM is no longer on the market due to the costs of production and low sales. LuxturnaTM is the first FDA approved AAV-based therapy that treats patients with leber's congenital amaurosis by delivering a human RPE65 gene using AAV2 to restore their vision.¹⁶ The most recent approval, ZolgensmaTM, is used to treat children below two years of age with spinal muscular atrophy, and has substantially extended the life span of

these patients.¹⁷ Aside from approved therapies, there are many on-going clinical trials that utilize AAV with promising results such as Pfizer's Duchenne Muscular Dystrophy(DMD) program or Spark Therapeutics' and Biogen's respective hemophilia programs. Pfizer has dosed DMD patients in a Phase I/II clinical trial with an AAV9 vector carrying a shortened version of the human dystrophin gene (mini dystrophin).¹⁸ Restoration of muscle functionality has been observed in patients allowing them to walk and run for longer periods of time. Hemophilia trials have also been very successful in restoring factor VIII and factor IX levels in severe hemophilia patients.^{19, 20} Treated patients have few to no occurrences of spontaneous bleeding events and most no longer require any recombinant factor VIII or IX injections. Table 2 includes more promising AAV-based therapies that are currently in clinical trials.

Despite the success of AAV, many hurdles remain that need to be overcome in order to progress the treatment of genetic diseases. Many of the challenges lay in developing new and improved AAV capsids. Currently, many genetic diseases are not treatable with AAV vectors due to low transduction efficiency in target organs such as the liver and CNS.²¹ Many groups have developed new AAV variants using directed evolution or rational engineering methods, but more improvement is still required to reach the full potential of the AAV capsid.²²

Immunogenicity is another hurdle that goes hand in hand with the AAV capsid as different AAV serotypes can illicit differing levels of immune responses.¹¹ In particular, the humoral response against the AAV capsid is a problem that largely does not have a solution. Antibodies that are generated against the AAV capsid prevent redosing of AAV and can also prevent patients from receiving AAV therapy if they have been previously exposed to wild type-AAV.²³ The cellular response against the AAV capsid has largely been managed with concurrent dosing of immunosuppressants, but other methods of avoiding immune response are being studied as

well.²⁴ Finally, production is also a concern as large amounts of AAV vectors are required for treatment of systemic diseases, increasing the production costs and prices of the therapies.²⁵ Development of new AAV capsids requires a deep understanding of the biology, structure, tropism, and immunogenicity of the virus.

1.2 AAV Biology

Understanding AAV biology is critical to developing the next generation of AAV-based therapies. AAV biology provides an understanding of the mechanisms of infection, methods of production, and triggers of an immune response, all of which can be utilized to improve AAV-based gene therapies. AAV, from the *Parvoviridae* family, is a single stranded, nonenveloped DNA virus that is roughly 22nm in diameter. The wt-AAV genome is 4.7 kbp in length and consists of three main elements, the inverted terminal repeats (ITR), the REP gene, and the CAP gene (Figure 1).²⁶ The ITRs are palindromic sequences that are 145 bases long and capable of folding into a T-shaped hairpin structure which gives the AAV genome a T-shaped double hairpin structure.²⁷ The ITRs function as important elements for DNA replication, genome packaging, and genome persistence.^{28, 29} It also has been characterized to have cryptic promoter activity that can potentially affect expression of a transgene.³⁰

The REP gene encodes for four non-structural rep proteins that are essential for AAV replication. The large Rep proteins, Rep 78 and 68, are alternative splicing products of mRNA transcribed from the p5 promoter (Figure 1). These two proteins are similar in function and are required for a vast majority of the AAV replication life cycle. Rep78/68 proteins have endonuclease and ATP-dependent helicase functions that initiate AAV gene expression. The REP proteins commence AAV replication by binding to the double stranded stem region of the ITRs and unwinding the AAV DNA strands via the helicase domain. The endonuclease domain

will then create a nick at the terminal resolution site(trs) to allow DNA polymerase access to one strand of the AAV genome.³¹⁻³⁵ Additionally, the large rep proteins allow the AAV genome to integrate into the AAVS1 locus in chromosome 19.³⁶ The expression of the smaller Rep 52 and Rep 40 proteins are driven by the p19 promoter and facilitate the packaging of the AAV genome into an assembled AAV capsid.^{31,37} The helicase region of the small REP proteins contains three Walker motifs that function as a motor to insert the AAV genome into the capsid.³⁸ The rep proteins can also regulate transcription of the wt-AAV genome by binding to the Rep Binding Elements (RBEs) in promoters p5 and p19.³⁹

The capsid gene encodes for the three structural proteins of the AAV capsid (Figure 1). These proteins, VP1, VP2, and VP3, are translated from two mRNAs that are encoded from the p40 promoter in the capsid gene.^{40,41} The first mRNA encodes for the VP1 protein while the second MRNA encodes for the VP2 and VP3 proteins (Figure 1). Due to the minor splicing acceptor site in the VP1 mRNA transcript, and the weak start codon (ACG) for VP2, the ratio between VP1, VP2, and VP3 is roughly 1:1:10.⁴² VP1, VP2, and VP3 share the same C-terminus, but have different functionalities. The VP3 protein and VP3 domains in the VP1/VP2 proteins form an icosahedral 60mer capsid shell and are responsible for the tropism of the AAV capsid. The unique region of the VP1 (VP1u) contains a phospholipase A₂ domain and nuclear localization signals that allow the virus to escape from the endosome and trafficking into the nucleus.⁴³⁻⁴⁵ An alternate start codon encodes for the assembly-activating protein (AAP), which facilitates assembly of AAV particles by targeting newly synthesized capsid proteins and trafficking them into the nucleus for assembly.⁴⁶ A recently discovered AAV accessory protein, the membrane-associated accessory protein (MAAP), is thought to be involved in competitive exclusion.⁴⁷ However, the exact function has not been thus far determined.

AAV is a replication deficient virus and requires helper functions from proteins encoded by other viruses such as adenovirus, herpes simplex virus (HSV), vaccinia virus, and human papilloma virus (HPV).⁴⁸⁻⁵¹ The helper functions of adenovirus have been studied extensively as AAV was isolated as a contaminant from an adenovirus preparation. Important adenoviral genes for AAV replication include E1A, E1B, E2a, E4 and VA RNA.⁵⁰ The most important helper gene is E1A which activates the other early genes of adenovirus and induces the cell to enter the S phase of cell cycle to provide the optimal conditions for replication of the AAV genome.⁵² E1A also binds the P5 promoter in the AAV genome and promotes expression of the Rep and Cap genes. The other adenoviral helper genes promote replication through a variety of methods that include mRNA stabilization, replication processing, and second strand synthesis.⁵³ Understanding AAV biology has allowed development of efficient production methods of AAV that are adenovirus free. The preferred method of AAV production is through the triple plasmid transfection method, in which a transgene flanked by AAV ITRs is transfected in HEK 293 cells along with a helper plasmid and packaging plasmid.

1.3 Structure of AAV Capsids

As previously mentioned, the AAV capsid is assembled from the VP1, VP2, and VP3 proteins at a ratio of 1:1:10 that forms a 60mer icosahedral structure (Figure 2C and 2D). The structures of AAV serotypes 1 through 9 have all been resolved using x-ray crystallography or cryo-electron microscopy.⁵⁴⁻⁶⁰ In each of these serotypes, the structure of the VP3 regions that constituted the 60mer capsid surface were successfully resolved, but the structure of the VP1u, VP1/VP2 common region, and a small fraction of the N terminus of the VP3 protein were unresolvable. This was likely due to the non-structured nature and low copy number of these regions. As such, there is still much that can be discovered about the VP1u and the VP1/VP2

common region and their functions in AAV infection. The AAV VP3 proteins contain many regions that are highly conserved between each serotype which are very resistant to changes in amino acid sequence. Mutations in these conserved regions typically cause loss of infectivity or production problems.⁶¹ These conserved regions are comprised of eight anti-parallel β sheets that form a jellyroll motif that is the central structure of the VP3 protein (Figure 2A).⁶⁰ Situated in between these conserved regions are loop regions that are typically variable between each serotype. Nine variable regions on the surface of the capsid have been associated with different aspects of the viral infection pathway that include receptor binding, internalization, and antigenicity. These variable regions are common spots for engineering and directed evolution of new AAV serotypes that have enhanced properties.

The VP3 monomers can interact with each other to form dimers, trimers, and pentamers that are called the two-fold, three-fold, and five-fold symmetry axes in the 60mer capsid. The three-fold axis can be identified on the capsid where three spiky protrusions are present; these protrusions have been identified to be extremely important for receptor binding (Figure 2B).⁶² The variable region VIII (VR-VIII) is present in the three-fold axis and confers much of the difference in tropism to different AAV serotypes due to variable sequences that bind different receptors. This particular region has been extensively studied and modified to develop new AAV serotypes that have increased tropism to a target organ. Additionally, many antigenicity studies have shown that the three-fold axis is a commonly targeted region by anti-AAV antibodies that can neutralize the virus and prevent infection.⁶³ The five-fold axis can be identified on the 60mer capsid by a central pore, which has been shown to be important for AAV genome and transgene packaging as well as externalization of the VP1/VP2 unique regions.⁶⁴ Studies have also shown that the REP protein interacts with the five-fold axis to inject the AAV genome through the pore

into an assembled capsid. The exact composition of the five-fold axis is not known, but likely averages out to four VP3 proteins and either a VP1 or VP2 protein. The two-fold axis has been characterized to change its conformation during endosomal trafficking, allowing the VP1u to unfold, externalize from the interior, and re-fold.⁶⁵ Additionally, the conformational changes also weakened the two-fold axis region, potentially allowing for more efficient uncoating and thus more viral genomes in nucleus that are available for second strand synthesis or annealing.⁶⁶

1.4 Entry Pathway of AAV

The infection pathway of wt-AAV and rAAV are essentially the same and begin initially with receptor binding (Figure 4). Receptor binding varies for each serotype and depends heavily on the sequences within the variable regions.⁶⁷ The AAV capsid will typically bind multiple receptors consisting of sialic acid, heparin sulfate, growth factor receptors, integrins, and other receptors to facilitate entry into the cell. The current theory is that the AAV capsid will first bind to a glycan receptor, undergo conformational change, and then interact or bind with its co-receptors.⁶⁸ The glycan or primary receptor for each AAV serotype varies and is summarized in Table 3. AAV2 and AAV3 bind heparin sulfate glycans where as AAV1, AAV4, and AAV5 bind some form of sialic acid.⁶⁸⁻⁷² AAV6 is the only serotype that has been characterized to bind both heparin sulfate and sialic acid.⁵⁵ AAV9, unlike the other serotypes, binds N-linked galactose, which could explain why its tropism is drastically different from other serotypes.^{73, 74} The secondary or co-receptors that each serotype binds is more varied between serotypes when compared to their glycan receptors (Table 3). AAV2, which has been extensively studied, was discovered to bind $\alpha 5\beta 1$ -integrin, $\alpha V\beta 5$ -integrin, human fibroblast growth factor receptor 1(hFGFR), human hepatocyte growth factor receptor (hHGFR), and laminin receptor (LamR).⁷⁵⁻
⁷⁸ The exact process in which AAV2 engages these receptors is not well understood; there is

little indication if concurrent binding of all these receptors is critical for AAV infection. Other serotypes, such as AAV3, bind hFGFR, hHGFR, and LamR, which explains its efficient transduction capabilities in primary human hepatocytes.^{77, 79} The remaining serotypes are not as well characterized in terms of co-receptors, only having one known co-receptor discovered for each serotype thus far. AAV8 and AAV9 both bind LamR, while AAV5 binds platelet derived growth factor receptor (PDGFR) and AAV6 binds epidermal growth factor receptor (EGFR).^{77, 80, 81} Once the AAV capsid is bound to its glycan receptor and co-receptors, most AAV serotypes will internalize via clathrin-coated vesicles.^{82, 83} AAV5 is the only serotype that does not only rely on clathrin-coated vesicles; it also can utilize caveoli-dependent entry.⁸⁴

Recently studies have identified a new receptor, the AAV receptor (AAVR), that is essential for AAV entry into the cell.⁸⁵ The exact role of AAVR in AAV internalization is not well understood; studies have suggested that binding to AAVR can either cause conformational changes in the AAV capsid allowing for extrusion of the VP1u domain from pore in the five-fold axis and/or traffic the AAV capsid to the trans-golgi network (TGN) where it will then escape the endosome.⁸⁶⁻⁸⁸ Data suggests that the theory that AAVR traffics AAV capsids to the TGN is likely as there is accumulation of AAVR along with AAV capsids in the TGN when endosomal escape of the AAV capsid is prevented. However, it is unknown whether the AAV capsid binds AAVR directly on the cell surface, or if an interaction occurs later during internalization.

Various studies have provided somewhat conflicting data on the exact location in which AAVR binds AAV, but all seem to suggest that AAVR is necessary for internalization of the capsid. The initial study detailing the discovery of AAVR initially suggested that the interaction between AAVR and AAV was on the cell surface due to disruption of internalization with soluble AAVR and polyclonal AAVR-specific antibodies.⁸⁹ Further studies have suggested the opposite in

which a direct interaction with AAVR at the cell surface is not required.⁸⁵ Regardless, it seems that AAVR is essential for infection for every serotype tested except AAV4. Infection mediated by AAV4 showed no significant differences in wt-Huh7 cells versus Huh7 AAVR KO cells.⁸⁵ Interestingly, AAV5, although dependent on AAVR for internalization, utilized the receptor differently when compared to other serotypes such as AAV2, AAV6 and AAV8.^{88, 90} AAV5 primarily bound the PKD1 domain of AAVR in contrast to other serotypes that primarily bound the PKD2 domain of AAVR.

Once the AAV capsid enters the cell it traffics through the early, late, and recycling endosomes, potentially with the aid of AAVR.⁹¹ During this process, the pH within the endosome drops, eliciting conformational changes in the AAV capsid. The VP1u, normally buried within the capsid, denatures and is extruded through the pore at the five-fold axis.⁴⁴ Once externalized, the VP1u refolds and can interact with the endosomal membrane and trigger escape. Recent studies using genome-wide CRISPR screens have identified GPR108, a member of the G-protein-coupled receptor family, as being critical for AAV entry and endosomal escape.⁹² GPR108 has been identified to interact with the VP1u portion of the AAV capsid, which is subsequently critical for endosomal escape. Additionally, the study found that GPR108 does not affect binding and is localized in the late endosome and TGN, leading to the hypothesis that the VP1u interacts with GPR108 to facilitate endosomal escape. AAV5 was the only serotype found to be independent of GPR108, once again illustrating its divergence from other AAV serotypes.

Following endosomal escape, the AAV capsid is released into the cytoplasm where it then traffics to the nucleus. The cytoskeleton has been characterized as an important factor in transporting the AAV capsid to the perinuclear region.⁹³⁻⁹⁵ Additionally, nuclear localization signals located in the VP1/VP2 common regions are externalized along with the phospholipase

domain and have been established as critical for nuclear entry.⁹⁶ Chemical modifications of certain serotypes such as AAV2 in the cytoplasm have also been detailed; one study found that phosphorylation of certain tyrosine residues on the AAV2 capsid was necessary for nuclear entry.⁹⁷ The exact method in which the AAV capsid enters the nucleus is not fully understood. Some studies have reported that AAV uses host nuclear import mechanisms such as the nuclear pore complex, but inhibition of these mechanisms did not lead to complete blocking of nuclear import, suggesting that AAV may also use other methods to enter the nucleus.⁹⁸ The intact AAV capsid is imported into the nucleus and undergoes uncoating which allows genome expression to occur.⁹⁹

In the case that a transgene is delivered, the single stranded(ss) DNA will have its second strand synthesized to allow transcription of the transgene. If a self-complementary(sc) transgene is delivered, the second strand synthesis step is eliminated, and transcription directly proceeds to allow for faster expression of the transgene.¹⁰⁰ However, the packaging size is more limited for self-complementary transgenes, and thus only smaller transgenes can be delivered in a self-complementary form. Efforts have been made to increase the size of the transgene delivered by splitting larger transgenes into two separate vectors.¹⁰¹⁻¹⁰³ After uncoating in the nucleus of the cell, the two halves of the transgene will undergo homologous recombination or splicing to form the fully intact large transgene. However, the efficacy of this method is low and therefore efficient delivery of the transgene is required. In the case of a wt-AAV genome, the second strand will be synthesized to allow for transcription of the Rep proteins to allow for genome replication.

1.5 Tropism of Naturally Isolated AAV Serotypes 1-9

As discussed before, AAV is a highly versatile vector in gene therapy applications due to its varied tropism from the numerous serotypes that have been discovered thus far. AAV has been characterized with the capability to transduce many different types of tissues and organs (Table 3). AAV2, the most characterized AAV serotype, transduces a wide variety of cells *in vitro* and *in vivo*.^{104, 105} AAV2 has robust transduction in several cell lines, making it a popular vector for ex-vivo transduction experiments and therapies. AAV2 also was initially used to deliver transgenes to the liver but has seen less use recently due to the discovery of more efficient hepatotropic AAV vectors.¹⁰⁴ AAV2 is also extensively used in ocular delivery to treat genetic eye diseases, and is the vector used in the FDA approved drug Luxturna.^{14, 16} AAV2 has also been used to transduce cells in the CNS via direct injection to varying degrees of success.¹⁰⁶ AAV1 and AAV6 are very similar in sequence and structure, and thus target very similar tissues. AAV1 and AAV6 show the most robust transduction of skeletal muscles out of any serotype when injected locally at the target site.^{107, 108} Both serotypes also demonstrate fairly efficient liver transduction.¹⁰⁹ AAV3 initially did not have much of a use, as it was demonstrated to have poor transduction in mouse liver. However, studies testing AAV3b in human liver cancer cells revealed extraordinarily strong hepatotropic qualities even when transducing normal human hepatocytes.¹¹⁰ AAV3b is in many cases the strongest transducer of human liver cells out of the original nine serotypes characterized. AAV4 has been characterized to transduce the heart and lungs, but other serotypes such as AAV9 and AAV5 transduce these tissues more efficiently than AAV4 and thus this serotype sees limited use in the clinic.^{111, 112} AAV5, the most divergent serotype, is primarily used to target the lungs and liver, but also has been shown to be efficient at transducing the brain when injected directly to bypass the blood brain barrier (BBB).¹¹³ AAV5

has seen extensive use in treatment of diseases requiring low amounts of expression in the liver such as hemophilia A and B.¹¹⁴ Although AAV5 is one of the more efficient serotypes at transducing the lung, the overall transduction levels are not nearly enough to produce a therapeutic effect for many lung genetic diseases.¹¹¹ AAV7 has been described to be similar to AAV8 in terms of transduction, yet little characterization of the serotype has been performed.¹¹⁵ AAV8 is a popular hepatotropic serotype that also transduces skeletal muscle efficiently.¹¹⁶ Use of AAV8 in liver diseases has decreased substantially following the discovery that its transduction capabilities in murine liver did not translate well to that of human liver.^{109, 117} AAV9 is perhaps the most important serotype discovered to date, primarily because of its ability to cross the blood brain barrier and its systemic tropism. AAV9 is the only serotype that has been discovered that can cross the BBB and transduce neurons and other cells present in the brain.¹¹⁸ Additionally, AAV9 exhibits efficient transduction in skeletal muscle, the heart, and the liver. This vector is widely used in the clinic; nearly every clinical trial involving treatment of a neurological or muscular disease utilizes AAV9. Other variants from different species such as rhesus macaques have been discovered as well that also have interesting tropisms.^{119, 120}

1.6 Immunogenicity of AAV

Initial studies in animal models suggested that AAV-based therapies did not elicit an immune response that would affect the efficiency of the therapy or lead to adverse side effects in a patient.^{121, 122} However, the first in-human trials utilizing AAV2 to deliver factor IX to treat hemophilia B revealed that the immune response against AAV was different in humans when compared to animal models. Loss of transgene expression was noted after 8 weeks of sustained expression, which was determined to be a result of a CD8⁺ T cell response against the transduced cell population.¹²³ It was quickly determined that the immune response in humans

was different due to prior exposure to AAV that could not occur in the laboratory setting for animals specifically bred for research. As such, an extensive effort has been made to understand the immune response against AAV in humans to develop better AAV therapies.

The immune response against AAV can be divided into two categories: the immune response against the AAV capsid and the immune response against the AAV transgene and its protein products. Exposure of the AAV transgene in the endosome can activate the innate immune response; specifically, the activation of innate immunity via toll-like receptors (TLR). Partial exposure of the transgene or complete exposure due to AAV premature uncoating can result in TLR9 activation. TLR9 is present in the endosome and plays an important role in detection of pathogens and can trigger a signaling cascade that results in effector cell activation. TLR9 signals through the myeloid differentiation primary response gene 88 (MyD88), which leads to degradation of an inhibitor of NF kappa B and results in activation of pro-inflammatory genes.¹²⁴ A study by Zhu et al discovered that AAV2 activated mouse plasmacytoid DCs (pDCs) by the TLR9 recognition pathway that resulted in the production of type I interferon (INF).¹²⁵ Studies into type I INF and its function revealed that upregulation of type I INF triggers the upregulation of effector immune cells that can target transduced cells and ablate gene expression.¹²⁶ Zhu et al also found that the CD8+ T cell responses against the AAV2 capsid were dependent on the TLR9 pathway, showing the importance of avoiding the innate immune response when using AAV-based therapies.¹²⁵ Subsequent studies into AAV and the innate immune response revealed that the activation of the TLR9 pathway was dependent on the CpG motifs within the AAV transgene. Faust et al utilized an immunogenic capsid, AAVrh32.33, to test the effects of removal of TLR9 on innate immunity activation and subsequently effector immune cell response against transduced cells.¹²⁷ In TLR9 knockout mice, the IFN- γ T Cell response was significantly

suppressed resulting in stable gene expression. Additionally, they found significantly decreased immune cell infiltration into transduced tissues as well as significantly reduced chemokine and cytokine expression in TLR9 knockout mice. Removal of CpG motifs in the transgene resulted in AAVrh32.33 vectors that could stably express their transgene with a suppressed effector cell response in wt-mice, indicating that CpG motif removal was an important strategy to prevent immune response against an AAV vector. CpG motif removal was also noted to be far more important for self-complementary vectors as a study revealed that administration of self-complementary vectors resulted in a far more heightened innate immune response when compared to single stranded vectors.¹²⁸ The exact reason for the increase in response is unclear, but it was noted in separate study that double 5' end, sense-antisense TLR9 agonists induced more robust immune stimulation compared with single 5'-end cytosine guanine dinucleotide oligonucleotides.¹²⁹ The difference could also potentially be attributed to capsid stability with self-complementary vectors resulting in more exposed transgenes for TLR9 to detect.¹²⁷ TLR2 has also been demonstrated to elicit an immune response against AAV2 and AAV8.¹³⁰ These data together suggest that the innate immune recognition of AAV occurs in animals, but it is unclear if it occurs to the same magnitude in humans. There have been not acute clinical responses noted in more than 300 subjects that were observed.¹³¹

Aside from the innate immune response detecting the AAV transgene, the protein product of the transgene can also elicit an immune response. This can occur in patients who have “null” mutations, or mutations that cause the gene to not express any protein. In these cases, the patient will not have any self-immune tolerance to a normal protein and can lose stable expression of the protein due to an immune response. However, due to AAV's low proinflammatory profile and low infectivity in dendritic cells, immune responses against the transgene product are seldomly

detected. For liver directed gene therapy, many groups have discovered a self-tolerogenic effect developed towards proteins that are produced by the liver after transduction by an AAV vector. Cao et al found that hepatic transfer-induced regulatory CD4⁺CD25⁺ T cells (T_{regs}) suppress CD4⁺CD25⁻ T cells that were found to be transgene product-specific.¹³² Additionally, depletion of CD4⁺CD25⁺ T reg cells lead to antibody formation against the transgene, indicating that these T reg cells were essential for the self-tolerogenic effect towards the transgene product. This effect can be extended to animals that already have neutralizing antibodies against a protein product. A study in which hemophilic mice and dogs with antibodies against factor VIII and IX were dosed with an AAV vectors expressing either factor VIII or factor IX found that the anti-FVIII and anti-FIX antibodies disappeared from circulation and were no longer produced.¹³³

The extent to which this self-tolerogenic effect occurs in humans given an AAV-based therapy appears to be similar to that of animal models, but does require more extensive studies to completely verify.^{134, 135} So far, most studies detailing the transduction of hepatocytes in a clinical setting have mainly been for Hemophilia A and B. No indications of an immune response against the therapeutic transgene products were detected, even in those who could not produce factor VIII and factor IX.^{123, 131} However, these studies precluded any patients who had inhibitors or neutralizing antibodies against factor VIII and factor IX, and therefore could not determine if the removal of neutralizing antibodies would occur in humans as it occurred in dogs and mice.

The route of injection greatly influences the corresponding immune response against the transgene. AAV-based therapies that inject the virus systemically typically do not have any recorded immune response against the transgene product, likely because the liver is an off target site that can express the transgene product and prevent an immune response.¹³⁴ However, for

therapies where the virus is injected directly into the muscle via intramuscular injections, the risk of a targeted immune response recognizing the transgene product and ablating expression is slightly higher. Most clinical trials utilizing intramuscular or intravascular routes have not detected immune responses against the transgene product with the exception of a few trials.¹³⁶ A clinical trial involving AAV-based treatment of DMD reported in 2010 that a few patients developed transgene-specific CD4⁺ and CD8⁺ T cells after intramuscular injection of an AAV vector encoding for a mini dystrophin gene.¹³⁷ Analysis of the vector distribution in these patients indicated that the dystrophin had expressed but was quickly ablated by a cellular response. Interestingly, two out of the four patients that developed transgene specific T cells were found to already have these T cells before vector administration, indicating that the immune response in these patients was likely not a result of the vector administration.¹³⁷ Other clinical trials involving intramuscular injection of AAV have also noted potential transgene product specific immune responses but have only observed a drop in circulating levels of therapeutic transgene and not complete ablation.¹³⁸ A few strategies have been employed to prevent transgene product specific responses in intramuscular injections. One popular method is to dose patients with short term immunosuppression to dampen the development of an immune response that is specific to the transgene product.¹³⁹ Immunosuppressants, such as prednisolone, are already being utilized to prevent capsid specific T-cell responses following vector administration and therefore can also help with transgene immune responses. Other methods include switching to intravascular injections, using micro RNA to de-target transgene expression in dendritic cells, and utilizing tandem promoters to prevent transgene immunity.¹⁴⁰⁻¹⁴²

Capsid-specific T cell responses are more predominant when compared to transgene-specific T cell responses.^{143, 144} Initially, animal models did not suggest that T cell responses would be a

barrier to successful treatment via AAV but was quickly found not to be the case in humans. A clinical trial utilizing AAV2 to deliver factor IX to treat Hemophilia B found a rapid disappearance of factor IX expression after weeks of stable expression.¹²³ This was accompanied by increases in liver enzyme levels such as aspartate aminotransferase(AST) and alanine aminotransferase(ALT) which are indicators of damage and inflammation in the liver. The time course of the increase in AST and ALT levels and the drop in transgene expression was in line with an immune response, but it was unclear if the response was towards the capsid, transgene, or both. Further analysis of peripheral blood mononuclear cells (PBMC) using immunospot assay revealed a response towards the AAV capsid, but not the transgene product. These studies led to the current theory of how AAV elicits a capsid specific cell response (Figure 3).¹⁴⁵ After administration, AAV enters the target cell via receptor endocytosis and traffics through the endosome. After the virus escapes from the endosome, it enters the nucleus where uncoating allows for the transgene to be expressed. However, a small portion of the capsid remains in the cytoplasm and undergoes proteasomal processing in which the capsid proteins are digested and transported to the endoplasmic reticulum. These capsid fragments are then loaded on the MHC I to form a complex that is then displayed on the cell surface. Capsid-specific memory CD8⁺ T cells that were generated from prior exposure to wt-AAV can then recognize the AAV epitopes and undergo expansion. The expanded capsid-specific CD8⁺ T cells then target any cells with AAV epitopes displayed and abrogate transgene expression.¹⁴⁶ Similar to preventing an immune response against a transgene product, the same method is employed to prevent a response to the capsid. Typically, patients in clinical trials that receive AAV-based therapies will first receive a high-dose of steroids to prevent activation of any circulating capsid-specific memory T-cells. This method has worked well, allowing for stable expression for long periods of time without

any increases in AST and ALT. Therapies targeting the eye or CNS typically detect no immune responses against the capsid, likely due to the “immune privilege” these organs have.¹³⁶

The use of immunosuppressants has largely solved the cellular response against the AAV capsid and AAV transgene. However, the humoral response against the AAV capsid is still challenging to overcome and represents one of the main barriers to developing effective systemic AAV-based gene therapies. Exposure to wt-AAV or rAAV induces the generation of neutralizing anti-AAV antibodies that can prevent potential patients from receiving AAV-based therapies. Neutralizing antibodies recognizing epitopes on the AAV capsid can quickly neutralize the virus and prevent transduction of target cells by blocking essential pathways of infection (Figure 4, Right Panel). The most predominant method of neutralization is through steric hinderance in which the antibody binds to a receptor binding domain on the AAV capsid and prevents attachment to essential receptors on the cell surface. Binding of antibodies to the AAV capsid can also cause aggregation and trigger complement activation.²³ In the first clinical trials with systemically dosed AAV, patients were screened for neutralizing anti-aav antibody titers, but were not excluded from the trials as it was unclear whether it would affect the treatment.¹³¹ The researchers working on the trial quickly found that low titers of anti-aav antibodies were enough to ablate transgene expression and render the therapy ineffective. As such, the standard of eligibility for receiving AAV therapies is to screen all patients for neutralizing factors and preclude any patients with titers of anti-AAV antibodies above a certain cut off.¹³¹

Due to its natural origin, wt-AAV infections are prevalent throughout the human population and thus a large fraction of patients cannot receive systemic AAV therapies (Table 3).^{147, 148} Co-infections with adenovirus can prompt replication of wt-AAV leading to generation of a robust

humoral response against the AAV capsid which can occur as early as two years of age.¹⁴⁹ A study in performed in France characterized the prevalence of neutralizing factors against AAV using serum from healthy human donors. Using an enzyme-linked immunosorbent assay, the study found that the prevalence of anti-AAV total IgG was high in the study population, ranging from ~70% for AAV1 and AAV2 to ~ 40% for AAV5 and AAV8. Testing the serum for neutralizing factors revealed that almost 59% and 50% of the study population had neutralizing factors against AAV1 and AAV2. The lowest observed seroprevalences were for AAV5 and AAV8 in which only 3.2% and 19% of the subjects were seropositive for neutralizing factors against those serotypes. Additionally, low titers of neutralizing factors were found in almost all subjects that were seropositive against AAV5 and AAV8.¹⁵⁰ Similar studies performed in other countries such as the United States have also found similar results; AAV1, AAV2, AAV3, and AAV6 typically have high seroprevalences where as AAV8 and AAV9 have medium levels of seroprevalence.^{151, 152} AAV5 is consistently the lowest seroreactive capsid among those serotypes tested. Studies in China paint a slightly different picture, with higher percentages of the study population testing positive for neutralizing factors against AAV in comparison to studies performed in the West. This may be due to differences in hygiene practices, but none-the-less emphasizes the problem of neutralizing antibodies. Depending on the serotype used, up to 60%-70% of potential patients could be precluded from receiving a life-saving therapy, which is not ideal for the advancement of AAV therapy.¹⁵³ Neutralizing factors against AAV are also passed down through maternal antibodies, but quickly decrease in titer a few months after the baby is born.¹⁴⁹ Thus, there is a small window in which the prevalence of neutralizing factors is lower but can only be exploited by therapies that target this age range. Therefore, the humoral response

problem is particularly troubling for most systemic AAV therapies due to the prevalence of neutralizing factors against AAV in the human population.

So far, there is no solution to treating patients with neutralizing factors against AAV. A few strategies have been devised to overcome humoral immunity to AAV, but none have been utilized in the clinic thus far. One method that has been described utilizing empty capsids or a higher vector dose to deplete anti-AAV antibodies, but fears of triggering an anti-capsid CTL response has prevented this method from seeing further development.¹⁵⁴ Others have described a method using immunosuppressants such as rapamycin to eradicate anti-AAV antibodies and anti-AAV B-cells.¹⁵⁵ While promising, this method is hard to validate as animal models that emulate pre-existing AAV immunity are not representative of pre-existing immunity in humans, and thus their translation of these strategies is challenging. Lastly, methods of engineering variants for reduced seroreactivity through rational engineering or directed evolution have been quite popular, but for the most part have not yielded very promising capsids due to the cross-reactivity of anti-AAV neutralizing antibodies across all AAV serotypes.^{156, 157}

1.7 Engineering of AAV for Improved Transduction Properties

As previously mentioned, AAV-based gene therapy still faces numerous challenges which include increasing transduction efficiency in target tissues and overcoming the immunogenicity of the capsid. While AAV is thought to be relatively efficient at targeting specific tissues; the reality is that our current toolkit of AAV serotypes can only properly treat several systemic diseases where transduction of a small portion of cells is enough for therapeutic efficacy. It is still extremely challenging to achieve high transduction levels in afflicted organs to treat cell-autonomous diseases.¹⁵⁸ As such, many of our current therapies can hinder the progression and ameliorate the effects of certain genetic diseases but cannot be considered curative. Since the

early 2000s, many groups have engineered new AAV variants using rational engineering or directed evolution to attempt to increase the transduction of AAV in tissues such as the liver, heart, muscle, and the CNS (Figure 5).¹⁵⁹⁻¹⁶⁵

In 2003, the first study utilizing directed evolution via a random peptide library insertion into the AAV2 capsid was performed by Muller et al. The capsid library was screened on human coronary artery endothelial cells and AAV2 variants with increased transduction in these cells were discovered.¹⁶⁶ A few years later, another group developed a different directed evolution method in which AAV capsids were randomly mutated utilizing error prone PCR (EPPCR) and staggered extension protocol (stEP). EPPCR randomly mutated single nucleotides(nt) and stEP diversified the resulting library by shuffling mutations around akin to DNA-shuffling. This method allowed for mutation of the entirety of the AAV capsid, rather just targeting one domain in the capsid. The study successfully isolated AAV variants that had increased affinities to heparin sulfate and increased ability to resist neutralizing antibodies.¹⁶⁷ The random mutagenesis method of evolving the AAV capsid also allows for identification of important amino acids that affect receptor binding and can contribute to further understanding of the AAV capsid structure. However, random mutagenesis lacks the ability to significantly mutate the amino acid sequence of the virus and drastically alter tropism in a manner akin to antigenic shift in influenza viruses. In 2008, a new method of randomly engineering chimeric AAV capsids was developed by Li et al which utilized DNA-shuffling to graft different segments of AAV capsids together. To generate their AAV libraries, the capsid genes from AAV serotypes 1-9 were fragmented and randomly joined via primer-less PCR. Screening of the library resulted in isolation of chimeric AAV variants with capsid contributions from multiple serotypes.¹⁶⁸ Shortly after, another group utilized a similar DNA-shuffling strategy to analyze chimeric AAV variants screened on 293

cells.¹⁶⁹ DNA shuffling was particularly useful for developing chimeric AAV capsids that had increased transduction to tissues with existing AAV tropism such as muscle, heart, and liver. However, it was quickly understood that while the DNA-shuffling method was a powerful tool to reengineer AAV, the screening process was paramount to selecting variants with translatable characteristics. In 2009, Yang et al performed a study in which a DNA-shuffled library was screened *in vivo* in a mouse model. The rationale was that *in vitro* screening did not properly recapitulate the environment in an animal. The library was generated from fragments of AAV serotypes 1-9, apart from AAV7, and subjected to 2 rounds of *in vivo* selection in mice. Their top capsid candidate, M41, was selected due to its high frequency in muscle and low frequency in liver. M41 transduced the heart similarly compared to AAV9, but had lower transduction in the muscle and liver, potentially limiting off target transduction.¹⁷⁰

Since then, many groups have developed their own AAV capsids using DNA-shuffling and screening in animal models. An important innovation was the addition of barcoded libraries and next-generation sequencing (NGS) that allowed for more efficient screening of AAV variants.¹⁷¹ However, even with the advances in library construction, the translatability of mouse models to humans was still a problem. Groups utilizing DNA-shuffling began screening their libraries in more appropriate animal models, which was particularly important for liver-tropic AAV capsids. AAV transduction is vastly different in mouse liver when compared to human liver, and many capsids that show efficient transduction in mouse liver, such as AAV8, have very poor transduction in human liver.¹⁷² Due to these differences, one group from Stanford developed a screening process utilizing a humanized liver mouse model to screen for chimeric variants with increased liver tropism. Humanized liver mice are produced by replacing mouse hepatocytes with human hepatocytes in an FRG mouse model. From these models, the group was able to

isolate AAV- LK03, a predominantly AAV3 virus, that had superior transduction in human hepatocytes when compared to other commonly used serotypes.¹⁷³ However, one drawback of this method is that the mouse hepatocytes cannot be completely removed, and thus some variants can still be screened through mouse liver. This problem did present itself as the most predominant chimeric AAV variant in their screening, LK01, had poor transduction in human hepatocytes.¹⁷³ Additionally, further studies with the LK03 capsid revealed that >50% of serum donors had neutralizing antibodies against LK03, indicating it was very seroreactive, similar to AAV3.¹⁷⁴ In order to reduce seroreactivity, the group applied the same library construction and screening methodology with an additional IVIG screening step to weed out seroreactive AAV variants.¹⁵⁶ However, this method produced capsids that had no significant difference in seroreactivity when compared to serotypes such as AAV8, further indicating the challenge in engineering AAV capsids with increased transduction and low seroreactivity. Particularly for DNA shuffled capsids, seroreactivity seems to be a predominant issue due to the higher immunogenicity of capsids that are highly infectious. Serotypes such as AAV2, AAV3, and AAV6 have very high infectivities in a variety of cell types, thus it is logical that these capsids have high levels of seroprevalence. Many shuffled capsids end up with sequences from these capsids, and therefore have similar antigenicity compared to their “ancestral” capsids. As such, many DNA shuffled capsids are quite seroreactive, and in a clinical setting many potential patients would still be precluded from therapies that utilize DNA-shuffled capsids.

Random peptide insertion libraries are still very popular in AAV capsid engineering, particularly when screening for variants in tissues with extremely low transduction efficiency such as the brain.¹⁷⁵ One study utilized cre-dependent screening of an AAV9 random peptide insertion library in mouse brain to obtain AAV PHP.B which significantly enhances transduction

in the CNS when compared to AAV9.¹⁷⁶ However, reports later on described PHP.B as being species dependent; AAV PHP.B did not show any differences with AAV9 in non-human primates.¹⁷⁷ The difference was present even in different strains of mice; AAV PHP did not have enhanced transduction either in BALB-C mice.^{177, 178} The phenomena was mainly present in C57BL6 mice, again illustrating the importance of having good animal models to produce capsids that are translatable to humans. Further examination of AAV PHP.B and similar variants revealed use of the LY6A receptor, which was mainly present in C57BL6 mice and not as much in other species.¹⁷⁹ The process of traversing the blood brain barrier and infecting brain cells is significantly different in mice compared to humans, thus finding a capsid that is capable of doing so in humans through a mouse model is exceedingly difficult. More recent studies have attempted to use non-human primates as the selection model, which may result in more clinically translatable capsids.

1.8 Significance and Specific Aims

Currently, there are no AAV capsids that combine low humoral seroreactivity and seroprevalence with highly efficient transduction of human hepatocytes. One serotype, AAV5, is interesting due to its low seroprevalence in the human population, particularly when compared to other commonly used AAV serotypes. However, studies have proven that AAV5 mediated transduction is poor versus other AAV serotypes, and thus AAV5 has limited use in treating diseases that only require a fraction of normal protein expression. However, decades of studies have shown that the AAV capsid is highly engineerable, and thus can be evolved to better transduce target cells. Therefore, we hypothesize that directed evolution and rational engineering of AAV5 will result in an AAV capsid with high human hepatocyte transduction and low seroprevalence. This thesis is split into three specific aims which include: Directed Evolution of

AAV5 for Increased Liver Transduction (Chapter 2), Analysis of Mutations in Evolved AAV5 Capsids (Chapter 3), and Rational Engineering of Evolved AAV5 Capsids for Further Improvement of Liver Transduction Capabilities (Chapter 4).

Table 1: Approved AAV Gene Therapy Products					
Drug Name	Target Organ	Indication	Company	AAV Serotype	Transgene Product
ZolgenSMA	Spinal Cord	Spinal Muscular Atrophy	AveXis	AAV9	SMN
Glybera	Liver	Lipoprotein Lipase Deficiency	Uniqure	AAV5	LPL
Luxturna	Eye	Leber's Congenital Amaurosis	Sparks	AAV2	RPE65

Table of approved AAV gene therapy products. Data was obtained from clinicaltrials.gov. Abbreviations include: SMN, survival of motor neuron; LPL, lipoprotein lipase; RPE65, retinal pigment epithelium-specific 65 kDa protein

Table 2: Selected Clinical Trials utilizing AAV-Gene Therapy						
Target Organ	Indication	Sponsor	AAV Serotype	Transgene Product	NCT Number	Phase
Liver	Hemophilia A	Biomarin	AAV 5	Factor VIII	NCT03392974	Phase III
Liver	Hemophilia A	Sparks	Engineered AAV8	Factor VIII	NCT03003533	Phase I/II
Liver	Hemophilia A	Bayer	AAV hu 37	Factor VIII	NCT03588299	Phase I/II
Liver	Hemophilia B	Uniqure	AAV 5	Factor IX	NCT03569891	Phase III
Liver	Hemophilia B	Pfizer/Sparks	Engineered AAV8	Factor IX	NCT03587116	Phase III
Liver	Hemophilia B	Shire	AAV 8	Factor IX	NCT01687608	Phase I/II
Liver	Crigler-Najjar Syndrome	Audentes	AAV 8	UGT1A1	NCT03223194	Phase I/II
Liver	OTC Deficiency	Ultragenyx	AAV 8	OTC	NCT02991144	Phase I/II
Eye	Choroideraemia	Biogen/Nightstar	AAV 2	REP 1	NCT03496012	Phase III
Eye	Wet AMD	RegenxBio	AAV 8	Anti-VEGF Antibody	NCT03066258	Phase I/II
CNS	Parkinson disease	Voyager	AAV 2	AADC	NCT03065192	Phase I
CNS	Giant Axonal Neuropathy	NINDS	AAV 9	GAN	NCT02362438	Phase I
CNS	Batten disease (CLN6)	NCH	AAV 9	CLN6	NCT02725580	Phase I/II
Muscle	Duchenne Muscular Dystrophy	Pfizer	AAV 9	Mini-dystrophin	NCT03362502	Phase I
Muscle	X-linked MTM	Audentes	AAV 9	MTM1	NCT03199469	Phase I/II

Table of selected clinical trials with promising results. Data was obtained from clinicaltrials.gov. Abbreviations include: UGT1A1, UDP glucuronosyltransferase family 1 member A1; OTC, ornithine transcarbamylase; REP1, RAB escort protein 1; AMD, age-related macular degeneration; VEGF, vascular endothelial growth factor; AADC, aromatic L-amino acid decarboxylase; GAN, gigaxonin; CLN6, neuronal ceroid lipofuscinosis type 6; MTM, myotubular myopathy.

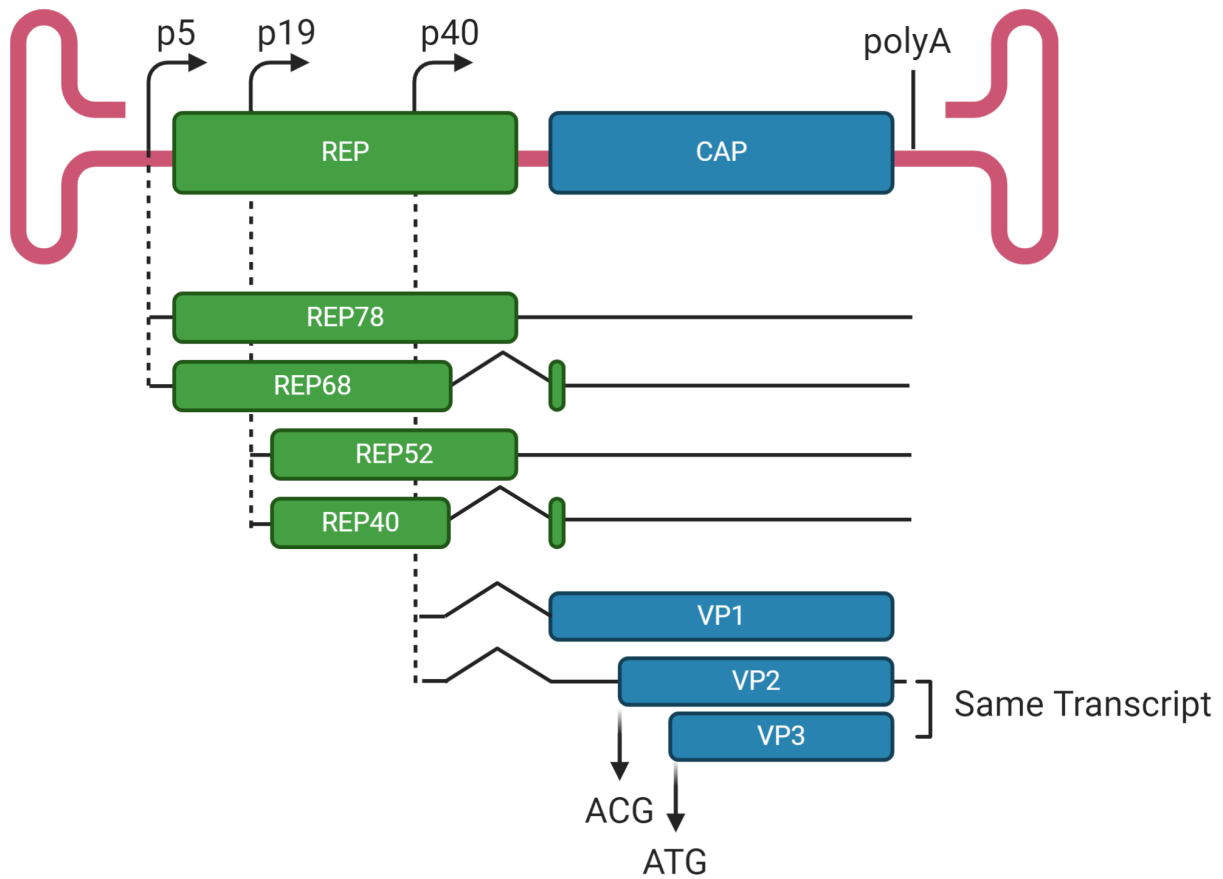


Figure 1: Wild-Type AAV Genome

There are two open reading frames between the hairpin ITRs for the wt-AAV genome. The Rep protein encodes four REP proteins that promote replication and packaging of the wt-AAV genome. The p5 and p19 promoters each drive transcription of two rep proteins each. The p40 promoter drives the transcription of two transcripts that encode for the VP1, VP2, VP3, and AAP (not shown) proteins. The VP1 transcript is spliced together by a weak splicing acceptor site. Alternative start codon ACG initiates transcription for VP2 protein, in contrast to the ATG for VP3. This results in a ratio of 1:1:10 of VP1 to VP2 to VP3 proteins. Figure made with Biorender.

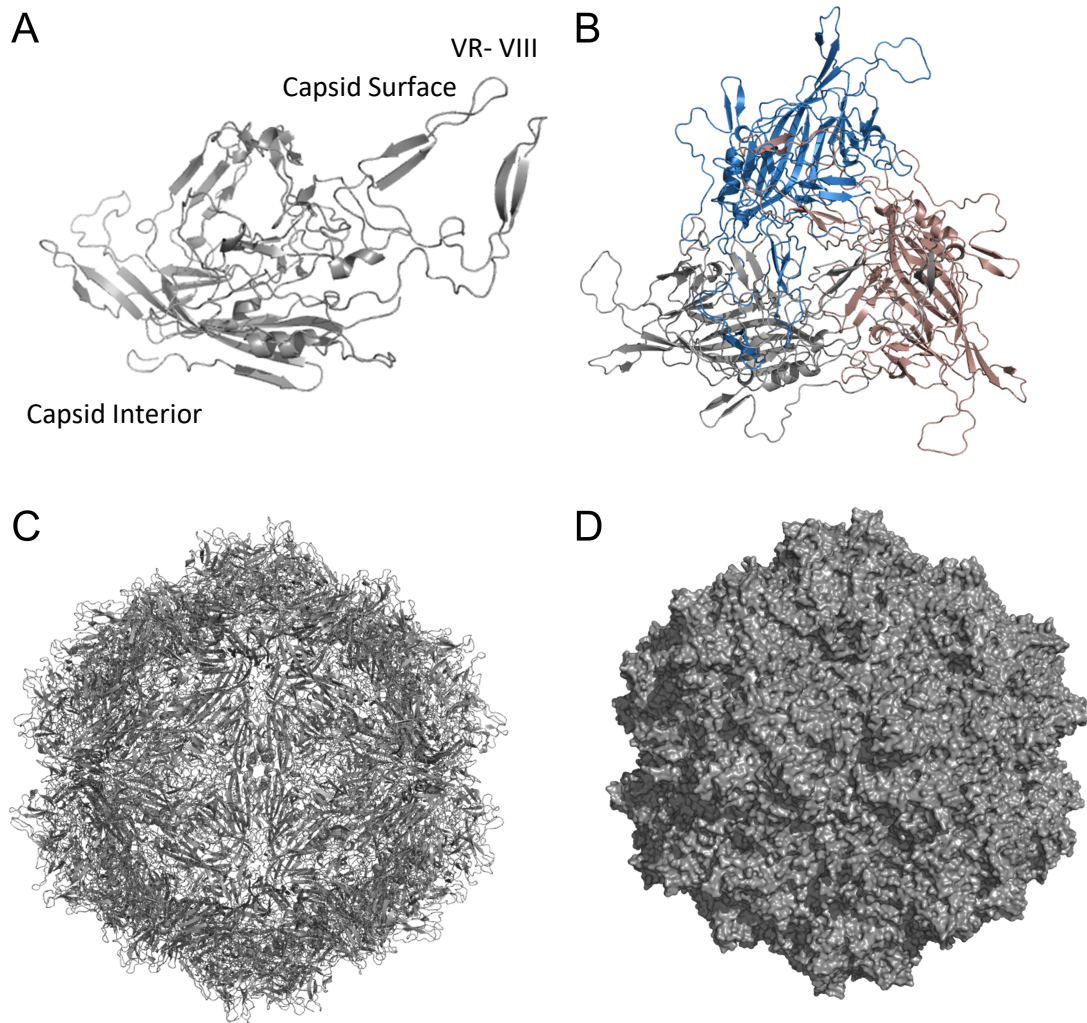


Figure 2: AAV VP3, Trimer, and 60mer Structures

(A) Ribbon cartoon rendering of AAV5 VP3 (PDB#3NTT). The domains near the capsid surface are labeled as such on the VP3 protein. These domains interact with receptors to facilitate binding and entry. The domains near the interior are important for proper capsid assembly. Mutation of these domains can cause drastic changes in stability and yield. One of the more studied domains, VR-VIII, is labeled. This domain is involved heavily with receptor binding and is different for each serotype. (B) Ribbon cartoon rendering of an AAV5 VP3 trimer. The blue, tan, and grey sections each signify a single VP3 unit. (C) A full ribbon cartoon rendering of the 60mer AAV5 capsid. The 60mer capsid was generated using viperdb. (D) Surface rendered 60mer AAV5 capsid.

Table 3: Receptors, Tropism, and Seroprevalence of AAV Serotypes

AAV Serotype	Glycan Receptor	Protein Receptors	<i>In Vivo</i> Tropism	Seroprevalence of Neutralizing Factors
1	N-linked α -2,3 sialic acid	AAVR	Muscle	High
2	Heparin Sulfate	AAVR, α 5 β 1-integrin, α V β 5-integrin, hHGFR, hFGFR,	Eye, Liver	High
3	Heparin Sulfate	hHGFR, hFGFR, LamR	Liver	High
4	O-linked α -2,6 sialic acid	Unknown	Eye	Unknown
5	N-linked α -2,3 sialic acid	PDGFR, AAVR	Liver, Lungs	Low, Medium
6	Heparin Sulfate, N-linked α -2,6 sialic acid	EGFR, AAVR	Muscle, Liver, Lung	High
7	Unknown	AAVR	Muscle, Liver	Unknown
8	Unknown	AAVR, LamR	Muscle, Liver	Medium
9	N-linked Galactose	AAVR, LamR	Liver, Heart, Muscle, CNS	Medium

Table showing AAV serotypes and their receptors, tropism, and seroprevalence. *In Vivo* tropism lists the most commonly targeted organs for each serotype. Most organs are targeted through i.v. injection for each serotype. For all eye targetting serotypes, direct injections into the eye are performed. AAV6 muscle tropism is through intra-muscular injection. Seroprevalence is the prevalence of neutralizing antibodies against the AAV serotype in the general public. Low = 0%-10%. Medium = 10%- 50%. High = 50%-100%. Seroprevalences are compiled from multiple studies.

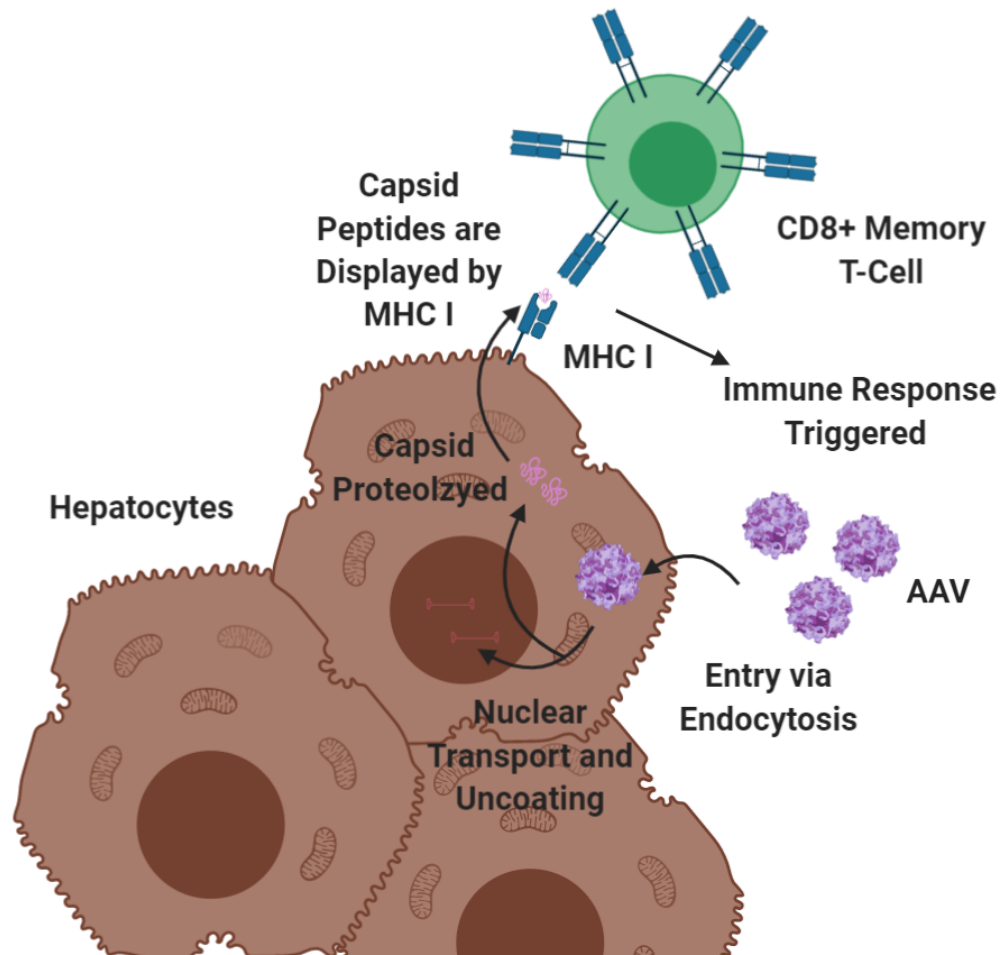


Figure 3: Working Theory of Cellular Response Against AAV Capsids

The working theory of the cellular response begins with AAV binding to the cell surface and entering via endocytosis. After trafficking through the endosome and escaping, the capsid can localize to the nucleus where it will uncoat allowing the transgene to be expressed. However, during this process, not all of the capsid particles will enter the nucleus. A fraction will be proteolyzed and the resulting peptides are displayed by the MHC I. CD8+ memory T cells that were generated by prior exposure to wt-AAV can recognize the capsid peptides and trigger an immune response that results in ablation of transduced cells and transgene expression. Figure made with Biorender.

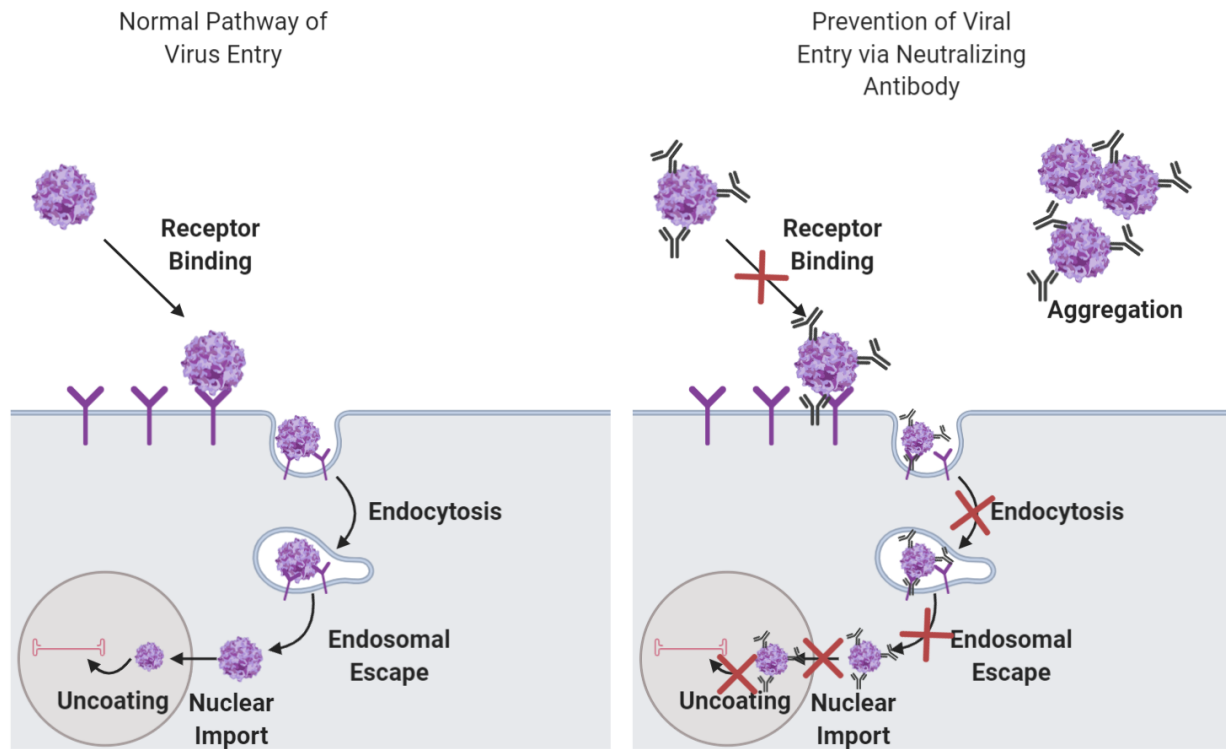


Figure 4: AAV Viral Entry Pathway and Prevention of Entry by Neutralizing Antibodies

The left panel described the normal AAV pathway of entry which begins with receptor binding to a glycan receptor. Conformational changes occur in the capsid to allow for additional co-receptors to bind the capsid. The capsid is then internalized via endocytosis and then escapes the endosomal as the pH decreases. The capsid will then traffic to the nuclear membrane where the entire capsid will be imported into the nucleus. Uncoating of the capsid subsequently frees the transgene inside for expression. The right panel describes how neutralizing antibodies can prevent the entry of the virus and thus prevent transgene expression. Neutralizing antibodies can bind to the surface of the capsid in regions responsible for receptor binding. Steric hindrance prevents binding and thus the virus cannot enter the cell. Additionally, neutralizing antibodies can cause aggregation of the virus and activate the complement. Figure made with Biorender.

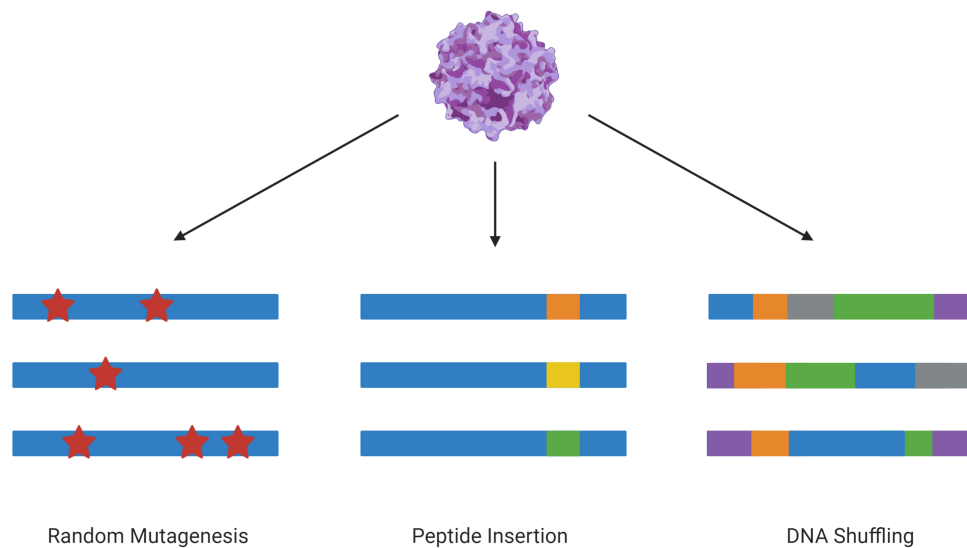


Figure 5: Diagram Depicting the Main Methods for Directed Evolution of the AAV Capsid

An AAV virus can be evolved using a multitude of techniques. Random mutagenesis involves using error prone PCR to randomly induce mutations in the capsid gene of the virus. This method is very similar to the natural evolution of DNA viruses. Peptide insertion involves insert peptide libraries into specific sites in the AAV capsid. This is typically the VR-VIII site, due to its flexibility and importance with receptor binding. The last method is DNA shuffling, in which the capsid genes of many different serotypes are fragmented and rejoined using primer-less PCR. This results in chimeric AAV capsids with drastic changes in properties. Figure made with Biorender.

CHAPTER 2

DIRECTED EVOLUTION OF AAV5 FOR INCREASED LIVER TRANSDUCTION¹

2.1 Overview

Hepatotropic recombinant adeno-associated virus (rAAV) capsids that are commonly used to deliver therapeutic genes to the human liver typically have significant seroprevalence in the human population, effectively reducing the patient pool that can receive AAV-based therapies to treat rare-genetic liver diseases. One AAV serotype, AAV5, does not face the same immunological limitations when compared to other widely used AAV serotypes. Only a small fraction of the human population has neutralizing antibodies against AAV5, which is much lower when compared to AAV2, AAV6, AAV8, and AAV9. However, in exchange for its favorable seroreactivity and seroprevalence, AAV5 suffers from poor transduction efficacy in human liver. As such, AAV5 is only practical to use for genetic diseases that require low amounts of transgene expression in order to produce a therapeutic effect. To increase the efficacy of AAV5 based gene therapy for liver diseases, we constructed a replication competent library of AAV5 mutants by error prone PCR (EPPCR) and staggered extension protocol(stEP) and screened for variants with increased liver transduction in Huh7 cells. Around 25 unique mutants were discovered and tested for yield and infectivity. The five best variants, MV1, MV18, MV20,

¹ This chapter includes a manuscript in submission: Qian R., Li J., Xiao X. *Directed Evolution of AAV Serotype 5 for Increased Liver Transduction and Retention of Low Humoral Seroreactivity.*

MV50, and MV53 were taken for further characterization in various human liver cell lines. Of the five selected mutants, MV50 and MV53 consistently demonstrated the most significant increases in liver transduction when compared with AAV5. These five mutants were also characterized in a non-humanized mouse to determine if the mutations changed tropism of the viruses in a mouse. Interestingly, some viruses exhibited increases in mouse lung transduction, indicating that they had potential uses in AAV5-based lung transduction. All variants were tested for their seroreactivity towards pooled human IVIG and compared with wild type AAV5. Most mutants had similar seroreactivities compared to AAV5, thus indicating that our mutations did not significantly alter the serological profiles of these viruses. These evolved AAV5 capsids have the potential to expand the patient population that can receive AAV-based liver gene therapies.

2.2 Introduction

Development of AAV-based gene therapies for genetic liver diseases has made substantial progress in the past decade, culminating in landmark clinical trials for diseases such as hemophilia A and B.^{19, 20, 180} However, successful clinical trials have mainly been limited to liver diseases that only require a small fraction of normal protein expression for therapeutic effect, which is readily achievable by using moderately high doses of commonly utilized hepatotropic rAAV capsids.¹⁸¹⁻¹⁸³ Treatment of liver diseases requiring more extensive and broad transduction of human hepatocytes remains a challenge as many of the clinically relevant hepatotropic rAAV capsids cannot achieve the required levels of gene expression for therapeutic efficacy.¹⁸¹

As such, much effort has been applied in developing engineered rAAV capsids through directed evolution or rational design for increased human hepatocyte infectivity.^{156, 172, 173} Although these methods have yielded capsids with significantly increased human liver

transduction, many of the evolved and engineered capsids still potentially suffer from having significant seroprevalence in the human population similar to their “ancestral” counterparts. These “ancestral” counterparts are typically AAV serotypes that are commonly used for in vivo hepatic delivery, such as AAV2, AAV3, AAV6, and AAV8, which have moderate to high levels of pre-existing neutralizing antibodies in the general population.^{150, 152, 153} Pre-existing neutralizing antibodies are a direct result of prior exposure to wild-type AAV and can often cross neutralize many different AAV serotypes.¹⁸⁴ As a result, evolved capsids for liver gene therapy still have a possibility of being neutralized to the same extent as their ancestral parents by pre-existing neutralizing antibodies targeting homologous domains on the capsid surface.¹⁷⁴ Interestingly, most evolved capsids contain little to no traces of AAV5 sequences, likely a result of AAV5 having the most divergent sequence and demonstrating significantly less transduction in human hepatocytes when compared to other serotypes.^{156, 172} Due to its divergent sequence, AAV5 has been consistently characterized as the serotype with the lowest seroprevalence of pre-existing neutralizing factors in the general human population.^{150, 151} Studies utilizing serum from health adult donors in Europe and America concluded that as low as ~3% and ~13% of their respective study population tested positive for neutralizing factors against AAV5 which was significantly lower compared to other serotypes such as AAV2, AAV6 and AAV8.^{150, 152} Additionally, clinical trials utilizing AAV5 for hemophilia A have also noted that patients with pre-existing anti-AAV5 antibodies had sustained levels of FVIII expression comparable to patients without neutralizing factors which indicates that AAV5 could be used even in the presence of neutralizing factors in serum.^{180, 185} Thus, evolved AAV5 vectors that have enhanced transduction capabilities could have tremendous advantages in evading neutralizing antibodies and improving liver gene therapy.

In this study, we engineered diverse libraries of AAV5 mutants using error prone pcr and the staggered extension protocol using previously established methods.^{167, 186, 187} Error prone PCR was utilized instead of other methods such as peptide insertion libraries to lower the possibility of significantly increasing the seroreactivity of AAV5. The infectious library was screened in Huh7 cells, a human liver carcinoma cell line, in the presence of wild-type adenovirus type 5 to allow for replicating screens. Other studies have noted replicative screening to be beneficial as it allows for selection in every step of the viral life cycle including binding, uptake, trafficking, uncoating, and gene expression.¹⁵⁶ Variants that infect liver cells more efficiently will replicate first, resulting in increased titers within the system and driving selection for that variant. Additionally, replicative screens allows production and yield to play a role in selection as variants that may have advantages in transduction may also have deficiencies in replication, which could potentially prevent a capsid from being used to treat diseases that require high doses of AAV. Variant AAV5 capsids were selected for their infectivity in Huh7 cells and their production yields. Mutant AAV5 capsids screened on Huh7 cells exhibited increased transduction in primary human hepatocytes while also retaining similar seroreactivity compared to AAV5. The result is AAV5 mutant capsids that have enhanced transduction in primary human hepatocytes and favorable seroreactivities.

2.3 Materials and Methods

Generation of Random Mutagenesis AAV5 Plasmid Library

The randomly mutated AAV5 plasmid library was generated by amplifying a wt-AAV5 capsid gene (XR5 plasmid) with error prone PCR using a GeneMorph II Random Mutagenesis Kit (Agilent) followed by subsequent amplification by staggered extension protocol (stEP). In brief, 10ng of the DNA template was amplified over thirty cycles using an error prone DNA

polymerase to achieve a wide range in the VP3 gene per each PCR fragment. To further diversify the mutant AAV5 plasmid library, the point mutations generated by error prone PCR were shuffled using stEP in which roughly 100ng of mutated AAV5 VP3 DNA was subjected to 100 extremely short cycles of denaturing (~20s), annealing (~5 seconds), and elongation(~10s). For both error prone pcr and stEP, the forward primer (5'-AGGCTCGGACCGAAGAGGACT-3') overlapped a RSRII restriction enzyme cutsite upstream of the VP3 gene while the reverse primer (5'-ATCGAGCGGCCGCAAGAGGCAGTATTTTAC-3') overlapped the NotI cutsite downstream of the VP3 gene to facilitate cloning of the PCR product into an “infectious”, or wildtype AAV5 plasmid.

The mutant VP3 stEP PCR amplicons were purified and digested to completion using RSRII/NotI restriction enzymes. Digested DNA was isolated using agarose gel purification and cloned into backbone containing an AAV2 REP gene and a partial AAV5 Capsid gene flanked by AAV2 ITR sequences to create an “infectious” plasmid, or a replication competent AAV plasmid. The resulting mixture was electroporated into DH10B electrocompetent bacteria and spread across LB agar plates containing ampicillin. A viral plasmid library of 5×10^5 independent clones was generated as determined by quantification of the number of colonies following bacteria transformation. To confirm the diversity of the library, 20 colonies were picked from the plates for miniprep and sequencing. Individual bacteria colonies were pooled together by washing the LB-agar plates with terrific broth medium and then cultured in four liters of TB medium. The propagated bacteria were then used for large-scale purification of the plasmid DNA library by ultracentrifugation with CsCl-ethidium bromide gradients.

AAV Library and Vector Production

Purified AAV vectors were produced via the triple transfection and cesium chloride density ultracentrifugation methods. Briefly, HEK293 cells were transfected with a helper plasmid, a self-complementary GFP (sc-GFP) or single stranded LacZ-nls vector plasmid, and a packaging plasmid containing capsid gene and an AAV2 rep gene. Cells were harvested 72 hours post transfection and isolated by centrifugation. The media was collected and stored while the cell pellet was resuspended and subjected to three freeze thaw cycles. The resulting cell lysate was incubated with DnaseI and RnaseA at 37C and centrifuged and the supernatant was collected. The virus from the supernatant and the media were then concentrated by PEG precipitation followed by two rounds of cesium chloride (CsCl) density ultracentrifugation. CsCl fractions containing virus were determined by DNA dotblot and combined and dialyzed using 5% sorbitol in PBS. Dialyzed virus preparations were again titered using DNA dot blot with a probe specific to reporter gene. All viruses that were tested were titered in the same dotblot to allow consistent measurement of viral titers.

The AAV5 viral library was produced using the same method as described before, but with only two plasmids. In brief, the plasmid library and a helper plasmid were transfected into human embryonic kidney (HEK293) cells at a 1:1 ratio via the calcium phosphate transfection method. After 72 hours post transfection, the transfected cells and media were collected. The viral particles were released via the freeze thaw method and purified using CsCl density centrifugation. For all AAV5 library experiments, the AAV titer was determined by the dotblot method using a probe specific to the AAV2 Rep gene.

Mutant AAV5 Library Selection in Huh7 Cells

The AAV5 viral library was added to Huh7 cells at a MOI of 5000 vector genomes per cell and coinfecting with wildtype-adenovirus type-5(wt-ad) at a MOI of 100 vg per cell. After 72 hours of infection, the cells were collected and lysed via three freeze thaw cycles with a dry ice and ethanol mixture. The cell lysate was then incubated at 56C for 1 hour to inactivate the wt-ad present in lysate. The cell lysate was then centrifuged at 15000rpm for 5 min and the supernatant containing the mutant viral particles was collected. The virus in the supernatant was titered by DNA dotblot. Huh7 cells were again infected with virus from the previous round of selection at a MOI of 5000 vg/cell. In total, 7 rounds of selection on Huh7 cells were performed. For the last round of selection, the infected cells were washed with PBS twice to remove any virus that did not manage to infect the cells. The viral DNA was then extracted from the cells via a modified Hirt Extraction as previously described by others.¹⁸⁸ In short, cells were suspended in 250 uls of a Tris-HCl/EDTA solution containing 100 ug/ml RNase A. Cells were lysed with the addition of a 1.2% sodium dodecyl sulfate solution and incubated for 5 min at room temperature. chromosomal DNA and cellular debris were precipitated with the addition of a cesium chloride, potassium acetate, and acetic acid solution and incubated on ice for 15 minutes. The mixture was then centrifuged at 4C for 15 minutes, and the supernatant was loaded onto a Qiagen Qiaprep Spin column. The bound DNA is then washed, eluted, and amplified via PCR using the same primers used for the error prone PCR. The resulting PCR amplicons are purified and subsequently digested with RSRII and NotI and ligated into a packaging plasmid containing AAV2 Rep and a partial AAV5 Cap gene. The ligation mixture was transformed into bacteria and spread onto agar plates containing ampicillin. After overnight incubation, individual colonies were picked for plasmid amplification via miniprep. Amplified plasmid DNA was incubated

with RNASEA, purified, and sequenced. Primers used to sequence mutant AAV5 capsids were: F1: 5'-GGCCAGGCTCTCATTTGTTC-3'; F2: 5'-GACGACACATCCTTCGGG-3'; F3: 5'-CAGCTGCCCTACGTCGTC-3'; F4: 5'-GGCACGTACAACCTCCAGGAAATC-3'

Transduction of Human Liver Cancer Cells by AAV Vectors

Variant AAV5 vectors were used to packaged sc-GFP reporter genes for comparison to wt-AAV5. Huh7 cells in 12 well plates were infected with AAV5 and mutant self-complementary(sc)-GFP encoding viruses at a MOI of 100,000 viral genomes(vg) per cell and co-infected with 5000 vg/cell of wt-ad5. Seventy-two hours after infection, cells were taken for fluorescent imaging and subsequent GFP quantification using the Fluorometric GFP Quantification Kit from Cellbio Labs. GFP activity was normalized by protein concentration as measured by Pierce BCA Protein Assay Kit (ThermoFisher Scientific).

Transduction of Primary Human Hepatocytes by AAV Vectors

Primary human hepatocytes (TRL HUM4037, Triangle Research Laboratory, NC) were cultured according to vendor's instructions. In brief, cells were thawed and plated at 2.5e5 cells per well in collagen coated 24 well plates (Corning BioCoat Collagen I 24 well plates). The next day, the primary human hepatocytes were infected with purified sc-GFP vectors at a MOI of 500,000 vg per cell. Media was changed 48 hours after infection, and once daily afterwards. Ninety-six hours post infection, cells were taken for fluorescent imaging and subsequent GFP quantification using the Fluorometric GFP Quantification Kit from Cellbio Labs. GFP activity was normalized by protein concentration as measured by Pierce BCA Protein Assay Kit (ThermoFisher Scientific).

Tissue Tropism of AAV Vectors in Mice after Systemic Administration

C57/BL6J mice were maintained in a 12-hr:12-hr light: dark artificial light cycle (0700-1900) at a temperature of 20C and a humidity of 55±5%. All animal protocols were approved by the University of North Carolina Animal Care and Use Committee. The mutant AAV5 capsid genes were used to package CB-LacZnl_s reporter gene which expresses B-galactosidase with a nuclear localization signal and compared to wt-AAV5. LacZ vectors were administered to eight-week-old male C57BL/6J mice by intravenous tail vein injection at a dose of 1e12 vg per mouse. After three weeks, the mice were sacrificed, and tissues were collected, and flash frozen in liquid nitrogen cooled 2-methylbutane. Tissues were stored at -80C until ready for use. Tissues were homogenized in lysis buffer from the Galacto-Star LacZ Assay Kit (Applied BioSystems) and measured for protein concentration using the Pierce BCA Protein Assay Kit (Thermo Fisher). Samples were diluted to similar protein concentrations. B-galactosidase enzyme activity in homogenized tissue lysates was measured using the Galacto-Star LacZ Assay Kit and readings were normalized by protein concentration.

HepG2 cells were transduced using the same methodology as described above. Quantification was performed in same manner as well.

AAV Neutralization Assays with Intravenous Immunoglobulin

Huh7 cells were seeded at 5e4 cells per well in a 96 well plate. The next day, 50 particles of wt-wt-Ad5 per cell was added to each well of the 96 well plate. AAV sc-GFP vectors (1e9 vg) were incubated with reciprocal dilutions of IVIG (Carimune NF, ZLB Behring). The first well corresponded to 25ug of IVIG, and each subsequent well contained half of the previous amount of IVIG. The combined IVIG and AAV vector mixtures were incubated for 1 hour at 37C and

then added to individual wells of Huh7 cells in a 96 well plate. Virus concentration was kept the same for each reciprocal dilution of IVIG. After 72 hours, the cells in each well were lysed and the crude lysate was assayed for GFP activity using a Fluorometric GFP Quantification Kit (CellBio Labs). The GFP activity was measured against a control well infected with only virus and no IVIG to obtain the percent of max GFP expression at each reciprocal dilution for each virus. The percent of max GFP activity was plotted against the log reciprocal dilution in GraphPad 8 to generate a fitted curve using nonlinear regression. The corresponding EC50, or reciprocal dilution required for 50% max GFP activity, was calculated using GraphPad 8, and compared to the EC50 of other AAV serotypes to determine the relative differences in seroreactivity to IVIG.

Statistics

Statistical analyses were conducted with GraphPad Prism 8. All statistical analyses were justified as appropriate and p-values <0.05 were considered statistically significant. For all statistical tests performed, intra-assay variation fell within the expected range and the variance across groups was similar. Comparison of experimental values from two groups were assessed using a Student's unpaired two-tailed t test. Experimental values for IVIG neutralization assays were first normalized and then plotted against the log transformed values for reciprocal dilutions before being compared using an Extra sum of squares F test.

2.4 Results

Generation and Screening of a Diverse AAV5 Capsid Library in Huh7 Cell Line

To evolve AAV5 for enhanced liver gene therapy, we constructed a diverse library of AAV5 capsids by utilizing a similar method previously described by Maheshri et al in which

error prone PCR(epPCR) and staggered extension protocol (stEP) are utilized to randomly generate point mutations in the AAV5 capsid gene.¹⁸⁷ Generation of the library was performed with primers overlapping the RSRII and NotI restriction enzyme cutsites up and down stream of the VP3 gene in the plasmid XR5 to limit mutations to the VP3 gene. Mutated AAV5 capsid genes were then further diversified through stEP and combined with the epPCR library, resulting in a diverse library of AAV5 capsid genes that were then cloned into an infectious vector containing AAV2 ITRs and a chimeric AAV2 and AAV5 rep gene. An infectious wt-like AAV5 library was produced using the triple plasmid transfection method followed by purification via cesium chloride density ultracentrifugation (Figure 6).

We screened the AAV5 library on Huh7 cells, a human hepatocyte derived carcinoma cell line, in an effort to develop more cost-effective screening systems for human liver transduction. Other groups have described AAV3 and AAV8 transduction efficacy of Huh7 cells as fairly representative of their infectivity in primary human hepatocytes, and thus we decided Huh7 cells would serve as an adequate selection model for human hepatocyte transduction. The purified AAV5 library was added to Huh7 cells followed by coinfection with wildtype adenovirus type 5 (Ad5). After 72 hours of Ad5 infection, the cells were collected and lysed to release AAV5 variants that successfully transduced and replicated. Supernatant containing the virus was titered and added back to fresh Huh7 cells. Viral DNA was extracted from a portion of the cells at rounds 5 and 7 via a modified Hirt Extraction and the isolated VP3 genes were amplified by PCR. Mutant VP3 genes were then cloned into a packaging plasmid, propagated, and sequenced (Figure 7).

Sequencing of AAV5 capsids selected from the 5th round of selection revealed that approximately half (31 out of 65) of the sequenced mutants contained an glycine to arginine

(G257R) mutation in the Loop1 or variable region I (VR I) of the AAV5 VP1 protein (Figure 8). Further enrichment of the mutants carrying the Loop1R mutation was observed after the 7th round of selection in which 73 out of 75 mutants carried the Loop1R mutation (Figure 8). All unique sequences obtained from the 5th and 7th rounds of selection were used to package self-complementary GFP (sc-GFP) vector and crudely assessed for infectivity and yield. The five best variants were selected for large scale production and purification for further analysis (Figure 9A and 9B).

Characterizing AAV5 Variants for Increases in Human Liver Cell Transduction

We next investigated the transduction efficacy of the AAV5 variants versus wt-AAV5, and additionally determined whether screening of AAV capsids on Huh7 cells was translatable to primary human hepatocytes. The sc-GFP vector was packaged into five variant capsids and wt-AAV5 and purified for in depth analysis of functional transduction in human liver cells. All viruses were titered on the same dotblot and found to have similar production titers when compared to wt-AAV5. Huh7 cells were transduced at a MOI of 1e5 vg per cell and co-infected with 5000 vg/cell of wt-Ad5 to accelerate the process of transgene expression. Imaging of GFP expression revealed that all five mutants had significantly increased GFP expression compared to AAV5 (Figure 10A). Variant MV50 was the best performing variant that was around 12x better than AAV5 in transduction of Huh7 cells (Figure 10B and 10C). The second and third best variants were MV53 and MV1, which were 11x and 10x better than AAV5, respectively (Figure 10B and 10C). These results confirmed previously noted sequencing data that suggested the Loop1R mutation was specifically enriched during screening in Huh7 cells. As such, the Loop1R mutation is contributing the most in terms of increasing infectivity in Huh7 cells while additional mutations are complimentary to the Loop1R mutation and add small increases in transduction.

The final mutant, MV20, contains no Loop1R mutation, but still shows a 6x increase in infectivity compared to AAV5 (Figure 10B and 10C). This suggests that the mechanism in which MV20 is increasing infectivity may be different compared to the other mutants.

Next, the variants were tested against AAV5 in HepG2 cells, a human liver cancer cell line, to evaluate if the increases in transduction seen in Huh7 cells were cell-line specific. Similar to the results from before, the variants exhibited significant increases in transduction compared to AAV5 in HepG2 cells, albeit at a lower magnitude when compared to the increases in Huh7 cells (Figure 11A). MV50 once again was the best performing variant with a 7x increase in GFP expression when compared to AAV5 while other variants exhibited slightly lower increases in transduction that ranged from around 4x-6x depending on the variant (Figure 11B and 11C). One potential reason for the slightly lower magnitude of increase in HepG2 versus Huh7 cells could be due to the tendency of HepG2 cells to grow in clusters, thus making it harder for AAV to bind to the surface of the cells and facilitate entry. Additionally, due to the nature of cancer cell lines, it is also a possibility that the expression levels of various entry receptors on the cell surface varies between Huh7 and HepG2, thus leading to different levels of transduction depending on the receptors that are utilized by AAV5 and the variants. Regardless, increased transduction in both liver cancer cell lines indicated that these mutant AAV5 were not Huh7-specific and have a higher likelihood of translating to human hepatocytes.

Next, the five AAV5 mutants were tested for their transduction capabilities in donor primary human hepatocytes in order to verify that their increased infectivity in Huh7 cells was translatable to human liver cells. Primary human hepatocytes were plated and infected with purified sc-GFP vectors at a MOI of 500,000 vg per cell. Ninety-six hours post-infection, the cells were taken for imaging of GFP expression and quantification of GFP activity. Similar to the

results from Huh7 cells, the AAV5 mutants were all significantly better at infecting primary human hepatocytes when compared with wt-AAV5 (Figure 12A). In particular, MV50 and MV53 were the two variants with the best transduction capabilities and both infected primary human hepatocytes roughly 10-fold better compared to AAV5, which was very consistent with the fold increase in Huh7 cells (Figures 12B and 12C). The increase in infectivity of the other three mutants, MV1, MV18, and MV20 over AAV5 were also very consistent with the results from Huh7 Cells, with the fold increase over AAV5 around 8-fold, 7-fold, and 5-fold, respectively (Figures 12B and 12C). The overall magnitude of the fold increases in infectivity in primary human hepatocytes are very consistent when compared to the results from Huh7 cells (Figure 12D), indicating that Huh7 cells and primary human hepatocytes are very similar in terms of characteristics influencing AAV infectivity, and also demonstrates the viability of using Huh7 cells to approximate infectivity in human liver cells.

B-galactosidase (LacZ) reporter gene vectors were packaged by our AAV5 variants and injected intravenously into non-humanized C57BL/6 mice (1×10^{12} vg/ mouse) to assess whether or not our variants had altered tropism in a mouse. Three weeks post injection, the mice were sacrificed, and their tissues were homogenized and assessed for LacZ activity. Unsurprisingly, the variants performed differently in mouse liver when compared to primary human hepatocytes, likely due to selection on human liver cells. LacZ quantitative enzyme assays showed that MV18, the variant with the lone G257R mutation, did not have significantly different mouse liver transduction when compared with wt-AAV5 (Figure 13A). Of note, MV1 and MV53 were the only variants that had slightly higher levels of LacZ activity in the mouse livers, indicating that their secondary mutations may have non-species-specific mechanisms of increasing functional transduction (Figure 13B). To see if our variants had any changes in tropism to other

organs, the lungs, heart, gastrocnemius, and brain were assessed for LacZ activity. No detectable changes were seen in skeletal muscle (GAS), heart, and brain (Figure 13A). However, we did see a significant increase(4x) in LacZ expression levels in mouse lungs transduced by Loop1 variants when compared to wt-AAV5, indicating that these mutations could also have potential applications in increasing lung transduction efficacy (Figure 13C). However, these mutations would likely need to be combined with other lung-specific mutations AAV5 mutations in order to pose any effectiveness in treating lung diseases.

Assessing neutralization of AAV5 variants with pre-existing antibodies in Pooled Human IgGs

Next, we investigated whether directed evolution of AAV5 also induced changes in seroreactivity of the capsids to neutralizing factors in pooled human IgG. We assessed seroreactivity via a neutralizing assay that utilized intravenous immunoglobulin (IVIg), or pooled immunoglobulin G from thousands of donors, to represent the overall prevalence of neutralizing antibodies against specific antigens in the overall human population. We compared our mutant viruses to two control serotypes, AAV5 and AAV9: one with very low prevalence of neutralizing antibodies, and one with a medium prevalence. Mutant viruses containing GFP reporter transgenes were incubated with increasing reciprocal dilutions, or two-fold dilutions, of IVIg for 1 hour and then added to individual wells of Huh7 cells in a 96 well plate. After 72 hours, the cells in each well were lysed and the crude lysate was assayed for GFP activity. The GFP activity was measured against a control well infected with only virus and no IVIg to obtain the percent of max GFP expression at each reciprocal dilution for each virus (Figure 14A). Plotting the percent max of GFP against the log reciprocal dilution and curve fitting using nonlinear regression allowed for the comparison of seroreactivity between different viruses.

From these curves, we determined that the seroreactivity of AAV5 and the MV mutants are fairly consistent with each other, and all of which are significantly shifted to the left of AAV9, indicating that AAV5 and the mutants require more IVIG to neutralize their infectivity when compared to AAV9 (Figure 14B). This signifies that the IVIG likely contains a higher titer of anti-AAV9 neutralizing antibodies, and thereby indicates that the donor population likely has a higher prevalence of anti-AAV9 antibodies compared to anti-AAV5 antibodies. The seroreactivity curve for MV18, or the mutant with only the Loop1R mutation, is shifted to the left of AAV5, signifying that MV18 is slightly less seroreactive than AAV5 and requires slightly more IVIG to achieve 50% inhibition of infectivity (Figure 14B and 14C). MV20 and MV53 are slightly more seroreactive when compared to AAV5 whereas MV1 and MV50 do not differ in seroreactivity in comparison to AAV5 (Figure 14B and 14C). Although the seroreactivity of the mutants towards IVIG seems to slightly vary in comparison to AAV5, we believe that the overall seroprevalence of antibodies against the mutants in the human population is unlikely to be significantly different when compared to AAV5. The variations in seroreactivity between the mutants are more likely to be attributed to changes in resisting neutralization.

2.5 Discussion

Engineering novel AAV capsids with increased liver tropism has progressed significantly in the past few years yet has also grown more challenging. Experience from clinical trials and literature has detailed the importance of balancing aspects of infectivity, immunogenicity, yield, and other factors when developing capsids for clinical use, increasing the complexity of library generation, screening systems, and capsid characterization process. Other groups have developed methods for evolving capsids based on these criteria using DNA shuffling and other techniques based on existing serotypes with hepatotropic properties but remain potentially problematic in

terms of seroreactivity. We decided to approach this problem of infectivity and seroprevalence by engineering AAV5, a serotype that has been shown to have significantly less seroprevalence when compared to more commonly used serotypes such as AAV2, AAV3, and AAV8. The purpose of this study was to increase the transduction efficacy of AAV5 in the human liver while minimizing any potential changes in seroreactivity to develop an AAV capsid that had both good transduction capabilities and favorable seroreactivity.

To accomplish this, we generated AAV5 capsid libraries via random mutagenesis, to avoid significant alterations in seroreactivity that other methods such as peptide insertion libraries could potentially cause. We decided ultimately to screen our AAV5 libraries in Huh7 cells to develop more cost-effective screening systems for human liver transduction. Other groups have described AAV3 and AAV8 transduction efficacy of Huh7 cells as fairly representative of their infectivity in primary human hepatocytes, and thus we decided they would serve as an adequate selection model for human hepatocyte transduction.¹⁸⁹ While others have noted that there are vast differences between *in vitro* and *in vivo* selection, we believe that the fenestrated nature of the endothelial lining in the liver allows for easier translation from *in vitro* to *in vivo*, as long as the screening system is of human hepatocyte origin.¹⁹⁰ Additionally, there is a wealth of evidence that supports the idea that non-humanized mouse models are not suited for screening of hepatotropic properties in human hepatocytes.^{172, 191} Even humanized liver mouse models present their own challenges which include factors such as variability of the number of implanted human hepatocyte versus existing mouse hepatocytes and morphology of the humanized livers.^{156, 192} All of these factors led us to believe that screening for human liver transduction in an *in vivo* model was not the only route that could be taken and that *in vitro* selection could potentially yield capsids with increased human liver infectivity.

Using these methods, we successfully developed novel AAV5 variant capsids with enhanced transduction capabilities in human liver cells that retained the advantageous low seroreactivity of wt-AAV5. Two capsids, MV50 and MV53, displayed significantly increased transduction in human hepatocytes by up to 10-fold over wt-AAV5. Similar results were found in Huh7 cells, indicating that Huh7 cells could accurately predict performance of the variants and wt-AAV5 in primary human hepatocytes. Other variants, such as MV1 and MV20, also showed increased transduction in human liver cells, but at slightly less efficacy when compared to MV50 and MV53. Mouse transduction studies unsurprisingly revealed that the AAV5 variants with increased human liver transduction did not drastically show increased transduction in mouse liver, which has been previously reported by many groups. In fact, many of the variants displayed de-targeting from mouse liver, which is again consistent with results from studies engineering human liver specific AAV capsids. Subsequent engineering of these AAV5 variants by combining mutations from different mutants did not further increase transduction efficacy, likely due to evolving separately and thus having conflicting mechanisms that impede infection. Further improvement of these capsids may be achieved by additional random mutagenesis and subsequent screening on human liver cells. Interestingly, highly mutated, and diverse AAV5 mutants were not selected for in this study, indicating that AAV5 may only tolerate small changes at once and thus any subsequent libraries generated may require minimal amounts of mutations and longer screening runs.

We also evaluated the seroreactivity of our variants using IVIG to represent the overall prevalence of neutralizing antibodies against the AAV Capsid in the human population. We found that our variants had neutralization curves that were quite similar to AAV5. The G257R mutation shifted the neutralization curve significantly to the left, indicating that more IVIG was

needed to neutralize MV18 when compared AAV5. The secondary mutations of MV50 and MV53 seemed to slightly increase the seroreactivity when compared with MV18, which is not surprising as these mutations likely enhance existing binding domains which leaves them more sensitive to IVIG disrupting binding. In particular, the shift from MV18 to MV53 is fairly large, which could be related to the conformational change of the VP1/VP2 common region during endosomal escape. One potential explanation is that the VP2/VP3 junction is more heavily influenced by steric interactions of neutralizing antibodies that bind nearby than other domains in the VP3 gene. However, even with the shifts of the seroreactivity curves, we believe that our mutants will have the same seroprevalence as AAV5. This is largely because all the mutations found from the selection process are all de novo mutations and do not exist in any other serotype (Figure 17). Coupled with the fact that the AAV5 is the most genetically divergent AAV serotype, it is extremely unlikely for any human to have been infected previously by these mutants and thus have developed neutralizing antibodies specifically targeting these de novo mutations. It is far more likely that the existing antibodies that already target AAV5 are interfering with the mutations ability to carry out their functions perhaps through steric hinderance of the region the mutation resides in. As such, we have concluded that the mutant AAV5 viruses are fairly consistent in terms of seroreactivity towards IVIG compared to AAV5, particularly compared to other serotypes such as AAV9, and therefore the overall prevalence of neutralizing factors in the human population against the mutants is likely to be very similar to AAV5.

Our engineered AAV5 capsids could potentially be used to improve current Hemophilia A and B therapies that utilize wt-AAV5 by increasing the expression levels of Factor VIII and XI at decreased doses. AAV5 based therapies typically require extremely high doses of AAV5,

which also add to the production cost of the treatments, rendering them less obtainable for potential patients. However, for liver diseases requiring higher transduction levels, the current capsids may need to be further modified via more directed evolution in order to reach therapeutic efficacy required. Further evolution of these mutants could also result in capsids that are even less seroreactive compared to wt-AAV5. For diseases requiring tropism to other areas such as the CNS or skeletal muscle, more drastic evolution of AAV5 is needed. In these cases, peptide insertion libraries, or targeted mutations of specific loops can be used, but more caution must be placed when determining the changes in seroreactivity.

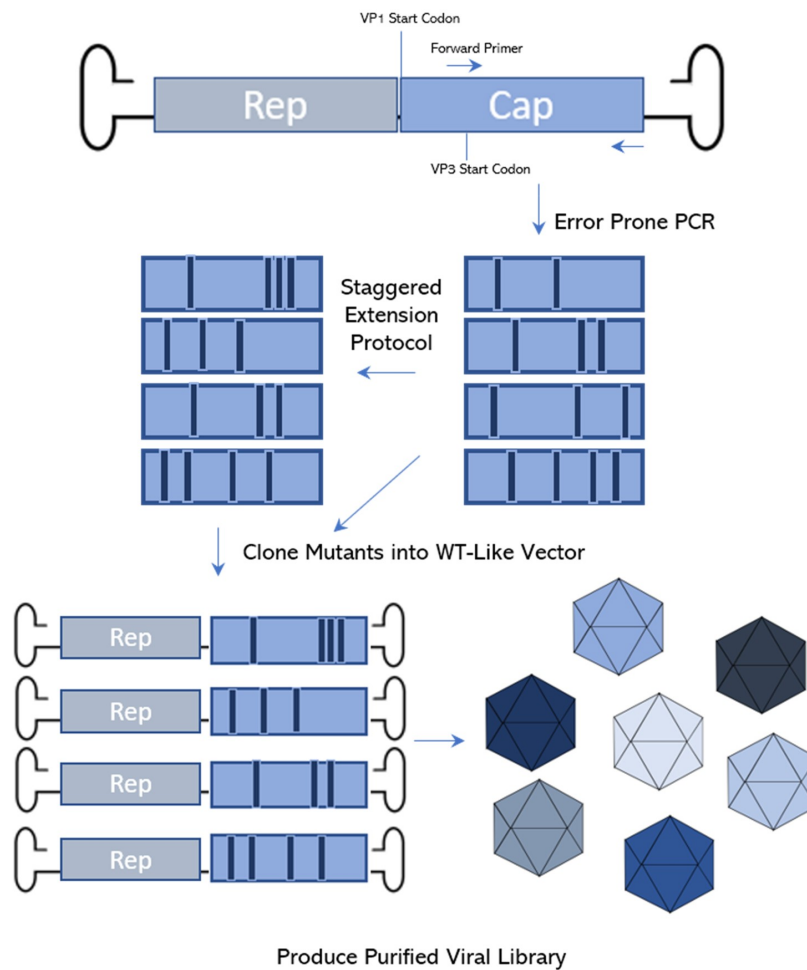


Figure 6: Directed Evolution of Adeno-Associated Virus Serotype 5 Capsid by Random Mutagenesis

Diagram illustrating the mutant AAV5 library creation process. WT-AAV5 capsid genes were PCR-amplified using an error prone polymerase and subsequently shuffled using the staggered extension protocol(stEP). The error prone and stEP amplicon libraries were pooled and cloned into a WT-like vector plasmid that could produce replicant competent AAV vectors. The plasmid library was then amplified and used to produce a purified AAV5 library using the cesium chloride density ultracentrifugation method.

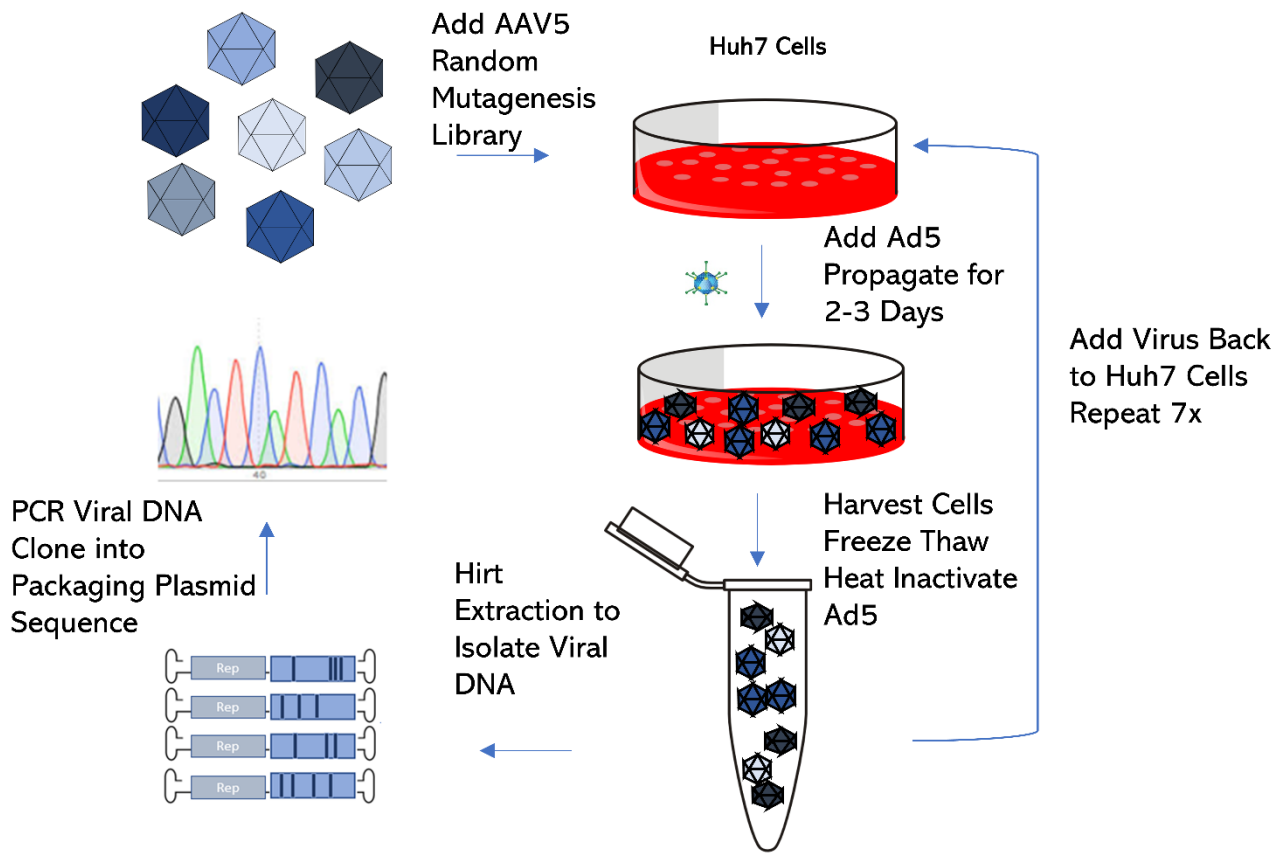


Figure 7: Sequential Screening of AAV5 Library in Huh7 Cells

Diagram depicting the screening process. Purified mutated AAV5 library was added to Huh7 cells which were coinfecting with wt-adenovirus type 5 to allow for replicative screening. Cells were harvested along with the supernatant and lysed using the freeze-thaw method. The lysate was centrifuged and the supernatant with the mutant AAV5 capsids was taken for the next round of screening. The screening process was repeated a total of 7 times. In the very last round of selection, the mutant AAV5 capsid DNA were extracted and amplified. After cloning into a packaging plasmid containing AAV2 rep, the plasmids were taken for amplification and screening.

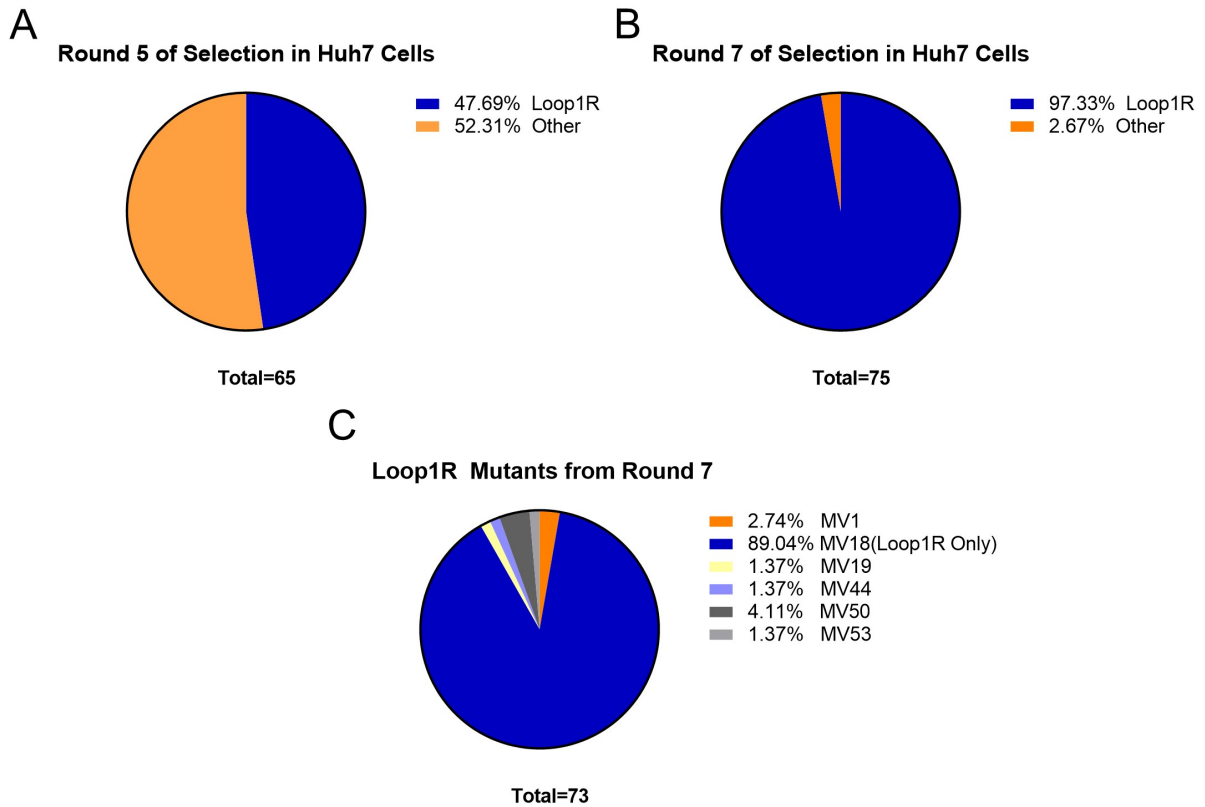
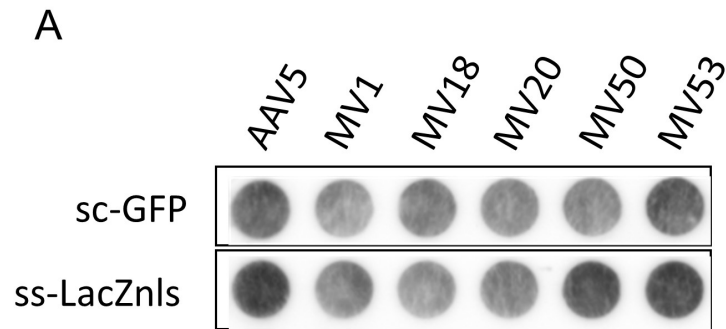


Figure 8: Sequencing of AAV5 Variants from 5th and 7th Rounds of Selection

(A) Percentage of sequenced AAV5 variants carrying the G257R mutation (Loop1R) from the fifth round of selection. (B) Percentage of sequenced AAV5 variants carrying the G257R mutation (Loop1R) from the seventh round of selection. (C) Breakdown of AAV5 variants carrying the the Loop1R mutation from the seventh round of selection. MV18 only contains the Loop1R mutation. All other mutants carry the Loop1R mutation plus an additional mutation.



B

AAV5 and MV Mutant Viral Titer

Virus	sc-GFP (vg/ml)	ss-LacZ (vg/ml)
AAV5	2.10E+12	3.78E+12
MV1	1.35E+12	1.46E+12
MV18	1.50E+12	1.96E+12
MV20	1.40E+12	2.36E+12
MV50	1.45E+12	3.54E+12
MV53	2.30E+12	3.76E+12

Figure 9: Production and Yield of Five Selected AAV5 Mutants

(A) DNA dotblot for the titer of each mutant and AAV5 for two versions of the virus, sc-GFP and ss-LacZnls. (B) Production titers for each capsid and each transgene version.

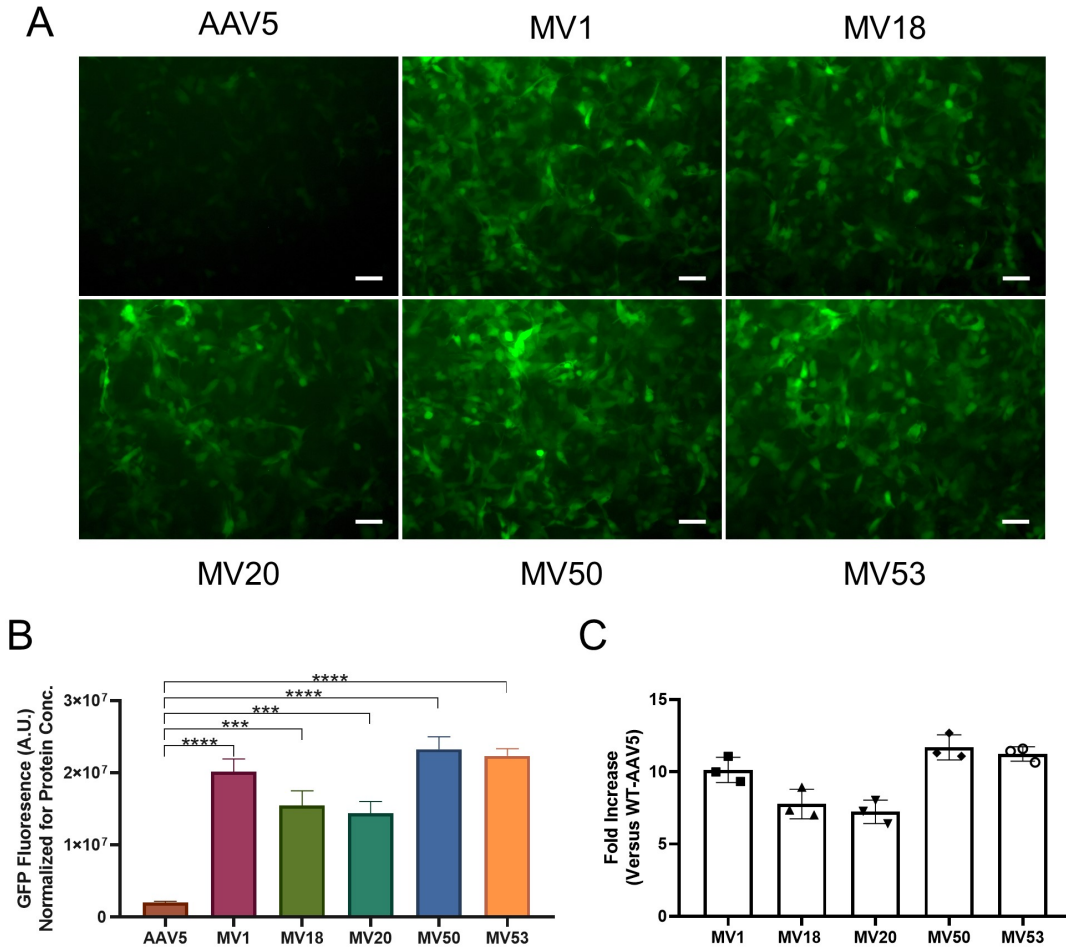


Figure 10: Evaluation of Huh7 Transduction for Select AAV5 Mutants

(A) Fluorescent imaging of Huh7 cells transduced with self-complementary GFP vectors with AAV5 and MV mutant capsid serotypes. Huh7 cells were transduced at a MOI of 1e5 vg/cell. Images were taken 96 hours after infection. Expression of GFP (green) indicates transduced cells. GFP expression was normalized by protein concentration. 10x magnification. Scale Bar: 100um. (B) Comparison of normalized GFP expression in Huh7 cells between AAV5 and MV mutants. Data are shown as mean values \pm SD. ***p<0.001; ****p<0.0001. (C) Fold increase in GFP expression of MV mutants versus wt-AAV5 in Huh7 cells.

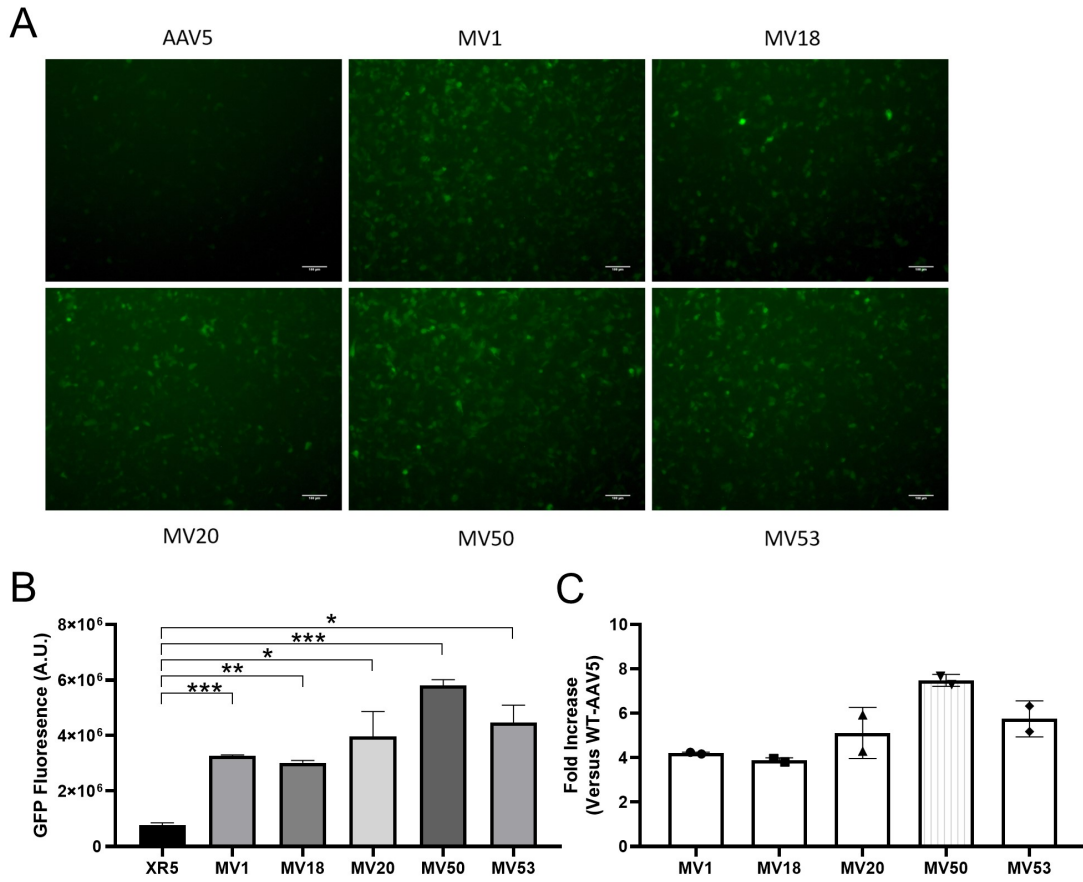


Figure 11: Evaluation of HepG2 Transduction for Select AAV5 Mutants

(A) Fluorescent imaging of HepG2 cells transduced with self-complementary GFP vectors with AAV5 and MV mutant capsid serotypes. HepG2 cells were transduced at a MOI of 1e5 vg/cell. Images were taken 96 hours after infection. Expression of GFP (green) indicates transduced cells. GFP expression was normalized by protein concentration. 10x magnification. Scale Bar: 100um. (B) Comparison of normalized GFP expression in Huh7 cells between AAV5 and MV mutants. Data are shown as mean values \pm SD. * $p < 0.05$; ** $p < 0.01$; *** $p < 0.0001$. (C) Fold increase in GFP expression of MV mutants versus wt-AAV5 in HepG2 cells.

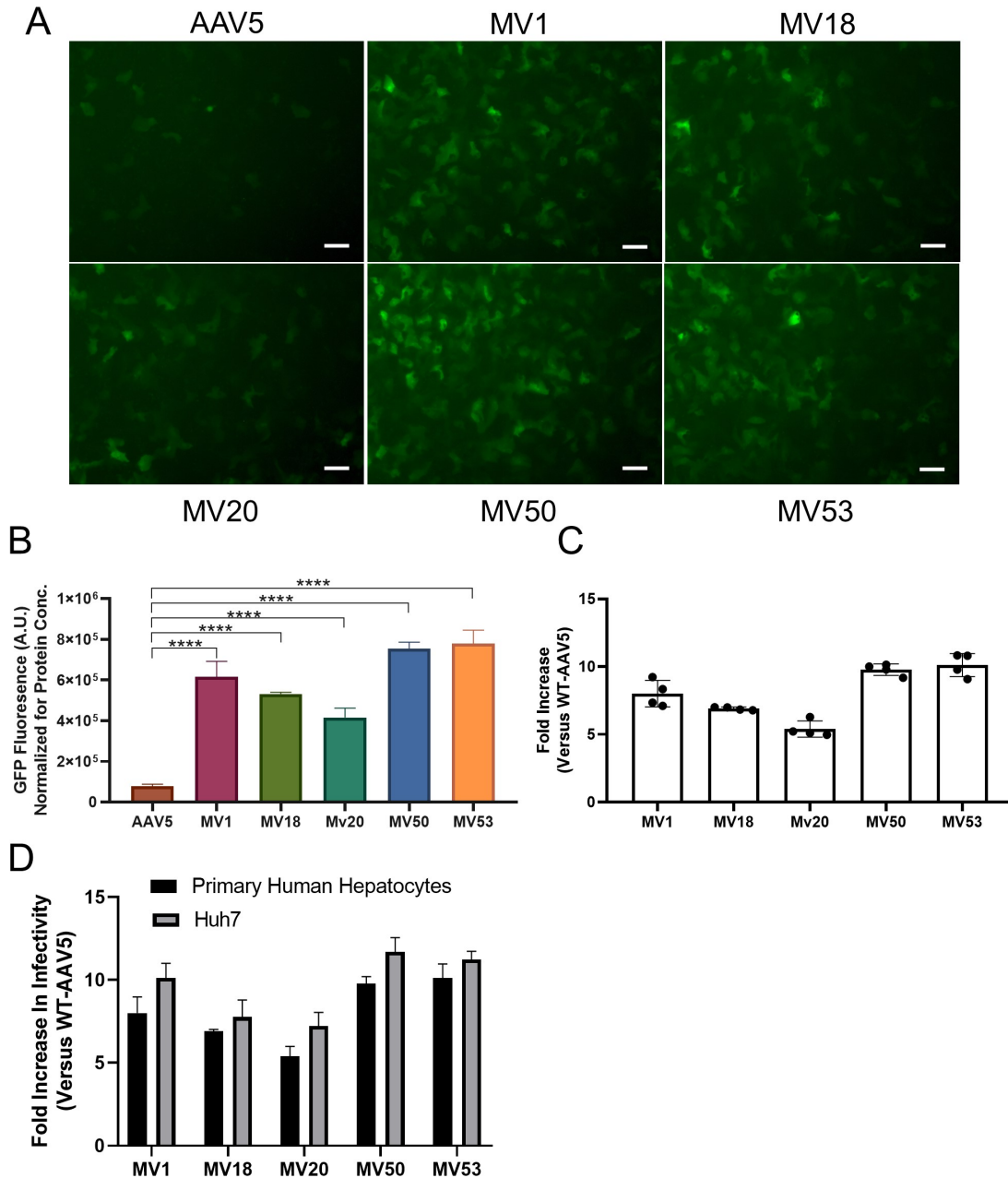


Figure 12: Evaluation of Primary Human Hepatocyte Transduction for Select AAV5 Mutants

(A) Fluorescent imaging of primary human hepatocytes (TRL) transduced with self-complementary GFP vectors with AAV5 and MV mutant capsid serotypes. Human hepatocytes were transduced at a MOI of 5e5vg/cell. Images were taken 96 hours after infection. Expression of GFP (green) indicates transduced cells. GFP expression was normalized by protein concentration. 10x magnification. Scale Bar: 100um. (B) Comparison of normalized GFP expression in primary human hepatocytes between AAV5 and MV mutants. Data are shown as mean values \pm SD. **** p <0.0001. (C) Fold increase in GFP expression of MV mutants versus wt-AAV5 in Huh7 cells. (D) Comparison of Fold Increases in GFP expression of MV mutants over wt-AAV5 in both Huh7 cells and primary human hepatocytes. Data are shown as mean values \pm SD.

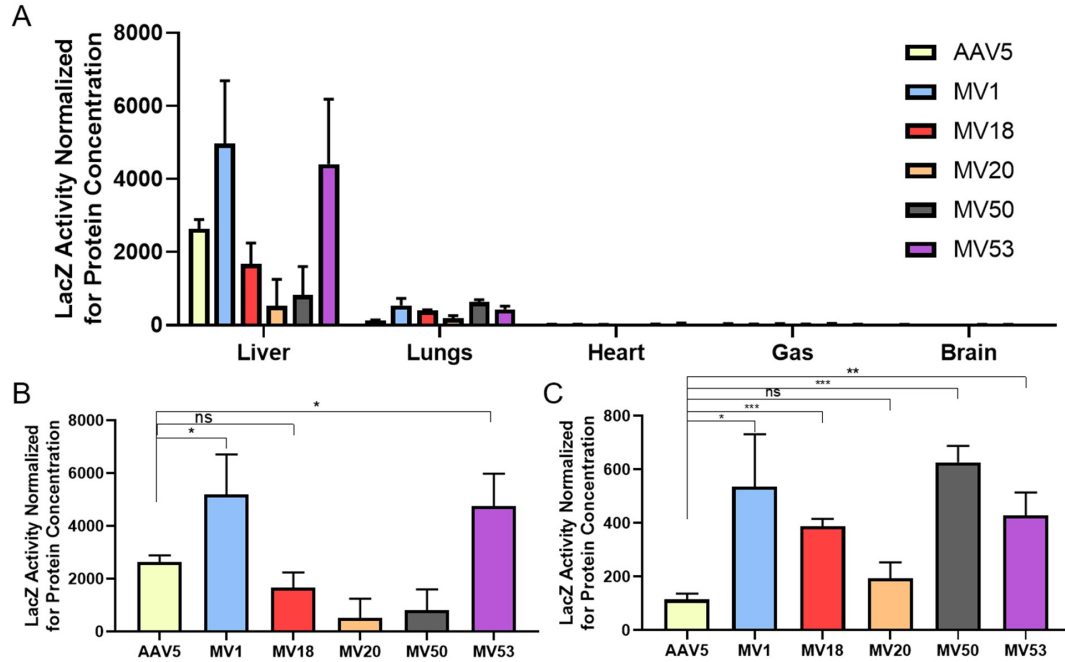


Figure 13: Comparison of Gene Transfer Efficiency in C57/BL6 Mice using a LacZ Vector

(A) Quantification of B-galactosidase(LacZ) activity in homogenized tissue samples of various organs in 8 week old C57/BL6 mice transduced by AAV5-CB-LacZnls, MV1-CB-LacZnls, MV18-CB-LacZnls, MV20-CB-LacZnls, MV50-CB-LacZnls, and MV53-CB-LacZnls. Each mouse was injected with 1×10^{12} vg via tail-vein injection. Tissues were collected 4 weeks post injection. Tissue samples were homogenized and assayed for LacZ activity. LacZ activity was normalized by protein concentrations for each tissue sample. A total of five organs were quantitated for LacZ activity: the liver, lungs, heart, gastrocnemius (GAS), and brain. Data are shown as mean values \pm SD. (B) Quantification of LacZ activity in homogenized mouse liver tissue. Data are shown as mean values \pm SD. * $p < 0.05$. (C) Quantification of LacZ activity in homogenized mouse lung tissue. Data are shown as mean values \pm SD. * $p < 0.05$. ** $p < 0.01$. *** $p < 0.001$.

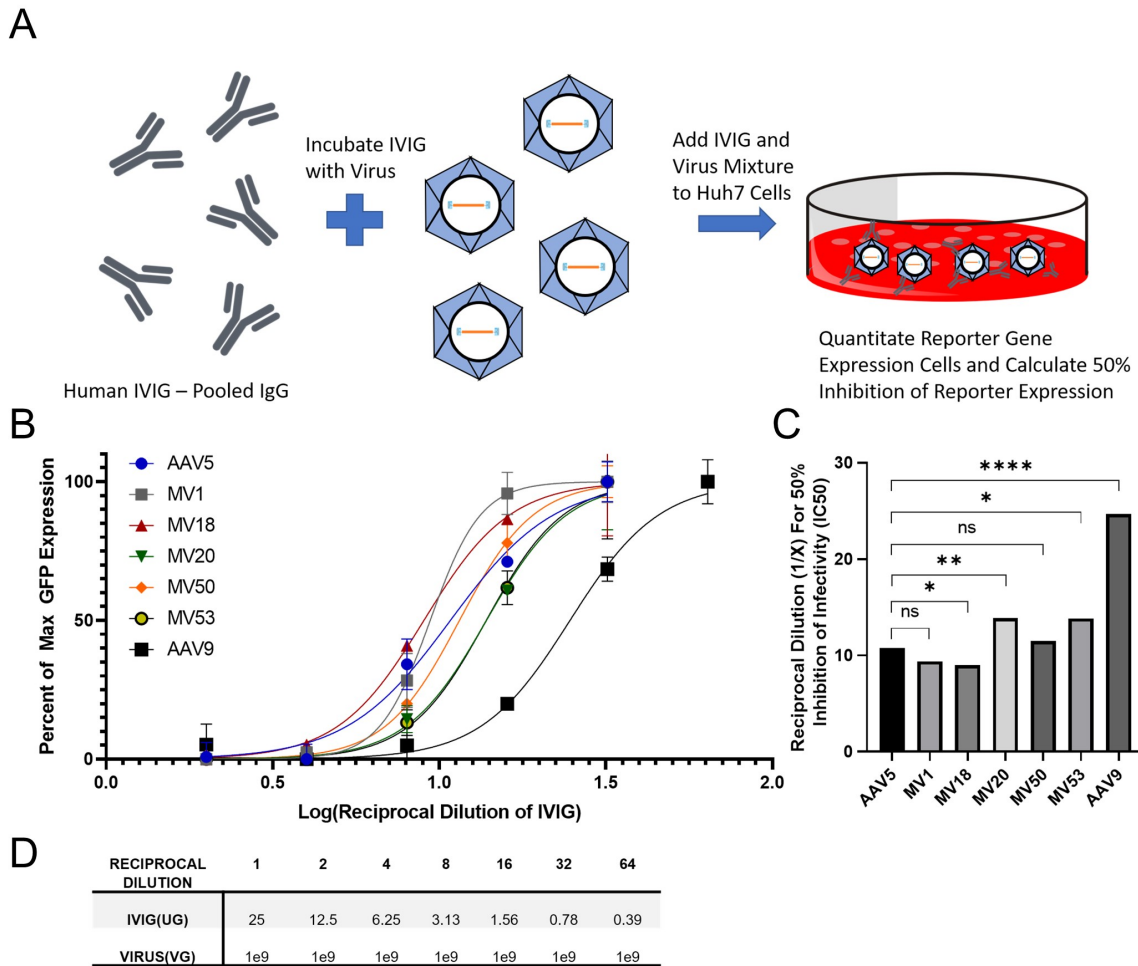


Figure 14. Seroreactivity of AAV5 and MV mutants using an IVIG Based Assay

(A) Diagram depicting IVIG assay. Virus is incubated with IVIG and added to Huh7 Cells that are co-infected with wt-adenovirus type 5. After 48 hours reporter gene expression is measured. (B) AAV Neutralization Assay using pooled human immunoglobulins from thousands of donors (IVIG Carimune NF, ZLB Behring) to assess seroreactivity. MV mutants were compared to AAV5 and AAV9 in their ability to resist neutralization by IVIG. Each capsid serotype containing sc-GFP was incubated with reciprocal dilutions of IVIG and added to Huh7 cells. After 72 hours, the GFP expression for each reciprocal dilution was quantified and compared to GFP expression of an infection control without the presence of IVIG. The percentage of max *gfp* expression at each reciprocal dilution for each virus was used to generate curves that represented the seroreactivity of each virus. Graphpad Prism 8 was used to curve fit the data. Serotypes with curves further to the right indicate less IVIG is needed to neutralize the virus. Serotypes with curves further to the left indicate more IVIG is needed to neutralize the virus. Plotted data points are shown as mean values \pm SD. (C) Reciprocal dilution at which 50% inhibition is achieved was calculated from the best fit curves for each capsid. Extra sum of squares F test was used to compare the best fit curves for each capsid and determine whether one capsid is more/less seroreactive compared to AAV5. * $p < 0.05$; ** $p < 0.01$; *** $p < 0.0001$. (D) Amount of IVIG and virus used for each reciprocal dilution.

CHAPTER 3

ANALYSIS OF MUTATIONS IN EVOLVED AAV5 CAPSIDS²

3.1 Overview

Understanding the functional differences of each mutation from the screened AAV5 variants is important for further engineering of these viruses. Sequence analysis revealed that each mutation in the library is a de novo mutation that is not found in the equivalent site in other AAV serotypes. Additionally, the mutations are generally spread out evenly across the AAV5 VP3 gene, with one mutation present in the VP1/VP2 common region. Four out of the five mutants contain the G257R, or Loop1R, mutation that has been previously been shown to greatly enhance human liver transduction. Three of the four mutants that carry the Loop1R mutation also contain an additional mutation that slightly enhances transduction compared to the Loop1R mutation alone. The variants that were screened were not highly mutated; the highest number of mutations in an individual mutant was three mutations. Structural analysis combined with binding/internalization assays revealed insights into locations of mutations and possible functions. The Loop1R mutation was found to increase both binding and internalization, whereas most other mutations in the library only increased binding. There was one mutation that did not affect binding or internalization, but likely was enhancing uncoating of the virus. Mutations were

² This chapter includes a manuscript in submission: Qian R., Li J., Xiao X. *Directed Evolution of AAV Serotype 5 for Increased Liver Transduction and Retention of Low Humoral Seroreactivity.*

combined to understand whether multiple mutation increasing binding would affect transduction in human liver cells. Only small differences were noted in Huh7 cells and primary human hepatocytes, indicating that multiple mutations combined did not significantly enhance transduction. Finally, the Loop1R mutation was tested in other serotypes, and found to have to have the opposite effect which reduced systemic transduction.

3.2 Introduction

The general process in which AAV infects cells is well understood as the infection pathway of AAV is similar to other widely studied viruses. Circulating AAV binds to a receptor on the cell surface, internalizes to the late endosome, escapes from the endosome, traffics to into the nucleus, and finally uncoats to allow expression of the transgene.⁶⁷ Only some of the mechanisms and functions of each domain in the AAV capsid and their interactions with each step of the viral infection pathway are currently known. Recent efforts have established important new factors that are critical for AAV internalization and endosomal escape.^{88, 89, 92} However, not all serotypes use the same factors in the same manner, indicating that each serotype needs to be studied separately. Past studies have revealed a few glycan or protein receptors for each serotype, but often the exact binding domains are not determined. This leads to challenges in rationally engineering AAV variants, as often what is thought as a logical idea does not work in the context of the AAV capsid. The divergence of AAV5 from other AAV serotypes adds to the difficulty of rationally engineering the AAV5 capsid. Therefore, further studies into the important domains that govern AAV5 viral entry is critical. Studies of the AAV5 capsid have revealed that AAV5 binds with at least three different receptors/glycans on the cell surface. Platelet Derived Growth Factor Receptor(PDGFR), AAV receptor (AAVR), and α -2,3-N-linked sialic acid are receptors that have all been described by others to be essential for

transduction.^{70, 80, 85} However, the exact residues that influence binding to these receptors is for the most part unknown.

Directed evolution of AAV5 using random mutagenesis can provide valuable data for understanding the functions of different domains in the AAV5 capsid. To further engineer the MV mutants, it is important to understand the general mechanism in which each mutation increases transduction efficiency, and which part of the viral infection pathway it plays a role in. The current study seeks to understand the various mutations in the MV mutants and the roles they play in enhancing liver transduction through sequence analysis, structure analysis, and binding/internalization assays. Additionally, the study seeks to understand if combinations of mutations found in the screened AAV5 mutants can further enhance transduction, and if the Loop1R mutation can affect other serotypes. Our results demonstrated that most of the mutations from the screened library affect binding, and that when combined they provide minimal increases in transduction over the original MV mutants. Only one mutation, the Loop1R mutation, affected both binding and internalization, and was found to be the critical mutation driving increased transduction in human liver cells. The Loop1R mutation does not work on other serotypes; in particular, an AAV9 capsid with the Loop1R mutation was de-targeted from many of the organs that wt-AAV9 readily infects. The insights gained from this study will allow for further rational engineering of the evolved AAV5 mutants further enhancing their liver transduction.

3.3 Materials and Methods

Sequence and Structure Analysis of AAV5 Variant Capsid Genes

DNA and Protein sequences of mutant AAV5 capsid genes screened in Huh7 cells were identified and aligned with Sequencher, AlignX and Clustal X. Amino acid mutations for each

variant were false-color mapped on to the AAV5 VP3 protein structure 3NTT using PyMol v2.3.0. 60mer AAV5 capsid structures were obtained by using 3NTT and viperdb to generate a 60mer consisting of 60 AAV5 VP3 proteins. The mutations from variant AAV5 capsids were false color mapped onto the 60mer structure.

AAV Library and Vector Production

Purified AAV vectors were produced via the triple transfection and cesium chloride density ultracentrifugation methods. Briefly, HEK293 cells were transfected with a helper plasmid, a self-complementary GFP (sc-GFP) or single stranded LacZ-nls vector plasmid, and a packaging plasmid containing capsid gene and an AAV2 rep gene. Cells were harvested 72 hours post transfection and isolated by centrifugation. The media was collected and stored while the cell pellet was resuspended and subjected to three freeze thaw cycles. The resulting cell lysate was incubated with DnaseI and RnaseA at 37C and centrifuged and the supernatant was collected. The virus from the supernatant and the media were then concentrated by PEG precipitation followed by two rounds of cesium chloride (CsCl) density ultracentrifugation. CsCl fractions containing virus were determined by DNA dotblot and combined and dialyzed using 5% sorbitol in PBS. Dialyzed virus preparations were again titered using DNA dot blot with a probe specific to reporter gene. All viruses that were tested were titered in the same dotblot to allow consistent measurement of viral titers.

Binding and Internalization Assay of AAV Vectors in Huh7 Cells

Binding of the AAV capsid to the surface of Huh7 cells was determined by incubating 2e3vg/cell of CB-LacZnls AAV vector with pre-cooled Huh7 Cells at 4C for 30min. Then, the cells were washed with cold PBS three times to wash away any unbound vector. Cells were

collected and resuspended in PBS. Total DNA was extracted using the DNeasy Blood and Tissue Kit (Qiagen, Hilden, Germany) and eluted with molecular grade water. The number of vector copies was determined in each sample via absolute qPCR quantification using primers and TaqMan probe specifically recognizing the CB-promoter sequence (Sigma Aldrich, St. Louis). The number of vector genomes was normalized to the number of endogenous glucagon gene copies. Internalization assay was performed similar to the binding assay, but instead allowing the bound virus to internalize at 37C for 1 hour. Cells were incubated with trypsin for 5 min at 37C to allow any un-internalized virus to be digested. After washing with PBS three times, total DNA was extracted from cells and eluted with molecular grade water. Vector copies was determined exactly the same as described before. Assays were performed on a 7300 Real-Time PCR system (Applied Biosystems) using GoTaq PCR Master Mix (Promega). The primers and probes used are as follows: CB-F: 5'-GTATGTTCCCATAGTAACGCCAATAG-3'; CB-R: 5'-GGCGTACTTGGCATATGATACT-3'; CB Probe: 5'-FAM-TCAATGGGTGGAGTATTTA-MGB-3'; Glucagon-F: 5'-AAGGGACCTTTACCAGTGATGTG-3'; Glucagon-R: 5'-ACTTACTCTCGCCTTCCTCGG-3'; Glucagon Probe: 5'-FAMCAGCAAAGGAATTCA-MGB-3'.

Site-directed Mutagenesis for Combining Mutations from Different Variants

Mutations were combined onto one capsid gene using site directed mutagenesis. A primer containing the mutation was used with a primer that covered half the ampicillin gene to amplify half of the MV mutant packaging plasmid. A primer set corresponding to the other half of the plasmid was also used to amplify the opposing half of the plasmid. The two PCR amplicons were purified and digested with DPN1 (NEB, Ipswich, MA) and purified using gel purification via QIAquick Gel Extraction Kit (Qiagen, Hilden, Germany). The purified fragments

were ligated together using blunt end ligation and transformed into DH10B competent cells. Transformed bacteria was then spread on an agar plate and allowed to grow overnight. Individual colonies were picked for DNA amplification and extraction. Extracted plasmids were then sent for sequencing to confirm proper incorporation of the mutations. Primers were used as follows: F417L MV1-F: TTCCACTCCAGCCTCGCTCCCAGT; F417L MV1-R: GGGCACCTCCTCAAAGTTGTA; A579T MV20-F: GACCGGCACGTACAACCTCCA; A579T MV20-R: GCGGGGGTAGTGGTGGAGC; S705G MV50-F: CACCGGGGAATACAGAAGCACC; S705G MV50-R: CCGTCCGGGGCAAAGTCCAC; Q179R MV53-F: CTGCGAATCCCAGCCCAACCA; Q179R MV53-R: CTGCTGGGATCCGCTGGGTC; AMP-R: ACTCACCAGTCACAGAAAAGCATC; AMP-F: ACTCAACCAAGTCATTCTGAGAATAG

Transduction of Human Liver Cancer Cells by AAV Vectors

Variant AAV5 vectors were used to packaged sc-GFP reporter genes for comparison to wt-AAV5. Huh7 cells in 12 well plates were infected with AAV5 and mutant self-complementary(sc)-GFP encoding viruses at a MOI of 100,000 viral genomes(vg) per cell and co-infected with 5000 vg/cell of wt-ad5. Seventy-two hours after infection, cells were taken for fluorescent imaging and subsequent GFP quantification using the Fluorometric GFP Quantification Kit (Cell BioLabs, San Diego, CA). GFP activity was normalized by protein concentration as measured by Pierce BCA Protein Assay Kit (ThermoFisher Scientific, Waltham, MA).

Transduction of Primary Human Hepatocytes by AAV Vectors

Primary human hepatocytes (TRL HUM4037, Triangle Research Labs, NC) were cultured according to vendor's instructions. In brief, cells were thawed and plated at 2.5×10^5 cells per well in collagen coated 24 well plates (BioCoat Collagen I 24 well plates, Corning, Corning, NY). The next day, the primary human hepatocytes were infected with purified sc-GFP vectors at a MOI of 500,000 vg per cell. Media was changed 48 hours after infection, and once daily afterwards. Ninety-six hours post infection, cells were taken for fluorescent imaging and subsequent GFP quantification using the Fluorometric GFP Quantification Kit from Cell Bio Labs (San Diego, CA). GFP activity was normalized by protein concentration as measured by Pierce BCA Protein Assay Kit (ThermoFisher Scientific, Waltham, MA).

Tissue Tropism of AAV Vectors in Mice after Systemic Administration

C57/BL6J mice were maintained in a 12-hr:12-hr light: dark artificial light cycle (0700-1900) at a temperature of 20C and a humidity of $55 \pm 5\%$. All animal protocols were approved by the University of North Carolina Animal Care and Use Committee. The mutant AAV5 capsid genes were used to package CB-LacZnl reporter gene which expresses B-galactosidase with a nuclear localization signal or self-complementary GFP and compared to wt-AAV5. LacZ vectors were administered to eight-week-old male C57BL/6J mice by intravenous tail vein injection at a dose of 1×10^{12} vg per mouse. GFP vectors were administered at 1×10^{11} vg per mouse. After three weeks, the mice were sacrificed, and tissues were collected, and flash frozen in liquid nitrogen cooled 2-methylbutane. Tissues were stored at -80C until ready for use. GFP injected mouse tissue samples were sectioned in to 10um sections and imaged for GFP using a fluorescent microscope. LacZ mouse tissues were homogenized in lysis buffer from the Galacto-Star LacZ Assay Kit (Applied BioSystems, Foster City, CA) and measured for protein concentration using

the Pierce BCA Protein Assay Kit (Thermo Fisher, Waltham, MA). Samples were diluted to similar protein concentrations. B-galactosidase enzyme activity in homogenized tissue lysates was measured using the Galacto-Star LacZ Assay Kit and readings were normalized by protein concentration.

Statistics

Statistical analyses were conducted with GraphPad Prism 8. All statistical analyses were justified as appropriate and p-values <0.05 were considered statistically significant. For all statistical tests performed, intra-assay variation fell within the expected range and the variance across groups was similar. Comparison of experimental values from two groups were assessed using a Student's unpaired two-tailed t test.

3.4 Results

Sequence alignment of the five variants with wt-AAV5 revealed that the selected mutations were primarily spread across the AAV5 VP3 gene, with only one variant, MV53, containing a mutation in the unique VP2 region (Figures 15 and 19A). Four (MV1, MV18, MV50, MV53) out of the five variants carried the Loop1R mutation, of which three mutants (MV1, MV50, MV53) were likely evolutionarily derived from a parental variant (MV18) that carried only the Loop1R mutation (Figures 16 and 19A). MV1, MV50, and MV53 sequences were not found in the sequencing data from the 5th round of selection, indicating that these variants may have arisen later in the selection process and hence derived from MV18. Structural analysis using false-color mapping onto the crystal structure of AAV5 revealed additional insights into each mutation's location and potential function. The primary Loop1R mutation, G257R, is located in a surface exposed part of the VR-I region of the AAV5 VP1 protein

(Figures 18, 19B). MV1 contains a secondary mutation (F417L) that is buried in the interior of the capsid in a fairly conserved region across AAV serotypes that likely does not play a role in altering binding of AAV5 (Figures 18, 19B). MV50 contains a secondary mutation (S705G) near the VR IX (Loop 9) region and is present on the surface of the capsid as determined by false-color mapping (Figures 18, 19B). This region has also been characterized to be involved with receptor binding and close to known antigenic sites on other serotypes.⁶³ Interestingly, MV53's secondary mutation could not be analyzed by structural analysis as the AAV5 VP2 unique protein and the N terminus of the AAV5 VP3 protein could not be resolved by x-ray crystallography (Figures 19B).⁵⁹ The only variant to not carry the Loop1R mutation is MV20, which instead contains three different amino acid mutations versus wt-AAV5 that are not found in any of the other variants (Figures 18, 19B). Only one of the three mutations (A579T) is located in a surface exposed region, VR VIII, which has been shown to be involved in binding sialic acid for AAV5 (Figures 18, 19B).¹⁹³ The remaining two mutations are located in regions that likely do not affect binding but could have potential implications in capsid stability.

Elucidating Potential Mechanisms for AAV5 Mutations

We next investigated our variants for changes in binding and internalization in order to understand how each mutation in each variant contributed to enhancing human liver tropism. We first probed the changes between MV18 and AAV5 to determine effect of the G257R mutation. Binding assays performed by incubating virus with Huh7 cells at 4C and quantitating bound vector genomes via RT-PCR revealed that the G257R mutation increased binding to the cell surface by a factor of 2.2 when compared to WT-AAV5 (Figure 20A). An internalization assay using the same procedure as the binding assay with an additional steps of incubation at 37C for an hour and digestion with trypsin showed that the percentage of bound virions that were

internalized was increased by 3.1-fold for the Loop1 mutation versus WT-AAV5 (Figure 20C). The internalization assay additionally indicated an overall 7 times difference in total virus internalized between AAV5 and the MV18, which was consistent with the difference in GFP expression reported previously (Figure 20B). The increase in internalized virus is likely a result of the increased binding, but whether the mutation is enhancing an existing binding domain or changing receptors is unknown.

Subsequent comparison of MV18 against MV1, MV50, and MV53 allowed us to isolate the effects of the secondary mutations and provided more insight into their potential functions. Using structural analysis, we previously speculated that the F417L mutation was unlikely to change receptor binding, viral entry, and endosomal escape due to its location in the capsid. Binding and internalization assays corroborated the theory as there was no significant differences in binding or internalization of the virus when the F417L mutation was added together with the Loop1 mutation (Figures 20D-F). However, transduction assays revealed a clear increase in infectivity for MV1 over MV18; as such, it is likely that the F417 mutation is affecting a process further downstream such as uncoating of the capsid that cannot be properly detected by an internalization assay that detects all viral genomes within the cell. Interestingly, MV1 has noticeably lower yield compared to the rest of the variants, adding evidence for the theory that the F417L mutation decreases the stability of the capsid which could facilitate uncoating in the nucleus of the cells (Figure 9A and 9B).

Structural analysis of MV50 revealed that the S705G mutation was likely on the surface of the capsid and potentially had implications in altering receptor binding. A binding assay comparing MV18 and MV50 confirmed that the S705G mutation further increased binding to the cell surface around 2-fold over the Loop1 mutation alone (Figure 20D). Interestingly, the

percentage of bound virions that were internalized decreased significantly when comparing MV50 and MV18, indicating that the increased binding did not result in an increased percentage of internalized virus (Figure 20F). Additionally, no difference between overall amount of virus internalized was observed between MV50 and MV18, signaling that the Loop1 mutation and its receptor are likely the main driver for the increase in the bound virus being internalized and increases in binding through the S705G mutation does not affect the internalization rate (Figure 20E). Interestingly, similar results were found for MV53, where binding to the cell was increased by the Q179R mutation, but the percentage of bound virions decreased significantly (Figure 20D and 20F). This suggests that MV53 is similar to MV50 in that the Q179R and S705G mutations likely influence binding to an attachment factor on the cell surface but have negligible influence on internalization when compared to the G257R mutation. The lack of a difference in overall internalized virus between MV18 and MV50/MV53 may also be a result of the static nature of the binding assay where receptor turnover and subsequent binding of new virions is not considered. Additionally, these data also show that although the VP2/VP3 junction near the five-fold axis is not resolvable by x-ray crystallography, its structure is likely on or near the surface of the capsid and plays a role in binding of the virion to the cell.

Finally, we compared the only non-loop1 mutant, MV20 to MV18. Interestingly, MV20 exhibited binding comparable to MV18, roughly a 2.2-fold increase when compared to AAV5. However, the A579T mutation does not significantly increase the percentage of bound virions that are internalized when compared to AAV5 (Figure 20A and 20C). As such, the A579T mutation seems to be increasing binding, but is not increasing internalization when compared to the Loop1 mutation. This indicates that affinity for receptors that are engaged by MV18 and MV20 are different, and perhaps for MV20 the increase in binding is against an attachment

factor such as sialic acid, but still relies on a different receptor for internalization and as such results in lower internalization when compared to the Loop1 mutation.

Combination of Mutations from Multiple AAV5 Variants

We combined mutations from multiple variants to test whether liver transduction could be further enhanced. Combination variants with the F417L mutation had extremely low yields, indicating that the capsids were extremely unstable with the F417L mutation. This lent extra credence to the theory that F417L decreased the stability of the capsid. In the end, two combinations were tested, MV50 with a A579T mutation (MV50.T) and MV50.T plus the Q179R mutation (MV50.53T) (Figure 21B). In Huh7 cells, both variants were only marginally better than MV50, indicating that addition of extra mutations from other variants did not contribute much to increased liver tropism (Figures 21A and 21C). Interestingly, both variants were slightly worse than their base variant MV50 in primary hepatocytes, suggesting that combination of mutations from the library was counterproductive in primary human hepatocytes, perhaps due to competition for receptor binding (Figures 21A and 21D). Additionally, yield of the viruses decreased as a result of combination (Data not shown). However, these combination variants could have drastically different tropisms in an *in vivo* due to off targeting of various organs, but that remains to be determined. As such, we concluded that the original variants of MV50 and MV53 were the best possible candidates for an AAV5 variant with enhanced liver transduction or for further evolution.

Loop1R Mutation in Other AAV Serotypes

We were interested in determining whether the Loop1R mutation would have an effect in other AAV serotypes. We introduced the Loop1R mutation into AAV6, AAV7, AAV8, and

AAV9 capsids at the equivalent amino acid for each serotype compared to AAV5. Loop1R versions of each serotype were packaged with a sc-GFP vector and tested in Huh7 cells. Interestingly, for each serotype, the wild type capsid was significantly better at transducing Huh7 cells when compared to the Loop1R versions (Figure 22A). Very little GFP expression was observed for the Loop1R viruses, indicating that the Loop1R mutation had adversely affected infectivity in Huh7 cells in contrast to increasing infectivity for AAV5. This is not surprising due to the significant differences in sequence in the Loop1 region of AAV5 versus the same region in other serotypes. However, a significant decrease in liver targeting is potentially advantageous as there is a possibility of the virus retargeting to other organs. Additionally, de-targeting the capsids from the liver can make the capsid more specific, potentially decreasing any unwanted side-effects as well as minimizing immune responses to capsid.

Therefore, we decided to test the Loop1R version of AAV9 due to its systemic delivery to the liver, skeletal muscle, heart, and CNS. C57/BL6 mice were i.v. injected (1e11vg) with sc-GFP vectors packaged by AAV9 and AAV9 Loop1R. Four weeks after vector administration, mice were sacrificed and their heart, liver, gastrocnemius, and brain were harvested and flash frozen. Tissues were sectioned and taken for fluorescent imaging to determine differences in GFP expression between AAV9 and AAV9 Loop1R. Fluorescent imaging of liver, heart, and gastrocnemius sections revealed decreases in GFP expression in mice injected with the AAV9 Loop1R GFP vectors when compared to mice injected with AAV9 GFP vectors (Figure 22B). AAV9 Loop1R seemed to be almost completely de-targeted from mouse liver and had drastically lower transduction in mouse heart. No obvious differences were seen in the gastrocnemius images between AAV9 and AAV9Loop1R, perhaps indicating that transduction in the gastrocnemius was not as affected by the Loop1R mutation compared to other organs. No

differences in the brain were detectable through fluorescent imaging (data not shown). In order to confirm the results from the gastrocnemius and brain, we tested lacZ versions of AAV9 and AAV9 Loop1R in mice to allow for quantification of LacZ activity using a more sensitive chemiluminescence assay. C57/BL6 mice were administered 1×10^{12} vg of AAV9-CB-LacZnls or AAV9Loop1R-CB-LacZnls via tail vein injections. Quantification of LacZ activity in homogenized brain tissue samples revealed essentially a completely de-targeting of AAV9 Loop1R from mouse brain that was no different from PBS injected mice (Figure 22C). We were also able to determine that AAV9 Loop1R did in fact decrease (2-fold) transduction in the gastrocnemius, but less so when compared to other organs. Overall, AAV9 Loop1R is significantly detargeted from mouse liver, brain, and heart, but less so from gastrocnemius making it an interesting vector that could be utilized for specific skeletal muscle delivery.

3.5 Discussion

Sequence and structural analysis of the MV mutants revealed interesting insights into the directed evolution process and the functionality of each mutation. Interestingly, it appeared that our best performing mutants, MV1, MV50, and MV53, were all evolved from MV18. Sequencing data from the 5th and 7th rounds indicated MV1, MV50, and MV53 were only present in the 7th round of selection where as MV18 was present at large quantities in both. Additionally, MV1, MV50, and MV53 all carry a secondary mutation along with the Loop1R mutation, suggesting that these viruses arose from natural evolution within the selection system and were not originally part of the random AAV5 library. This is not surprising as the DNA replication system of cell lines can induce mutations into the sequence of the AAV5 capsid as it replicates, demonstrating another benefit of replication competent screening. However, this process likely requires many rounds of selection as the original library first must be screened for

variants with increased transduction before subsequent mutation and evolution of the screened variants can occur. The screened variants must make up a large portion of the AAV sequences within the system before any natural evolution can occur. Another interesting observation was that the highly mutated sequences in the library were not selected for, which was not surprising as other studies have typically reported that optimal mutation numbers range from 2-5 mutations per 1000 base pairs (bp).¹⁹⁴ As such, we could further improve the directed evolution process by introducing an iterative element by producing a library with few mutations and screening it for a three rounds of selection before inducing more mutations in the newly screened mutants.

All three of the best performing variants (MV1, MV50, MV53) shared a G257R mutation in the VRI or Loop1 region, which we described as the primary mutation that was driving the overall increase in infectivity in human liver cells. Our results demonstrated that the G257R mutation increased receptor binding and internalization but could not concretely establish which aspect of internalization was affected as the internalization assay only measured virus that entered the cell and did not account for location within the cell. The location of the Loop1 mutation in the VRI region suggests that it should not have any purpose in endosomal escape as the VP1u region of the VP1 protein is responsible for escaping the endosome.⁴⁴ Additionally, because the fold change in overall amount of virus internalized and the fold change in GFP expression are consistent, we believe it suggests that that change in GFP expression is primarily due to an increase in overall amount of virus entering the cell, and less likely due increases in endosomal escape or cellular trafficking. For these reasons, we believe that the Loop1 mutation is primarily responsible for increasing binding to a receptor that internalizes more quickly compared to other receptors used by AAV5, thereby increasing the overall amount and rate of virus internalized. Others have found that the VRI region is heavily involved with binding of the

AAV receptor (AAVR) for most serotypes except AAV5.⁸⁵⁻⁸⁸ As such, it is not clear what receptors, if any, the VRI region of AAV5 interacts with. Thus, we are not able to conclude if the G257R mutation is enhancing binding to an existing receptor such as AAVR or allowing binding of a different receptor that AAV5 previously did not target.

The F417L mutation found in MV1 is particularly interesting because the binding and internalization data suggest that the mutation does not affect receptor binding and entry. Due to decreases in yield, and its location in the capsid, we believe that this mutation is decreasing the stability of the capsid which in turn is leading to more efficient uncoating. Uncoating has been reported to be the limiting step of gene expression in hepatocytes, and thus a potential increase in uncoating efficiency could lead to higher gene expression.¹⁹⁵ Studies have also shown AAV5 to be the most thermostable serotype, which prompts question on whether its stability is negatively affecting uncoating.¹⁹⁶ The other mutations found in the AAV5 variants are all surface mutations and seem to significantly affect binding of the virus to the cell membrane. A similar mutation to A579T in MV20 has been reported before in a study detailing a chimeric AAV5 mutant (A581T) with enhanced human lung transduction.^{197, 198} In their study and subsequent studies, they noted that their mutant with a A581T mutation played a role in sialic acid recognition and binding, which could be a potential mechanism for our A579T mutation.¹⁹⁸ Interestingly, MV20 did not show enhanced transduction capabilities in mouse lung, which mirrors their finding that the A581T mutation alone does not affect lung transduction significantly. The S705G and Q179R mutations that are present in MV50 and MV53, respectively, seem to primarily affect binding to receptors that are not essential for internalization. It is likely that they are binding attachment factors and enhance transduction by allowing more association of the capsid with the cell membrane. The Q179R mutation is particularly interesting as it lies in the unique VP2 gene of

AAV5, meaning that in a 60mer capsid the presence of this mutation is significantly lower than a mutation that resides in the VP3 gene. Yet, the Q179R mutation is still able to significantly influence binding at comparable levels to the S705G mutation. The location is also of great interest as the VP1/VP2 common region and the first 15 amino acid residues of the VP3 region for AAV5 were not resolvable by x-ray crystallography, so the conformation of these regions is unknown. There has been some speculation that the junction of the VP1/VP2 common region and the N terminus of the VP3 region, or VP2/VP3 junction, is near the surface of the capsid. Our data comparing MV18 and MV53 with various assays complements this theory with additional evidence to suggest that not only is this particular region on the surface, but also that it plays a role in binding and seroreactivity. Binding assays revealed that the Q179R mutation increased binding to the cell surface, while also slightly increasing the seroreactivity of the capsid against IVIG, both of which suggest that this region is on the surface and interacting with receptors. This could have interesting implications on the understanding and engineering of AAV5 as there have been no other reports of binding domains found in the VP1/VP2 common region thus far for AAV5 or any other serotype. It is also possible that the VP2/VP3 junction of other AAV serotypes shares similar characteristics and further analysis of this region could provide further insights in to AAV structure and binding domains. The analysis of each mutation's location in the AAV5 VP3 structure and its potential mechanism are summarized in Table 4

Combining the mutations from each variant did not achieve the intended effect of further increasing transduction in human hepatocytes. The F417L mutation did not stably work with other mutations and resulted in extremely low yields of virus. Combining surface mutations seemed to have a positive effect in Huh7 cells, but no significant difference in human

hepatocytes. This could be a result of differing receptor expression levels in Huh7 cells compared to primary human hepatocytes leading to slight differences in transduction levels. Addition of multiple mutations responsible for increasing binding to the cell surface could have some detrimental effects on capsid conformation, delaying proper binding of all the receptors required for internalization. Additionally, the A579T mutation could also be interfering with the internalization provided by the Loop1R mutation. The combined mutants MV50.T and MV50.53T were only tested on one set of human hepatocytes, and thus it is unclear if similar results would be found in other human hepatocytes. Regardless, the small differences in infectivity indicate that this method of combining mutations is inadequate for increasing transduction significantly.

After analysis of the Loop1R mutation, we wanted to explore this mutation in the context of other AAV serotypes. Studies have shown that all serotypes that utilize AAVR, except for AAV5, interact with the receptor via residues in the VR I/ Loop1 region. AAV5 was discovered to primarily use VR II and VR IV to bind to AAVR, indicating that the Loop1 region of AAV5 was used for an unknown purpose.⁸⁸ We were curious if the G257R mutation in other serotypes would achieve higher transduction, or whether it would negatively impact infectivity. The data showed that both *in vitro* and *in vivo* comparisons of AAV9 and AAV9 Loop1R were similar; addition of the glycine to arginine mutation substantially decreased infectivity, particularly in the liver, heart, and brain. This data matches fairly well with a study that investigated AAV8 transduction in AAVR KO mice in which AAV8 was significantly de-targeted from mouse liver.⁸⁵ Therefore, it is possible that the addition of the Loop1R mutation into AAV9 has prevented AAVR binding, leading to decreases in infectivity across all organs tested. Interestingly, the gastrocnemius seemed to be the least affected tissue, with AAV9 Loop1R

exhibiting only a 2-fold decrease in infectivity. This could signify that skeletal muscle mediated AAV9 transduction is not as reliant on AAVR for cellular entry in comparison to the liver, heart, and brain. As such, this vector has potentially interesting applications for targeted skeletal muscle delivery. Classic vectors for muscle delivery, such as AAV8 and AAV9, also target the liver and other tissues, which can lead to stronger immune responses to the capsid and transgene due to the off targeting of AAV. However, AAV9 Loop1R could circumvent these problems as it does not target the liver, which could allow for use of significantly higher doses of AAV. Further modifications could be performed on AAV9 Loop1R to enhance its muscle-specific transduction as well.

>MV1

MSFVDHPPDWLEEVGEGREFLBLEAGPPKPKPNQQHQDQARGLVLPGYNYLGPNGNLDREGP
VNRADDEVAREHDISYNEQLEAGDNPYLKYNHADAFAEFQEKLADDTSGGNGLGAQVFAKRVLE
PFGLVEEGAKTAPTGKRIDDHFPKRKKARTEEDSKPSTSSDAEAGPSGSQQLQIPASSLGADT
MSAGGGGGLGDNNQGADGVGNASGDWHCDSTWMGDRVVTKSTRTWVLPYNNHQQYREIKSG
SVD^RSNANAYFGYSTPWGYFDNRFHSHWSPRDWQRLINNYWGFRPRSLRVKIFNIQVKEVTVQ
DSTTTIANNTSTVQVFTDDDDYQLPYVVGNGTEGCLPAFPQVFTLPQYGYATLNRDNTENPTER
SSFFCLEYFPSKMLRTGNNFEFTYNFEEVPHSS^LAPSQNLFLKLANPLVDQYLYRFVSTNNTGGV
QFNKNLAGRYANTYKNWFPGMGRTOGWNLGSGVNRASVSAFATTNRMELEGASYQVPPQPN
GMTNNLQGSNTYALENTMIFNSQPANPGTTATYLEGNMLITSESETQPVNRVAYNVGGQMATN
NQSSTTAPATGTYNLQEIIVPGSVWMERDVYLQGPWAKIPETGAHFHPSAMGGFGLKHPPPM
LIKNTVPVGNITSFSDVPVSSFITQYSTGQVTVEMEWELKKENSKRWNPEIQYTNNYNDPQFVDF
APDSTGEYRSTRPIGTRYLTRPL

>MV18

MSFVDHPPDWLEEVGEGREFLBLEAGPPKPKPNQQHQDQARGLVLPGYNYLGPNGNLDREGP
VNRADDEVAREHDISYNEQLEAGDNPYLKYNHADAFAEFQEKLADDTSGGNGLGAQVFAKRVLE
PFGLVEEGAKTAPTGKRIDDHFPKRKKARTEEDSKPSTSSDAEAGPSGSQQLQIPASSLGADT
MSAGGGGGLGDNNQGADGVGNASGDWHCDSTWMGDRVVTKSTRTWVLPYNNHQQYREIKSG
SVD^RSNANAYFGYSTPWGYFDNRFHSHWSPRDWQRLINNYWGFRPRSLRVKIFNIQVKEVTVQ
DSTTTIANNTSTVQVFTDDDDYQLPYVVGNGTEGCLPAFPQVFTLPQYGYATLNRDNTENPTER
SSFFCLEYFPSKMLRTGNNFEFTYNFEEVPHSS^FAPSQNLFLKLANPLVDQYLYRFVSTNNTGGV
QFNKNLAGRYANTYKNWFPGMGRTOGWNLGSGVNRASVSAFATTNRMELEGASYQVPPQPN
GMTNNLQGSNTYALENTMIFNSQPANPGTTATYLEGNMLITSESETQPVNRVAYNVGGQMATN
NQSSTTAPATGTYNLQEIIVPGSVWMERDVYLQGPWAKIPETGAHFHPSAMGGFGLKHPPPM
LIKNTVPVGNITSFSDVPVSSFITQYSTGQVTVEMEWELKKENSKRWNPEIQYTNNYNDPQFVDF
APDSTGEYRSTRPIGTRYLTRPL

>MV20

MSFVDHPPDWLEEVGEGREFLBLEAGPPKPKPNQQHQDQARGLVLPGYNYLGPNGNLDREGP
VNRADDEVAREHDISYNEQLEAGDNPYLKYNHADAFAEFQEKLADDTSGGNGLGAQVFAKRVLE
PFGLVEEGAKTAPTGKRIDDHFPKRKKARTEEDSKPSTSSDAEAGPSGSQQLQIPASSLGADT
MSAGGGGGLGDNNQGADGVGNASGDWHCDSTWMGDRVVTKSTRTWVLPYNNHQQYREIKSG
SVDG^SSNANAYFGYSTPWGYFDNRFHSHWSPRDWQRLINNYWGFRPRSLRVKIFNIQVKEVTV
QDSTTTIANNTSTVQVFTDDDDYQLPYVVGNGTEGCLPAFPQVFTLPQYGYATLNRDNTENPTER
RSSFFCLEYFPSKMLRTGNNFEFTYNFEEVPHSS^FAPSQNLFLKLANPLVDQYLYRFVSTNNTGG
VQFNKNLAGRYANTYKNWFPGPI^GRTOGWNLGSGVNRASVSAFATTNRMELEGASYQVPPQPN
GMTNNLQGSNTYALENTMIFNSQPANPGTTATYLEGNMLITSESETQPVNRVAYNVGGQMATN
NQSSTT^TIPATGTYNLQEIIVPGSVWMERDVYLQGPWAKIPETGAHFHPSAMGGFGLKHPPPM
LIKNTVPVGNITSFSDVPVSSFITQYSTGQVTVEMEWELKKENSKRWNPEIQYTNNYNDPQFVDF
APDSTGEYRSTRPIGTRYLTRPL

>MV50

MSFVDHPPDWLEEVGEGREFLBLEAGPPKPKPNQQHQDQARGLVLPGYNYLGPNGNLDREGP
VNRADDEVAREHDISYNEQLEAGDNPYLKYNHADAFAEFQEKLADDTSGGNGLGAQVFAKRVLE
PFGLVEEGAKTAPTGKRIDDHFPKRKKARTEEDSKPSTSSDAEAGPSGSQQLQIPASSLGADT

MSAGGGGPLGDNNQGADGVGNASGDWHCDSTWMGDRVVTKSTRTWVLP SYN NHQYREIKSG
SVD^RSNANAYFGYSTPWGYFDNRFHSHWSPRDWQRLINNYWGFRPRSLRVKIFNIQVKEVTVQ
DSTTTIANNLTSTVQVFTDDDDYQLPYVVGNGTEGCLPAFPQVFTLPQYGYATLNRDNTENPTER
SSFFCLEYFPSKMLRTGNNFEFTYNFEEVPFHSSFAPSQNLFKLANPLVDQYLYRFVSTNNTGGV
QFNKNLAGRYANTYKNWFPGPMGRTQGWNLGSGVNRASVSAFATTNRMELEGASYQVPPQPN
GMTNNLQGSNTYALENTMIFNSQPANPGTTATYLEGNMLITSESETQPVNRVAYNVGGQMATN
NQSSTTAPATGTYNLQEIVPGSVWMERDVYLQGPWAKIPETGAHFHPSPAMGGFGLKHPPPM
LIKNTVPVGNITSFSDVPVSSFITQYSTGQVTVEMEWELKKENSKRWNPEIQYTNNYNDPQFVDF
APD^GTGEYRSTRPIGTRYLTRPL

>MV53

MSFVDHPPDWLEEVGEGREFLGLLEAGPPKPKPNQQHQDQARGLVLPGYNYLGPNGLDREGP
VNRADDEVAREHDISYNEQLEAGDNPYLKYNHADAFAEFQEKLADDTSGGNGLKAQVQAKKRVLE
PFGLVEEGAKTAPTGKRIDDHFPKRKKARTEEDSKPSTSSDAEAGPSGSQQL^RIPAQPASSLGADT
MSAGGGGPLGDNNQGADGVGNASGDWHCDSTWMGDRVVTKSTRTWVLP SYN NHQYREIKSG
SVD^RSNANAYFGYSTPWGYFDNRFHSHWSPRDWQRLINNYWGFRPRSLRVKIFNIQVKEVTVQ
DSTTTIANNLTSTVQVFTDDDDYQLPYVVGNGTEGCLPAFPQVFTLPQYGYATLNRDNTENPTER
SSFFCLEYFPSKMLRTGNNFEFTYNFEEVPFHSSFAPSQNLFKLANPLVDQYLYRFVSTNNTGGV
QFNKNLAGRYANTYKNWFPGPMGRTQGWNLGSGVNRASVSAFATTNRMELEGASYQVPPQPN
GMTNNLQGSNTYALENTMIFNSQPANPGTTATYLEGNMLITSESETQPVNRVAYNVGGQMATN
NQSSTTAPATGTYNLQEIVPGSVWMERDVYLQGPWAKIPETGAHFHPSPAMGGFGLKHPPPM
LIKNTVPVGNITSFSDVPVSSFITQYSTGQVTVEMEWELKKENSKRWNPEIQYTNNYNDPQFVDF
APDSTGEYRTRPIGTRYLTRPL

Figure 15: Amino Acid Sequence for Best Performing AAV5 Variants

The VP1 amino acid sequences for best performing variants. The mutations that differ from AAV5 are highlighted in red.

AAV5 1 MSFVDHPPDWLEEVGEGFLREFLGLGAEAGPPKPKPNQQHQDQARGLVLPGYNYLGPNGGLDR
MV1 1 MSFVDHPPDWLEEVGEGFLREFLGLGAEAGPPKPKPNQQHQDQARGLVLPGYNYLGPNGGLDR
MV18 1 MSFVDHPPDWLEEVGEGFLREFLGLGAEAGPPKPKPNQQHQDQARGLVLPGYNYLGPNGGLDR
MV20 1 MSFVDHPPDWLEEVGEGFLREFLGLGAEAGPPKPKPNQQHQDQARGLVLPGYNYLGPNGGLDR
MV50 1 MSFVDHPPDWLEEVGEGFLREFLGLGAEAGPPKPKPNQQHQDQARGLVLPGYNYLGPNGGLDR
MV53 1 MSFVDHPPDWLEEVGEGFLREFLGLGAEAGPPKPKPNQQHQDQARGLVLPGYNYLGPNGGLDR

AAV5 61 GEPVNRADDEVAREHDI SYNEQLEAGDNPYLKYNHADADEFQEKLADDTSFGGNLGKAVFQA
MV1 61 GEPVNRADDEVAREHDI SYNEQLEAGDNPYLKYNHADADEFQEKLADDTSFGGNLGKAVFQA
MV18 61 GEPVNRADDEVAREHDI SYNEQLEAGDNPYLKYNHADADEFQEKLADDTSFGGNLGKAVFQA
MV20 61 GEPVNRADDEVAREHDI SYNEQLEAGDNPYLKYNHADADEFQEKLADDTSFGGNLGKAVFQA
MV50 61 GEPVNRADDEVAREHDI SYNEQLEAGDNPYLKYNHADADEFQEKLADDTSFGGNLGKAVFQA
MV53 61 GEPVNRADDEVAREHDI SYNEQLEAGDNPYLKYNHADADEFQEKLADDTSFGGNLGKAVFQA

AAV5 121 KKRVLPEPFLVEEGAKTAPTGKRIDDHFPKRKKARTEEDSKPSTSSDAEAGPSGSQQLQI
MV1 121 KKRVLPEPFLVEEGAKTAPTGKRIDDHFPKRKKARTEEDSKPSTSSDAEAGPSGSQQLQI
MV18 121 KKRVLPEPFLVEEGAKTAPTGKRIDDHFPKRKKARTEEDSKPSTSSDAEAGPSGSQQLQI
MV20 121 KKRVLPEPFLVEEGAKTAPTGKRIDDHFPKRKKARTEEDSKPSTSSDAEAGPSGSQQLQI
MV50 121 KKRVLPEPFLVEEGAKTAPTGKRIDDHFPKRKKARTEEDSKPSTSSDAEAGPSGSQQLQI
MV53 121 KKRVLPEPFLVEEGAKTAPTGKRIDDHFPKRKKARTEEDSKPSTSSDAEAGPSGSQQLRI

AAV5 181 PAQPASSLGADTMSAGGGGPLGDNNQGADGVGNASGDWHCDSTWMGDRVVTKSTRTWVLP
MV1 181 PAQPASSLGADTMSAGGGGPLGDNNQGADGVGNASGDWHCDSTWMGDRVVTKSTRTWVLP
MV18 181 PAQPASSLGADTMSAGGGGPLGDNNQGADGVGNASGDWHCDSTWMGDRVVTKSTRTWVLP
MV20 181 PAQPASSLGADTMSAGGGGSLGDNNQGADGVGNASGDWHCDSTWMGDRVVTKSTRTWVLP
MV50 181 PAQPASSLGADTMSAGGGGPLGDNNQGADGVGNASGDWHCDSTWMGDRVVTKSTRTWVLP
MV53 181 PAQPASSLGADTMSAGGGGPLGDNNQGADGVGNASGDWHCDSTWMGDRVVTKSTRTWVLP

AAV5 241 SYNHHQYREIKSGSVDGNSANAYFGYSTPWGYDFNRFHSHWSPRDWQRLINNYWGFRRP
MV1 241 SYNHHQYREIKSGSVDNSANAYFGYSTPWGYDFNRFHSHWSPRDWQRLINNYWGFRRP
MV18 241 SYNHHQYREIKSGSVDNSANAYFGYSTPWGYDFNRFHSHWSPRDWQRLINNYWGFRRP
MV20 241 SYNHHQYREIKSGSVDGNSANAYFGYSTPWGYDFNRFHSHWSPRDWQRLINNYWGFRRP
MV50 241 SYNHHQYREIKSGSVDNSANAYFGYSTPWGYDFNRFHSHWSPRDWQRLINNYWGFRRP
MV53 241 SYNHHQYREIKSGSVDNSANAYFGYSTPWGYDFNRFHSHWSPRDWQRLINNYWGFRRP

AAV5 301 SLRVKIFNIQVKEVTVQDSTTTIANNLSTVQVFTDDDDYQLPYVVGNNGTEGCLPAFPQV
MV1 301 SLRVKIFNIQVKEVTVQDSTTTIANNLSTVQVFTDDDDYQLPYVVGNNGTEGCLPAFPQV
MV18 301 SLRVKIFNIQVKEVTVQDSTTTIANNLSTVQVFTDDDDYQLPYVVGNNGTEGCLPAFPQV
MV20 301 SLRVKIFNIQVKEVTVQDSTTTIANNLSTVQVFTDDDDYQLPYVVGNNGTEGCLPAFPQV
MV50 301 SLRVKIFNIQVKEVTVQDSTTTIANNLSTVQVFTDDDDYQLPYVVGNNGTEGCLPAFPQV
MV53 301 SLRVKIFNIQVKEVTVQDSTTTIANNLSTVQVFTDDDDYQLPYVVGNNGTEGCLPAFPQV

AAV5 361 FTLPQYGYATLNRDNTENPTERSSFFCLEYFPSKMLRTGNNFEFTYNFEEVPHSSIFAPS
MV1 361 FTLPQYGYATLNRDNTENPTERSSFFCLEYFPSKMLRTGNNFEFTYNFEEVPHSSIFAPS
MV18 361 FTLPQYGYATLNRDNTENPTERSSFFCLEYFPSKMLRTGNNFEFTYNFEEVPHSSIFAPS
MV20 361 FTLPQYGYATLNRDNTENPTERSSFFCLEYFPSKMLRTGNNFEFTYNFEEVPHSSIFAPS
MV50 361 FTLPQYGYATLNRDNTENPTERSSFFCLEYFPSKMLRTGNNFEFTYNFEEVPHSSIFAPS
MV53 361 FTLPQYGYATLNRDNTENPTERSSFFCLEYFPSKMLRTGNNFEFTYNFEEVPHSSIFAPS

AAV5 421 QNLFKLANPLVDQYLYRFVSTNNTGGVQFNKNLAGRYANTYKNWFPGPMMGRTQGWNLLGSG

```

MV1      421  QNLFKLANPLVDQYLYRFVSTNNTGGVQFNKNLAGRYANTYKNWFFPGPMMGRTQGWNLGSG
MV18     421  QNLFKLANPLVDQYLYRFVSTNNTGGVQFNKNLAGRYANTYKNWFFPGPMMGRTQGWNLGSG
MV20     421  QNLFKLANPLVDQYLYRFVSTNNTGGVQFNKNLAGRYANTYKNWFFPGPIIGRTQGWNLGSG
MV50     421  QNLFKLANPLVDQYLYRFVSTNNTGGVQFNKNLAGRYANTYKNWFFPGPMMGRTQGWNLGSG
MV53     421  QNLFKLANPLVDQYLYRFVSTNNTGGVQFNKNLAGRYANTYKNWFFPGPMMGRTQGWNLGSG

AAV5     481  VNRSVSAFATTNRMELEGASYQVPPQPNGMTNNLQGSNTYALENTMIFNSQPANPGTTA
MV1      481  VNRSVSAFATTNRMELEGASYQVPPQPNGMTNNLQGSNTYALENTMIFNSQPANPGTTA
MV18     481  VNRSVSAFATTNRMELEGASYQVPPQPNGMTNNLQGSNTYALENTMIFNSQPANPGTTA
MV20     481  VNRSVSAFATTNRMELEGASYQVPPQPNGMTNNLQGSNTYALENTMIFNSQPANPGTTA
MV50     481  VNRSVSAFATTNRMELEGASYQVPPQPNGMTNNLQGSNTYALENTMIFNSQPANPGTTA
MV53     481  VNRSVSAFATTNRMELEGASYQVPPQPNGMTNNLQGSNTYALENTMIFNSQPANPGTTA

AAV5     541  TYLEGNMLITSESETQPVNRVAYNVGGQMATNNQSSTTAPATGTYNLQEIVPGSVWMERD
MV1      541  TYLEGNMLITSESETQPVNRVAYNVGGQMATNNQSSTTAPATGTYNLQEIVPGSVWMERD
MV18     541  TYLEGNMLITSESETQPVNRVAYNVGGQMATNNQSSTTAPATGTYNLQEIVPGSVWMERD
MV20     541  TYLEGNMLITSESETQPVNRVAYNVGGQMATNNQSSTTAPATGTYNLQEIVPGSVWMERD
MV50     541  TYLEGNMLITSESETQPVNRVAYNVGGQMATNNQSSTTAPATGTYNLQEIVPGSVWMERD
MV53     541  TYLEGNMLITSESETQPVNRVAYNVGGQMATNNQSSTTAPATGTYNLQEIVPGSVWMERD

AAV5     601  VYLQGPIWAKIPETGAHFHPSPAMGGFGLKHPPPMLIKNTPVPGNITSFSDVPVSSFIT
MV1      601  VYLQGPIWAKIPETGAHFHPSPAMGGFGLKHPPPMLIKNTPVPGNITSFSDVPVSSFIT
MV18     601  VYLQGPIWAKIPETGAHFHPSPAMGGFGLKHPPPMLIKNTPVPGNITSFSDVPVSSFIT
MV20     601  VYLQGPIWAKIPETGAHFHPSPAMGGFGLKHPPPMLIKNTPVPGNITSFSDVPVSSFIT
MV50     601  VYLQGPIWAKIPETGAHFHPSPAMGGFGLKHPPPMLIKNTPVPGNITSFSDVPVSSFIT
MV53     601  VYLQGPIWAKIPETGAHFHPSPAMGGFGLKHPPPMLIKNTPVPGNITSFSDVPVSSFIT

AAV5     661  QYSTGQVTVEMEWELKKENSKRWNPEIQYTNNYNDPQFVDFAPDSTGEYRTTRPIGTRYL
MV1      661  QYSTGQVTVEMEWELKKENSKRWNPEIQYTNNYNDPQFVDFAPDSTGEYRTTRPIGTRYL
MV18     661  QYSTGQVTVEMEWELKKENSKRWNPEIQYTNNYNDPQFVDFAPDSTGEYRTTRPIGTRYL
MV20     661  QYSTGQVTVEMEWELKKENSKRWNPEIQYTNNYNDPQFVDFAPDSTGEYRTTRPIGTRYL
MV50     661  QYSTGQVTVEMEWELKKENSKRWNPEIQYTNNYNDPQFVDFAPDGTGEYRTTRPIGTRYL
MV53     661  QYSTGQVTVEMEWELKKENSKRWNPEIQYTNNYNDPQFVDFAPDSTGEYRTTRPIGTRYL

AAV5     721  TRPL
MV1      721  TRPL
MV18     721  TRPL
MV20     721  TRPL
MV50     721  TRPL
MV53     721  TRPL

```

Figure 16: Amino Acid Sequence Alignment of AAV5 and MV Mutants

Alignment of the VP1 amino acid sequences for each of the MV mutants and AAV5. The mutations that differ from AAV5 are highlighted in black with white font.

AAV1 MAADGYLPDWLEDNLSEGIREWWDLKPAPKPKANQQKQDDGRGLVLPGYKYLGPFGNDL
AAV6 MAADGYLPDWLEDNLSEGIREWWDLKPAPKPKANQQKQDDGRGLVLPGYKYLGPFGNDL
AAV2 MAADGYLPDWLEDNLSEGIREWWDLKPAPKPKANQQKQDDGRGLVLPGYKYLGPFGNDL
AAV3 MAADGYLPDWLEDNLSEGIREWWDLKPAPKPKANQQKQDDGRGLVLPGYKYLGPFGNDL
AAV7 MAADGYLPDWLEDNLSEGIREWWDLKPAPKPKANQQKQDDGRGLVLPGYKYLGPFGNDL
AAV8 MAADGYLPDWLEDNLSEGIREWWDLKPAPKPKANQQKQDDGRGLVLPGYKYLGPFGNDL
AAV9 MAADGYLPDWLEDNLSEGIREWWDLKPAPKPKANQQKQDDGRGLVLPGYKYLGPFGNDL
AAV4 -MTDGYLPDWLEDNLSEGIREWWDLKPAPKPKANQQKQDDGRGLVLPGYKYLGPFGNDL
MV MSFVDHPPDWLEEVG-EGLEFLGLEAGPPKPKPNQQHQDQARGLVLPGYNYLGPFGNDL
. : *****: **. * : : * . * * * . : : : * : *****: *****: *****

AAV1 KGEVNAADAAALEHDKAYDQQLKAGDNPYLRYNHADAEEFQERLQEDTSFGGNLGRAVFQ
AAV6 KGEVNAADAAALEHDKAYDQQLKAGDNPYLRYNHADAEEFQERLQEDTSFGGNLGRAVFQ
AAV2 KGEVNEADAAALEHDKAYDQQLDSDGNPYLKNHADAEEFQERLKEDTSFGGNLGRAVFQ
AAV3 KGEVNEADAAALEHDKAYDQQLKAGDNPYLRYNHADAEEFQERLQEDTSFGGNLGRAVFQ
AAV7 KGEVNAADAAALEHDKAYDQQLKAGDNPYLRYNHADAEEFQERLQEDTSFGGNLGRAVFQ
AAV8 KGEVNAADAAALEHDKAYDQQLKAGDNPYLRYNHADAEEFQERLQEDTSFGGNLGRAVFQ
AAV9 KGEVNAADAAALEHDKAYDQQLKAGDNPYLRYNHADAEEFQERLKEDTSFGGNLGRAVFQ
AAV4 KGEVNAADAAALEHDKAYDQQLKAGDNPYLRYNHADAEEFQERLQEDTSFGGNLGRAVFQ
MV RGEVNRADDEVAREHDISYNEQLEAGDNPYLRYNHADAEEFQERLQEDTSFGGNLGRAVFQ
: ***** * * . * * * : * . * . : *****: *****: * * * * * : * * * * *

AAV1 AKKRVLEPLGLVEEGAKTAPGKKRPVEQSPQE-PDSSSGIGKTGQQPAKRLNFGQTGDS
AAV6 AKKRVLEPLGLVEEGAKTAPGKKRPVEQSPQE-PDSSSGIGKTGQQPAKRLNFGQTGDS
AAV2 AKKRVLEPLGLVEEPVKTAPGKKRPVEHSPVE-PDSSSGTGKAGQQPARKRLNFGQTGDA
AAV3 AKKRILEPLGLVEEAAKTAPGKKRPVDQSPQE-PDSSSGVGKSGKQPARKRLNFGQTGDS
AAV7 AKKRVLEPLGLVEEGAKTAPAKKRPVEPSPQRS PDSSSTGIGKKGQQPARKRLNFGQTGDS
AAV8 AKKRVLEPLGLVEEGAKTAPGKKRPVEPSPQRS PDSSSTGIGKKGQQPARKRLNFGQTGDS
AAV9 AKKRILLEPLGLVEEAAKTAPGKKRPVEQSPQE-PDSSAGIGKSGAQPAKRLNFGQTGDT
AAV4 AKKRVLEPLGLVEQAGETAPGKKRPLIESPQQ-PDSSSTGIGKKGQPAKRLNFGQEDTGA
MV AKKRVLEPLGLVEEGAKTAPGKKRPLIDHFPKR-----KKARTEEDSKPSTSSDAE
****:***:****: :*** ** * . : . . .

AAV1 ESVPDPQPLGEPATPAAVGPTMASGGGAPMADNNEGADGVGNASGNWHCDS TWLGDRV
AAV6 ESVPDPQPLGEPATPAAVGPTMASGGGAPMADNNEGADGVGNASGNWHCDS TWLGDRV
AAV2 DSVPDPQPLGQPPAAPSGLTNTMATGSGAPMADNNEGADGVGNSSGNWHCDS TWMGDRV
AAV3 ESVPDPQPLGEPAPAPTSLSGNTMASGGGAPMADNNEGADGVGNSSGNWHCDS QWLGDV
AAV7 ESVPDPQPLGEPAPAPSSVSGTVAAGGGAPMADNNEGADGVGNASGNWHCDS TWLGDRV
AAV8 ESVPDPQPLGEPAPAPSGVGPNTMAAGGGAPMADNNEGADGVGSSGNWHCDS TWLGDRV
AAV9 ESVPDPQPLGEPAPAPSGVSLTMAAGGGAPVADNNEGADGVGSSGNWHCDS QWLGDV
AAV4 GDGPP-----EGSTSGAMSDDSEMRAAGAAVEGGQAGDGVGNASGDWHCDS TWSEGHV
MV AGPSGSQQLRIPAQPASSLGADTMSAGGGPLGDNNQAGDGVGNASGDWHCDS TWMGDRV
. . . . : . : : * . * . : : : *****: ***** * * : *

AAV1 ITTSTRTWALPTYNNHLYK---QIS-SASTGASNDNHYFGYSTPWGYFDNRFHCHFSR
AAV6 ITTSTRTWALPTYNNHLYK---QIS-SASTGASNDNHYFGYSTPWGYFDNRFHCHFSR
AAV2 ITTSTRTWALPTYNNHLYK---QIS-SQSG-ASNDNHYFGYSTPWGYFDNRFHCHFSR
AAV3 ITTSTRTWALPTYNNHLYK---QIS-SQSG-ASNDNHYFGYSTPWGYFDNRFHCHFSR
AAV7 ITTSTRTWALPTYNNHLYK---QISSETAG-STNDNTYFGYSTPWGYFDNRFHCHFSR
AAV8 ITTSTRTWALPTYNNHLYK---QISNGTSGATNDNTYFGYSTPWGYFDNRFHCHFSR
AAV9 ITTSTRTWALPTYNNHLYK---QISNSTSGGSSNDNAYFGYSTPWGYFDNRFHCHFSR
AAV4 TTTSTRTWALPTYNNHLYKRLG-----ESLQSNYNGFSTPWGYFDNRFHCHFSR
MV VTKSTRTWALPTYNNHLYK---EIKSGSVDRSNANAYFGYSTPWGYFDNRFHSHWSPR
* . *****: ***** * : : * * * : *****: *****: *****

AAV1 DWQRLINNNWGFRPKRLNFKLFNIQVKEVTNDGVTTIANNLTSTVQVFS DSEYQLPYVL
AAV6 DWQRLINNNWGFRPKRLNFKLFNIQVKEVTNDGVTTIANNLTSTVQVFS DSEYQLPYVL
AAV2 DWQRLINNNWGFRPKRLNFKLFNIQVKEVTQNDGTTT IANNLTSTVQVFTDSEYQLPYVL
AAV3 DWQRLINNNWGFRPKKLSFKLFNIQVKEVTQNDGTTT IANNLTSTVQVFTDSEYQLPYVL
AAV7 DWQRLINNNWGFRPKKLRFKLFNIQVKEVTNDGVTTIANNLTSTIQVFS DSEYQLPYVL
AAV8 DWQRLINNNWGFRPKRLSFKLFNIQVKEVTQNEGTKT IANNLTSTIQVFTDSEYQLPYVL
AAV9 DWQRLINNNWGFRPKRLNFKLFNIQVKEVTDNNGVKT IANNLTSTVQVFTDSYQLPYVL

AAV4 DWQRLINNNWGMRPKAMRVKIFNIQVKEVTSNGETTANNLTSTVQIFADSSYELPYVM
MV DWQRLINNYWGFRRPSLRVKIFNIQVKEVTVQDSTTTIANLNTSTVQVFTDDDYQLPYVV
***** **:*** : .*:***** :. . *:*****:*.*:*.**:****:

AAV1 GSAHQGCLPPFPADVPMI PQYGYLTLNNG---SQAVGRSSFYCLEYFPSQMLRTGNNFTF
AAV6 GSAHQGCLPPFPADVPMI PQYGYLTLNNG---SQAVGRSSFYCLEYFPSQMLRTGNNFTF
AAV2 GSAHQGCLPPFPADVFMV PQYGYLTLNNG---SQAVGRSSFYCLEYFPSQMLRTGNNFTF
AAV3 GSAHQGCLPPFPADVFMV PQYGYLTLNNG---SQAVGRSSFYCLEYFPSQMLRTGNNQF
AAV7 GSAHQGCLPPFPADVPMI PQYGYLTLNNG---SQSVGRSSFYCLEYFPSQMLRTGNNFEF
AAV8 GSAHQGCLPPFPADVPMI PQYGYLTLNNG---SQAVGRSSFYCLEYFPSQMLRTGNNQF
AAV9 GSAHEGCLPPFPADVPMI PQYGYLTLNDG---SQAVGRSSFYCLEYFPSQMLRTGNNQF
AAV4 DAGQEGSLPPFPNDVFMV PQYGYCGLVTGNTSQQQTDRNAFYCLEYFPSQMLRTGNNFEI
MV GNGTEGCLPAFPQVFTLPQYGYATLNRDN-TENPTERSSFYCLEYFPSKMLRTGNNFEF
. . :*.**.**:** :** :***** * . . : . *:*****:***** :

AAV1 SYTFEEVFPFHSSYAHSQSLDRLMNPLIDQYLYLNRTO-NQSGSAQNKDLLFSRGSPAGM
AAV6 SYTFEDVFPFHSSYAHSQSLDRLMNPLIDQYLYLNRTO-NQSGSAQNKDLLFSRGSPAGM
AAV2 SYTFEDVFPFHSSYAHSQSLDRLMNPLIDQYLYLNRTO-NQSGSAQNKDLLFSRGSPAGM
AAV3 SYTFEDVFPFHSSYAHSQSLDRLMNPLIDQYLYLNRTO-NQSGSAQNKDLLFSRGSPAGM
AAV7 SYTFEDVFPFHSSYAHSQSLDRLMNPLIDQYLYLNRTO-NQSGSAQNKDLLFSRGSPAGM
AAV8 SYTFEDVFPFHSSYAHSQSLDRLMNPLIDQYLYLNRTO-NQSGSAQNKDLLFSRGSPAGM
AAV9 SYTFEDVFPFHSSYAHSQSLDRLMNPLIDQYLYLNRTO-NQSGSAQNKDLLFSRGSPAGM
AAV4 SYTFEDVFPFHSSYAHSQSLDRLMNPLIDQYLYLNRTO-NQSGSAQNKDLLFSRGSPAGM
MV TYNFEEVFPFHSSLAAPSQNLFLKLANPLVDQYLYRFVSTN-----NTGGVQFVNKNLAGRY
: * *.***** * *.*: * :* ***:***: : * *

AAV1 SVQPKNWLPGPCYRQQRVSKTKTD-----NNNSNFTWTGASKYNLNGRESI INPGTAMAS
AAV6 SVQPKNWLPGPCYRQQRVSKTKTD-----NNNSNFTWTGASKYNLNGRESI INPGTAMAS
AAV2 RDQSRNWLPGPCYRQQRVSKTSAD-----NNNSEYSWTGATKYHLNGRDSL VN--PAMAS
AAV3 SLQARNWLPGPCYRQQRVSKTKTD-----NNNSNFTWTGASKYNLNGRESI INPGTAMAS
AAV7 AEQAKNWLPGPCYRQQRVSKTKTD-----NNNSNFTWTGATKYHLNGRDSL VNPGVAMAT
AAV8 ANQAKNWLPGPCYRQQRVSKTKTD-----NNNSNFTWTGATKYHLNGRDSL VNPGVAMAT
AAV9 AVQGRNYI PGPSYRQQRVSTTVTQ-----NNNSEFAWPGASSWALNGRNSLMNPGPAMAS
AAV4 SNFKKNWLPGPSIKQQGFSK TANQNYKI PATGSDSLIKYETHSTLDGRWSALT PGPPMAT
MV ANTYKNWFPGPMGRTQGWNLGSGVN-----RASVSATFATNRMELEGASYQVPPQPNGMT
:***:*** : * . * . **:

AAV1 HKDDEDKFFPMSGVMI FGKESAGA---SNTALDNVMI TDEEEIKATNPVATERFGTVAVN
AAV6 HKDDEDKFFPMSGVMI FGKESAGA---SNTALDNVMI TDEEEIKATNPVATERFGTVAVN
AAV2 HKDDEEKFFPMSGVLI FGKQSGEK---TNVNIKVMITDEEEIGTTPVATEQYGSVSTN
AAV3 HKDDEEKFFPMHGNI LFGKEGTTA---SNAELDNVMI TDEEEIRTTNPVATEQYGTVANN
AAV7 HKDDEDRFPPSSGVLI FG-KTGAT---NKTTLENVLMTNEEEIRPTNPVATEEYGVSSN
AAV8 HKDDEERFFPSSGILIFGKQNAAR---DNADYSDVMLTSEEEIKTTNPVATEEYGVADN
AAV9 HKEGEDRFPPSSGLIFGKQGTGR---DNVDADKVMITNEEEIKTTNPVATESYGVQVATN
AAV4 AGPADSKFS-NSQLIFAGPKQNGN---TATVPGTLIFTSEEEELAAATNATDTDMWGNLPGG
MV NNLQGSNTYALENTMIFNSQPANPGTTATYLEGNMLITSESETQPVNRVAYNVGGQMATN
. . :. . : :*.**.**:** :** :***:***: :* **:

AAV1 FQSSSTDPATGDVHAMGALPGMVWQDRDVYLQGPWIWAKI PHTDGHFHPSPLMGGFGLKHP
AAV6 FQSSSTDPATGDVHVMGALPGMVWQDRDVYLQGPWIWAKI PHTDGHFHPSPLMGGFGLKHP
AAV2 LQRGNRQAATADVNTQGVLPGMVWQDRDVYLQGPWIWAKI PHTDGHFHPSPLMGGFGLKHP
AAV3 LQSSNTAPTTRTVNDQGALPGMVWQDRDVYLQGPWIWAKI PHTDGHFHPSPLMGGFGLKHP
AAV7 LQAANTAAQTQVNNQGALPGMVWQNRDVYLQGPWIWAKI PHTDGNFHPSPLMGGFGLKHP
AAV8 LQQONTAPQIGTVNSQGALPGMVWQNRDVYLQGPWIWAKI PHTDGNFHPSPLMGGFGLKHP
AAV9 HQSAQAQAQTGWVQNGILPGMVWQDRDVYLQGPWIWAKI PHTDGNFHPSPLMGGFGMKHP
AAV4 DQSNLPTVDRLTALGAVPGMVWQNRDIYYQGPWIWAKI PHTDGHFHPSPLIGGFGLKHP
MV NQSSSTPATGTYNLQEI VPGSVWMERDVYLQGPWIWAKI PETGAHFHPSPAMGGFGLKHP
* . :** ** :**.* ******.**:***** :*****:***:

AAV1 PPQILIKNTPVPANPPAEFSATKFAFITQYSTGQVSVEIEWELQKENS KRWNPEVQYTS
AAV6 PPQILIKNTPVPANPPAEFSATKFAFITQYSTGQVSVEIEWELQKENS KRWNPEVQYTS
AAV2 PPQILIKNTPVPANPSTTFAAKFAFITQYSTGQVSVEIEWELQKENS KRWNPEIQYTS
AAV3 PPQIMIKNTPVPANPPTTFAAKFAFITQYSTGQVSVEIEWELQKENS KRWNPEIQYTS


```

AAV7      PPQILIKNTPVPANPPEVFTPAKFASFITQYSTGQVSVEIEWELQKENSKRWNPEIQYTS
AAV8      PPQILIKNTPVPADPPTTFNQSKLNSFITQYSTGQVSVEIEWELQKENSKRWNPEIQYTS
AAV9      PPQILIKNTPVPADPPTAFNKDKLNSFITQYSTGQVSVEIEWELQKENSKRWNPEIQYTS
AAV4      PPQIFIKNTPVPANPATTFSSTPVNSFITQYSTGQVSVQIDWEIQERSKRWNPEVQFTS
MV        PPMLLIKNTFVPGN-ITSFSDVPVSSFITQYSTGQVTVEMEWELKKENSKRWNPEIQYTN
**  : :*****.:      * . . *****: * : : * : * . *****: * : * .

AAV1      NYAKSANVDFTVDNNGLYTEPRPIGTRYLTRPL
AAV6      NYAKSANVDFTVDNNGLYTEPRPIGTRYLTRPL
AAV2      NYNKSVMRGLTVDTNGVYSEPRPIGTRYLTRNL
AAV3      NYNKSVMNDFTVDTNGVYSEPRPIGTRYLTRNL
AAV7      NFEKQTGVDFAVDSQGVYSEPRPIGTRYLTRNL
AAV8      NYKSTSVDFAVNTEGVYSEPRPIGTRYLTRNL
AAV9      NYYKSNNVEFAVNTEGVYSEPRPIGTRYLTRNL
AAV4      NYGQQNSLLWAPDAAGKYTEPRAIGTRYLTHHL
MV        NYNDPQFVDFAPDGTGEYRSTRPIGTRYLTRPL
* : .      : : * * ..*.*****: *

```

Figure 17: Alignment of All Mutations found in MV Mutants with Other AAV Serotypes

Alignment of AAV serotypes 1 through 9 against MV which contains all the mutations found in the MV mutants pooled into one sequence. Mutations are highlighted in red.

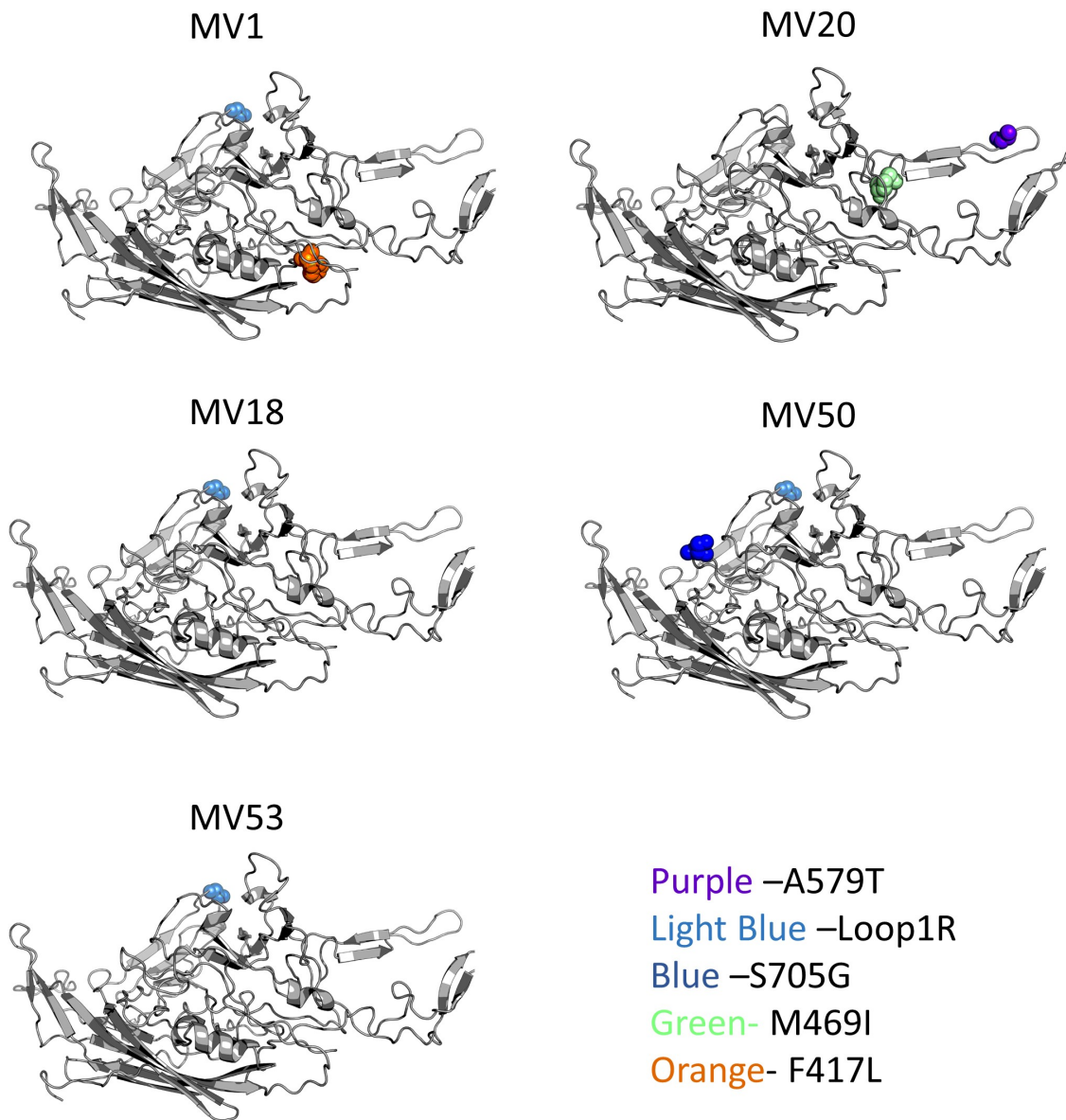


Figure 18: False Color Mapping of Mutations in each MV Variant onto the AAV5 VP3 Structure

The mutations in each AAV5 variant were mapped onto the AAV5 VP3 protein crystal structure (3NTT). Mutations are represented by spheres of differing colors that represent different mutations. Purple, A579T; Light Blue, G257R (Loop1R); Blue, S705G; Green, M469I; Orange, F417L.

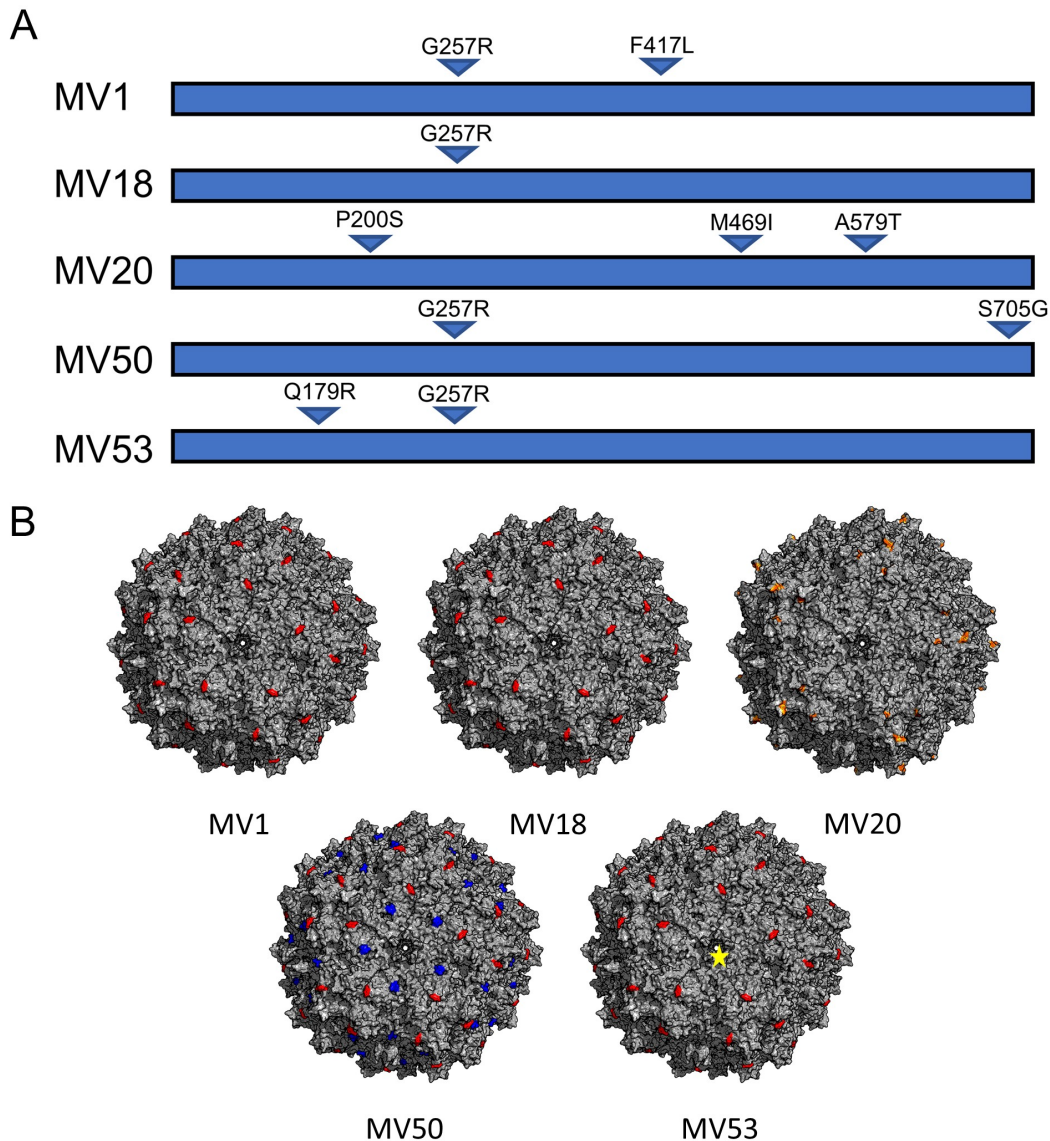


Figure 19: Sequence and Structural Analysis of Mutant AAV5 Capsids with Increased Human Liver Transduction

(A) Five selected mutants with the best yield and transduction capabilities. Location of amino acid mutations in the AAV5 VP1 amino acid sequence are indicated by triangles. The exact mutation is indicated above the triangle. (B) Mutations for each variant were false color mapped onto the surface of the 60mer crystal structure of AAV5. The G257R mutation is colored in red, the A579T mutation is colored in orange, and the S705G mutation is colored in blue. The F417L and M469I mutations do not show up as they are located in the interior of the MV1 and MV20 capsid. The exact structure of the domain that the Q179R resides in is unknown. The yellow star in MV53 indicates a possible location for the mutation, if the domain it is in resides near or on the surface of the MV53 capsid. False-color mapping of the mutations onto the AAV5 capsid was exaggerated by also highlighting the adjacent amino acids to allow for better visualization of the mutations on the capsid.

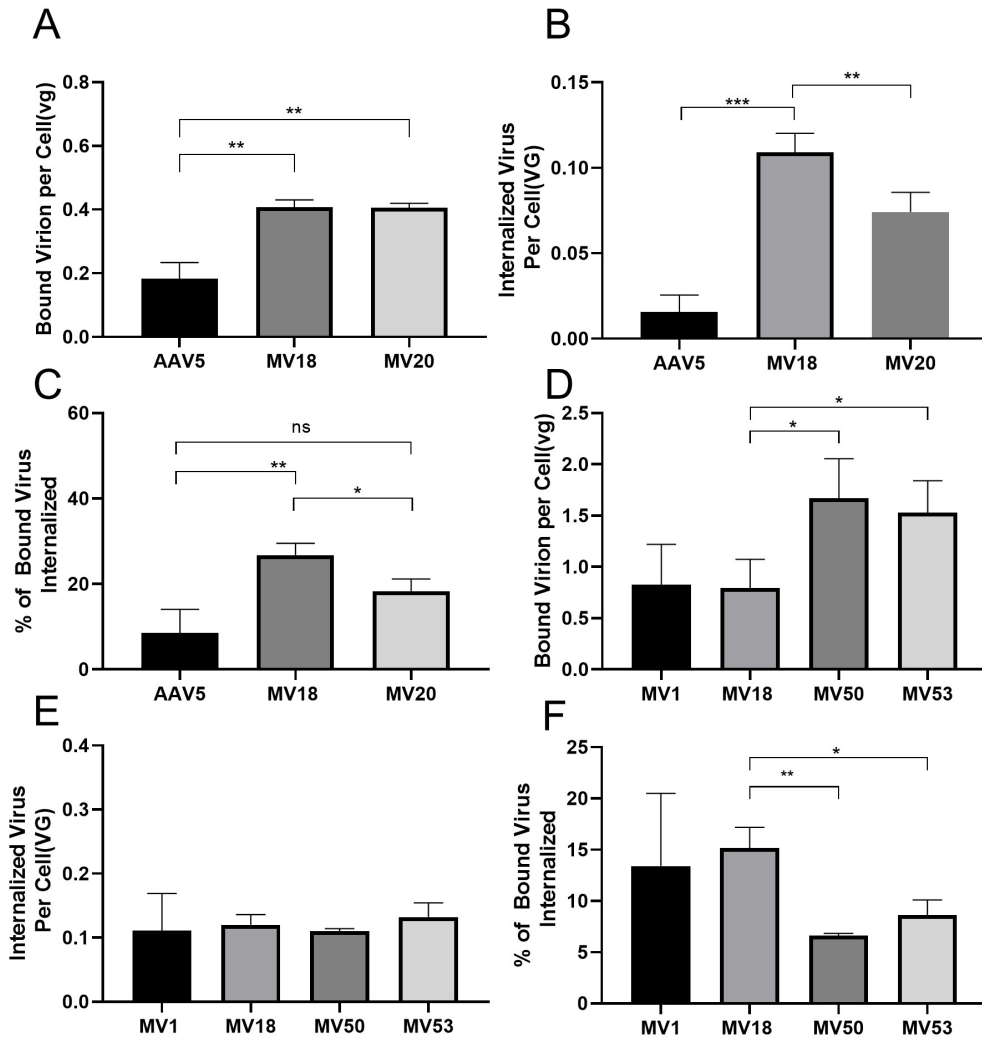


Figure 20: Comparison of Binding and Internalization between AAV5 and MV Mutants

(A) Binding assay comparing binding of capsid to Huh7 cell surface between AAV5, MV18, and MV20. Data shown are mean values ± SD. ** $p < 0.01$. (B) Internalization assay comparing amount of internalized virus in Huh7 cells between AAV5, MV18, and MV20. Data shown are mean values ± SD. ** $p < 0.01$; *** $p < 0.001$. (C) Percentage of bound viral genomes that are internalized comparison between AAV5, MV18, and MV20. Data shown are mean values ± SD. * $p < 0.05$; ** $p < 0.01$. (D) Binding assay comparing binding of capsid to Huh7 cell surface between MV1, MV18, MV50, and MV53. Data shown are mean values ± SD. ** $p < 0.01$. (E) Internalization assay comparing amount of internalized virus in Huh7 cells between MV1, MV18, MV50, and MV53. Data shown are mean values ± SD. (F) Percentage of bound viral genomes that are internalized comparison between MV1, MV18, MV50, and MV53. Data shown are mean values ± SD. * $p < 0.05$; ** $p < 0.01$.

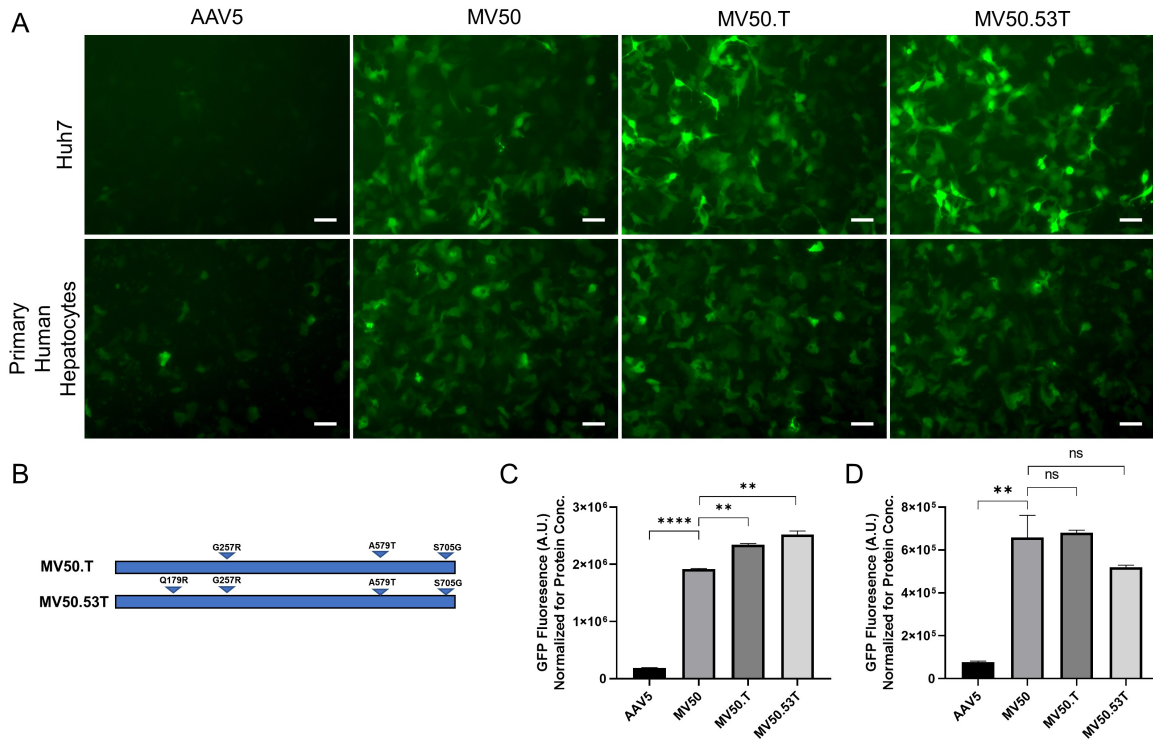


Figure 21: Combination of Mutations from multiple AAV5 Variants

(A) Fluorescent imaging of Huh7 cells and primary human hepatocytes(TRL) transduced with self-complementary GFP vectors with AAV5, MV50, MV50.T, and MV50.53T. Huh7 cells were transduced at a MOI of 1e5 vg/cell and human hepatocytes were transduced at a MOI of 5e5vg/cell. Images were taken 96 hours after infection. Expression of GFP (green) indicates transduced cells. 10x magnification. Scale Bar: 100um. (B) Depiction of the combined mutations that are in MV50.T and MV50.53T. Location of amino acid mutations in the AAV5 VP1 amino acid sequence are indicated by triangles. The exact mutation is indicated above the triangle. (C) Comparison of normalized GFP expression in Huh7 cells between AAV5, MV50, MV50.T, and MV50.53T. Data are shown as mean values \pm SD. ** $p < 0.01$; **** $p < 0.0001$. (D) Comparison of normalized GFP expression in primary human hepatocytes between AAV5, MV50, MV50.T, and MV50.53T. Data are shown as mean values \pm SD. ** $p < 0.01$.

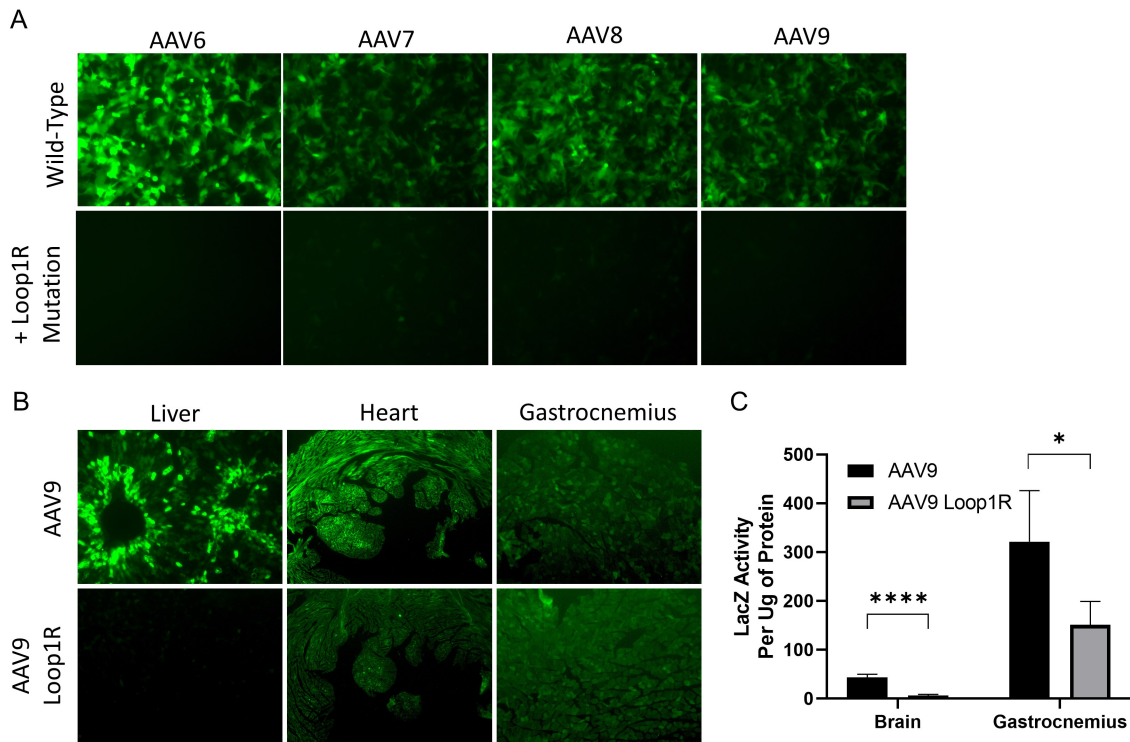


Figure 22: Loop1R Mutation in Other AAV Serotypes

(A) Fluorescent imaging of Huh7 cells transduced with self-complementary GFP vectors with AAV6, AAV7, AAV8, AAV9, and Loop1R versions. Huh7 cells were transduced at a MOI of 5×10^4 vg/cell and coinfecting with MOI of 500 of wt-AD. Images were taken 72 hours after infection. Expression of GFP (green) indicates transduced cells. 10x magnification. (B) Fluorescent Images of GFP expression in different mouse organs. Mice were injected with 1×10^{11} vg of GFP vector packaged by either AAV9 or AAV9 Loop1R. After 3 weeks, mice were sacrificed and their heart, gastrocnemius, and liver were harvested. Organs were sectioned and imaged for GFP fluorescence (Green). Liver sections are 10x magnification, while heart and gastrocnemius are 4x magnification. (C) Quantification of B-galactosidase (LacZ) activity in homogenized tissue samples of mouse brain and gastrocnemius transduced by AAV9-ssLacZnl and AAV9 Loop1R-ssLacZnl. Mice were i.v. injected with 1×10^{12} vg of vector and tissues were harvested 3 weeks after injection. Data are shown as mean values \pm SD. * $p < 0.01$.

Table 4: Mutations of AAV5 Variants with Increased Liver Tropism

Variant	Mutation	Region/Probable Function
<u>MV1</u>	G257R	Surface Exposed in VR-I/Loop1 Region, Increases Binding and Internalization
	F417L	Buried in Interior of Capsid, Affects Stability of Capsid and Perhaps Uncoating
<u>MV18</u>	G257R	Surface Region in VR-I/Loop1, Increases Binding and Internalization
<u>MV20</u>	P200S	Near VP2/VP3 Junction
	M469I	Interior Mutation
	A579T	Surface Exposed in VR-VIII/Loop 8 Region, Near Sialic Acid Binding Pocket and Increases Binding
<u>MV50</u>	G257R	Surface Region in VR-I/Loop1, Increases Binding and Internalization
	S705G	Surface Mutation Near Known Antigenic Site
<u>MV53</u>	Q179R	Near VP2/VP3 Junction, Increases Binding, No Effect on Internalization
	G257R	Surface Region in VR-I/Loop1, Increases Binding and Internalization

Location of the mutations was obtained by false color mapping of the mutations on to the crystal structure of the AAV5 capsid. Probable function was determined through structure analysis and binding/internalization assays

CHAPTER 4

RATIONAL ENGINEERING OF EVOLVED AAV CAPSIDS³

4.1 Overview

Experimental data from mechanistic studies of the evolved AAV5 mutants revealed that the dominant mutation, G257R, increased binding and the overall amount of virus internalized into the cell. Additional mutations enhanced either binding or uncoating, but likely did not affect any process after internalization of the virus. Structural analysis also suggested that there were no mutations affecting processes such as internalization, cellular trafficking, or nuclear import. As such, we theorized that combining the G257R mutation with a mutation or domain that could increase endosomal escape or cellular trafficking would greatly enhance the ability of our AAV5 mutants to transduce human liver cells. The VP1 protein for AAV has been characterized as essential for endosomal escape and cellular trafficking. In particular, the lipase domain located in the VP1 unique region (VP1u) is responsible for late endosomal escape. However, the AAV5 VP1u is significantly divergent from the VP1u of all other serotypes, indicating that the AAV5 VP1u may function differently. As such, we swapped the coding sequence for AAV5 VP1 unique region and VP1/VP2 common region with the equivalent regions from hepatotropic serotypes such as AAV3, AAV8, and AAV9 in order to enhance endosomal escape. Using site

³ This chapter includes a manuscript in preparation: Qian R., Li J., Xiao X. *Rational Engineering of the VP1/VP2 proteins of AAV5 Mutants Results in Further Enhancement of Liver Transduction.*

directed mutagenesis, we added the Loop1R mutation found in our AAV5 mutants to the chimeric AAV5 capsids. These capsids, called 3(5) Loop1R, 8(5) Loop1R, and 9(5) Loop1R, were tested on Huh7 cells for their transduction efficacy. The capsids with swapped VP1 regions showed increases in transduction that were significantly enhanced when combined with the Loop1R mutation. The 8(5) Loop1R and 9(5) Loop1R capsids were then tested in primary human hepatocytes. The 8(5) Loop1R capsids transduced three different hepatocyte donors on average 25x better than AAV5. The 9(5) Loop1R capsid was markedly better than 8(5) Loop1R, with an average 70-fold increase in GFP expression versus AAV5, and an average of 210x fold increase in LacZ Activity versus AAV5. Interestingly, the mutants were de-targeted from mouse liver, but significantly enhanced in mouse lung. Seroreactivity assays revealed that the chimeric Loop1R mutants had very similar seroreactivities against IVIG compared to AAV5. Binding and internalization assays for 9(5) Loop1r versus 9(5) and AAV5 indicated that addition of the AAV9 VP1/VP2 unique regions significant decreased binding and overall amount of virus internalized. Nuclear vector copy assays showed that the amount of virus that entered the nucleus is far greater for both 9(5) and 9(5) Loop1R, suggesting that the addition of the AAV9 VP1/VP2 regions decreased the amount of binding and internalized virus, but enhanced the escape of the virus from the endosome which resulted in an overall increase in the number of vector copies in the nucleus. Further studies into the effects of different serotypes VP1 regions revealed significant changes in binding for each serotype tested when compared to AAV5. AAV8 and AAV9 VP1 chimeric AAV5 viruses decreased binding significantly compared to AAV5. However, no differences were noted in the overall amount of virus internalized. AAV6 VP1 chimeric variants instead increased binding to the cell surface. This data indicates that the VP1/VP2 could potentially have domains that are involved with binding and is corroborated with

data from the AAV5 library that showed mutations in the AAV5 VP2 region could also enhance binding to the cell surface. Finally, chimeric AAV6 and AAV5 variants with different sequences of the AAV5 VP1/VP2 swapped showed that having more of the AAV5 sequences near the VP2/VP3 junction could enhance yield of the virus, but significantly decreased transduction capabilities. In this study, we developed chimeric AAV5 variants with a Loop1R mutation that significantly had increased transduction in primary human hepatocytes and are very promising for use in human liver gene therapy.

4.2 Introduction

While directed evolution of AAV5 using random mutagenesis yielded AAV5 variants with enhanced liver transduction, the overall increase was not substantial enough to markedly change the landscape of potential capsids for liver diseases requiring transduction of a large percentage of hepatocytes in the human liver. The evolved AAV5 variants likely would only be able to enhance hemophilia A and B therapies and would have limited capability in treatment of liver diseases such as OTC deficiency or Crigler-Najjar. These mutants are still inadequate in terms of liver transduction when compared to more relevant engineered hepatotropic rAAV capsids, such as LK03 or NP59.^{156, 173} As such, further engineering of the AAV5 mutants was required. Previous experimental data detailing the binding and internalization of AAV5 mutants with a G257R, or Loop1R mutation, showed that receptor binding and endocytosis were significantly enhanced when compared to AAV5. There was no evidence to suggest the mutations were causing any differences in endosomal escape, cellular trafficking, or nuclear import. Structural analysis supported this theory as most mutations were on the surface of capsid and not involved in any regions that were characterized as important for endosomal escape.

Studies on AAV5 and other AAV serotypes have identified the VP1u to be critical for endosomal escape and cellular trafficking. In particular, the VP1u domain in the VP1 unique region has a phospholipase A-2 (PLA-2) domain that is necessary for efficient endosomal escape.⁶⁴ At extracellular and early endosomal conditions, the VP1u domain is folded inside of the AAV capsid. Once the pH drops in the late endosome, the VP1u unfolds, passes through the five-fold axis, and refolds on the outside of the capsid, allowing interaction between the lipase and endosomal membrane.⁶⁵ Additionally, the factor GPR108 has been identified to be crucial for endosomal escape, and the VP1u is thought to interact with GPR108 in the endosomal membrane. However, in those studies, AAV5 was the only virus where endosomal escape was independent of GPR108.⁹² This is likely signified by the divergent VP1u sequence for AAV5 that is only 68% identical to the VP1u sequence in other serotypes (Figure 24). Additionally, the VP1/VP2 sequences contain nuclear localization signals and other peptide motifs that are critical for cellular trafficking.

As such, rational engineering of AAV5 VP1 and VP2 unique regions could drastically enhance the transduction capabilities of our AAV5 Loop1R mutants. Combining the binding and internalization increases of the Loop1R mutation with increases in endosomal escape and/or cellular trafficking could lead to chimeric variants that are highly efficient in human liver cells. Additionally, due to the location of the VP1/VP2 regions, there likely will not be any significant increases in seroreactivity of the engineered mutants as the VP1/VP2 regions are presumably located within the virus in most conditions outside of the cell. This means that chimeric AAV5 variants containing the VP1/VP2 domains of more seroreactive viruses such as AAV8 or AAV9 will not have many non-AAV5 domains located on the surface of the capsid, thus minimizing the impact on changes in seroreactivity.

In this study, we rationally engineered AAV5 mutants using PCR based cloning to swap the VP1 and VP2 unique sequence of various AAV serotypes on to AAV5. Substantial increases in infectivity were observed following the “VP1 swap” on to AAV5 for serotypes 3, 8 and 9 (3(5), 8(5), and 9(5)). Further increases in transduction were noted when a G257R mutation was combined with the chimeric AAV5 viruses (8(5) Loop1R and 9(5) Loop1R) on Huh7 cells and primary human hepatocytes. The 9(5) Loop1R capsid exhibited significantly increases (70x for GFP and 210x for LacZ) in infectivity in primary human hepatocytes when compared to AAV5 and even 8(5) Loop1R. Experiments probing the binding, internalization, and nuclear localization of the vector genomes revealed that the “VP1 swaps” decreased binding, but significantly increased the amount of nuclear vector copies. The Loop1R further enhanced the internalization of the chimeric AAV5 capsids, resulting in viruses with significantly improved human liver transduction. Binding studies revealed that the “VP1 swaps” altered binding profiles of the capsids and indicated the presence of a novel uncharacterized binding domain in the VP1/VP2 common region. Seroreactivity assays confirmed that the chimeric Loop1R mutants had similar seroreactivity profiles compared to AAV5. The result was chimeric variants that were highly efficient at transducing human liver cells while also having extremely favorable seroreactivity.

4.3 Materials and Methods

AAV Library and Vector Production

Purified AAV vectors were produced via the triple transfection and cesium chloride density ultracentrifugation methods. Briefly, HEK293 cells were transfected with a helper plasmid, a self-complementary GFP (sc-GFP) or single stranded LacZ-nls vector plasmid, and a packaging plasmid containing capsid gene and an AAV2 rep gene. Cells were harvested 72 hours

post transfection and isolated by centrifugation. The media was collected and stored while the cell pellet was resuspended and subjected to three freeze thaw cycles. The resulting cell lysate was incubated with DnaseI and RnaseA at 37C and centrifuged and the supernatant was collected. The virus from the supernatant and the media were then concentrated by PEG precipitation followed by two rounds of cesium chloride (CsCl) density ultracentrifugation. CsCl fractions containing virus were determined by DNA dotblot and combined and dialyzed using 5% sorbitol in PBS. Dialyzed virus preparations were again titered using DNA dot blot with a probe specific to reporter gene. All viruses that were tested were titered in the same dotblot to allow consistent measurement of viral titers.

Generation of Chimeric AAV5 Variants

The VP1 unique and VP1/VP2 common region of AAV3b, AAV6, AAV8, and AAV9 were swapped into the AAV5 capsid through PCR based cloning. In brief, one set of primers amplified the VP3 gene to half of the ampicillin gene in the plasmid XR5, while the other set of primers covered the remaining half of the ampicillin gene to the end of the VP1/VP2 common region. PCR amplicons were purified and digested with DPNI (NEB, Ipswich, MA) and purified using gel purification via QIAquick Gel Extraction Kit (Qiagen, Hilden, Germany). The purified fragments were ligated together using blunt end ligation and transformed into DH10B competent cells. Transformed bacteria was then spread on an agar plate and allowed to grow overnight. Individual colonies were picked for DNA amplification and extraction. Extracted plasmids were then sent for sequencing to confirm proper swapping of the AAV VP1/VP2 regions.

The Loop1R mutation was incorporated using site directed mutagenesis. A primer containing the mutation was used with a primer that covered half the ampicillin gene to amplify half of the chimeric AAV5 mutant packaging plasmid. A primer set corresponding to the other

half of the plasmid was also used to amplify the opposing half of the plasmid. The two PCR amplicons were purified and digested with DPN1 (NEB, Ipswich, MA) and purified using gel purification via QIAquick Gel Extraction Kit (Qiagen, Hilden, Germany). The purified fragments were ligated together using blunt end ligation and transformed into DH10B competent cells. Transformed bacteria was then spread on an agar plate and allowed to grow overnight. Individual colonies were picked for DNA amplification and extraction. Extracted plasmids were then sent for sequencing to confirm proper incorporation of the mutation.

The primers and probes used are as follows: Loop1M-F:

CGACAGAAGCAACGCCAAC; Loop1M-R: ACGGAGCCGCTTTTGATCT; AMP-R:
ACTCACCAGTCACAGAAAAGCATC; AMP-F: ACTCAACCAAGTCATTCTGAGAATAG;
AAV5Vp1_15AA-F: CTGCAAATCCCAGCCCAACC; AAV6VP1_15AA-R:
AGGTTGTGGGTCGGGGACTG; AAV5Vp1_40AA-F: AAGGCTCGGACCGAAGAG;
AAV6VP1_40AA-R: TGTCTTGCCAATGCCCGAGG; AAV6(5) F:
CCTGGGGTGCCTAATGAGTG; AAV6VP1/2 R : TGTAGTAGGTCCCACAGCAGCG;
AAV5 VP3 F: ATGTCTGCGGGAGGTGGCGGC; AAV5 VP3 R:
CAGGGTTTTCCCAGTCACGA; AAV9-R: TGTAAGAGATCCCACACCTGAGGG; AAV8-
R: TGTATTAGGTCCCACACCAGAG

Transduction of Human Liver Cancer Cells by AAV Vectors

Chimeric AAV5 vectors were used to packaged sc-GFP reporter genes for comparison to wt-AAV5. Huh7 cells in 12 well plates were infected with AAV5 and mutant self-complementary(sc)-GFP encoding viruses at a MOI of 100,000 viral genomes(vg) per cell and co-infected with 5000 vg/cell of wt-ad5. Seventy-two hours after infection, cells were taken for fluorescent imaging and subsequent GFP quantification using the Fluorometric GFP

Quantification Kit (Cell BioLabs, San Diego, CA). GFP activity was normalized by protein concentration as measured by Pierce BCA Protein Assay Kit (ThermoFisher Scientific, Waltham, MA).

Transduction of Primary Human Hepatocytes by AAV Vectors

Primary human hepatocytes (TRL HUM4037, TRL HUM4016, TRL HUM4021, Triangle Research Labs, NC) were cultured according to vendor's instructions. In brief, cells were thawed and plated at 2.5×10^5 cells per well in collagen coated 24 well plates (BioCoat Collagen I 24 well plates, Corning, Corning, NY). The next day, the primary human hepatocytes were infected with purified sc-GFP vectors or ss-LacZnl vectors at a MOI of 500,000 vg per cell. Media was changed 48 hours after infection, and once daily afterwards. Ninety-six hours post infection, cells were taken for fluorescent imaging and subsequent GFP quantification using the Fluorometric GFP Quantification Kit from Cell Bio Labs (San Diego, CA). GFP activity was normalized by protein concentration as measured by Pierce BCA Protein Assay Kit (ThermoFisher Scientific, Waltham, MA). Cells infected by ss-LacZnl vectors were lysed and the resulting lysate measured for protein concentration using the Pierce BCA Protein Assay Kit (Thermo Fisher, Waltham, MA). Samples were diluted to similar protein concentrations. B-galactosidase enzyme activity in homogenized tissue lysates was measured using the Galacto-Star LacZ Assay Kit and readings were normalized by protein concentration.

Tissue Tropism of AAV Vectors in Mice after Systemic Administration

C57/BL6J mice were maintained in a 12-hr:12-hr light: dark artificial light cycle (0700-1900) at a temperature of 20C and a humidity of $55 \pm 5\%$. All animal protocols were approved by the University of North Carolina Animal Care and Use Committee. The chimeric AAV5 capsid

genes were used to package CB-LacZnl reporter gene which expresses B-galactosidase with a nuclear localization signal and compared to wt-AAV5. LacZ vectors were administered to eight-week-old male C57BL/6J mice by intravenous tail vein injection at a dose of 1×10^{12} vg per mouse. After three weeks, the mice were sacrificed, and tissues were collected, and flash frozen in liquid nitrogen cooled 2-methylbutane. Tissues were stored at -80°C until ready for use. Tissues were homogenized in lysis buffer from the Galacto-Star LacZ Assay Kit (Applied BioSystems, Foster City, CA) and measured for protein concentration using the Pierce BCA Protein Assay Kit (Thermo Fisher, Waltham, MA). Samples were diluted to similar protein concentrations. B-galactosidase enzyme activity in homogenized tissue lysates was measured using the Galacto-Star LacZ Assay Kit and readings were normalized by protein concentration.

AAV Neutralization Assays with Intravenous Immunoglobulin

Huh7 cells were seeded at 5×10^4 cells per well in a 96 well plate. The next day, 50 particles of wt-ad5 per cell was added to each well of the 96 well plate. AAV ss-CB-LacZnl vectors (1×10^9 vg) were incubated with reciprocal dilutions of IVIG (Carimune NF, ZLB Behring, King of Prussia, PA). The first well corresponded to 25ug of IVIG, and each subsequent well contained half of the previous amount of IVIG. The combined IVIG and AAV vector mixtures were incubated for 1 hour at 37°C and then added to individual wells of Huh7 cells in a 96 well plate. Virus concentration was kept the same for each reciprocal dilution of IVIG.

After 72 hours, the cells in each well were lysed and the crude lysate was assayed for lacZ activity using a Galacto-Star LacZ Assay Kit (Applied BioSystems, Foster City, CA). The LacZ activity was measured against a control well infected with only virus and no IVIG to obtain the percent of max LacZ expression at each reciprocal dilution for each virus. The percent of max LacZ activity was plotted against the log reciprocal dilution in GraphPad 8 to generate a

fitted curve using nonlinear regression. The corresponding EC50, or reciprocal dilution required for 50% max GFP activity, was calculated using GraphPad 8, and compared to the EC50 of AAV5 to determine the relative differences in seroreactivity to IVIG.

Binding and Internalization Assay of AAV Vectors in Huh7 Cells

Binding of the AAV capsid to the surface of Huh7 cells was determined by incubating 2e3vg/cell of CB-LacZnl5 AAV vector with pre-cooled Huh7 Cells at 4C for 30min. Then, the cells were washed with cold PBS three times to wash away any unbound vector. Cells were collected and resuspended in PBS. Total DNA was extracted using the DNeasy Blood and Tissue Kit (Qiagen, Hilden, Germany) and eluted with molecular grade water. The number of vector copies was determined in each sample via absolute qPCR quantification using primers and TaqMan probe specifically recognizing the CB-promoter sequence (Sigma Aldrich, St. Louis). The number of vector genomes was normalized to the number of endogenous glucagon gene copies. Internalization assay was performed similar to the binding assay, but instead allowing the bound virus to internalize at 37C for 1 hour. Cells were incubated with trypsin for 5 min at 37C to allow any un-internalized virus to be digested. After washing with PBS three times, total DNA was extracted from cells and eluted with molecular grade water. Vector copies was determined exactly the same as described before. Assays were performed on a 7300 Real-Time PCR system (Applied Biosystems) using GoTaq PCR Master Mix (Promega). The primers and probes used are as follows: CB-F: 5'-GTATGTTCCCATAGTAACGCCAATAG-3'; CB-R: 5'-GGCGTACTTGGCATATGATACT-3'; CB Probe: 5'-FAM-TCAATGGGTGGAGTATTTA-MGB-3'; Glucagon-F: 5'-AAGGGACCTTTACCAGTGATGTG-3'; Glucagon-R: 5'-ACTTACTCTCGCCTTCCTCGG-3'; Glucagon Probe: 5'-FAMCAGCAAAGGAATTCA-MGB-3'.

Modified Internalization and Nuclear Localization Assays

Huh7 cells were incubated with 2e3vg/cell of CB-LacZnl AAV vector for 4 hours. For the modified internalization assay, cells were incubated with trypsin for 5 min at 37C to allow any un-internalized virus to be digested. After washing with PBS three times, total DNA was extracted from cells and eluted with molecular grade water. For the nuclear localization, cells were incubated with trypsin for 5 min at 37C to digest any un-internalized virus. After washing with PBS three times, cells were incubated with hypotonic buffer for 15 minutes on ice. 5 ul of 10% NP40 was added to the cells and vortexed for 10 seconds. The homogenate was centrifuged at 4C for 10min at 3000rpm. 200 ul of hypotonic buffer + 0.5% NP40 was added to the pellet and vortex for 10 second and spun down again at 4C at 3000rpm for 10 min. This process was repeated once more. The nuclei were then taken for total DNA extraction. Nuclei fractions were verified to be free of cytoplasmic contamination using GADPH. DNA gel electrophoresis and PCR were used to confirm presence of genomic DNA. The number of vector copies was determined in each sample via absolute qPCR quantification using primers and TaqMan probe specifically recognizing the CB-promoter sequence (Sigma Aldrich, St. Louis). The number of vector genomes was normalized to the number of endogenous glucagon gene copies. Assays were performed on a 7300 Real-Time PCR system (Applied Biosystems) using GoTaq PCR Master Mix(Promega). The primers and probes used are as follows: CB-F: 5'-GTATGTTCCCATAGTAACGCCAATAG-3'; CB-R: 5'-GGCGTACTTGGCATATGATACT-3'; CB Probe: 5'-FAM-TCAATGGGTGGAGTATTTA-MGB-3'; Glucagon-F: 5'-AAGGGACCTTTACCAGTGATGTG-3'; Glucagon-R: 5'-ACTTACTCTCGCCTTCCTCGG-3'; Glucagon Probe: 5'-FAMCAGCAAAGGAATTCA-MGB-3'.

Statistics

Statistical analyses were conducted with GraphPad Prism 8. All statistical analyses were justified as appropriate and p-values <0.05 were considered statistically significant. For all statistical tests performed, intra-assay variation fell within the expected range and the variance across groups was similar. Comparison of experimental values from two groups were assessed using a Student's unpaired two-tailed t test. Experimental values for IVIG neutralization assays were first normalized and then plotted against the log transformed values for reciprocal dilutions before being compared using an Extra sum of squares F test.

4.4 Results

Engineering the VP1/VP2 regions of AAV5 and AAV5 Loop1R Mutants

In order to potentially enhance endosomal escape and cellular trafficking, the VP1 genes sans the VP3 coding sequences were taken from other AAV serotypes and swapped on to wt-AAV5. The sequences encoding the VP1 and VP2 unique regions of packaging plasmids containing hepatotropic AAV serotypes 3b, 8, and 9 capsids were amplified and cloned into an wt-AAV5 packaging plasmid using PCR based cloning (Figure 23). Forward and reverse primers were designed to facilitate easy swapping of the VP1/VP2 regions from one plasmid to another. The same packaging plasmid backbone and rep gene were used for each of the viruses to minimize any differences in vector production quality affecting transduction efficacies. Sited directed mutagenesis was used to clone the G257R mutation (Loop1R mutation) in to the VP1 swapped chimeric AAV5 viruses (Figure 23). Six chimeric AAV capsids were generated, three with swapped VP1 regions (3(5), 8(5), 9(5)), and three with swapped VP1 regions and a G257R

mutation (3(5) Loop1R, 8(5) Loop1R, 9(5) Loop1R) that were taken for characterization in Huh7 cells and primary human hepatocytes.

Characterization of the Chimeric VP1 swapped Loop1R Mutants

We next investigated the transduction efficacy of the six chimeric capsids in Huh7 cells, a human hepatocarcinoma cell line. We have previously found this cell line to be a robust predictor of AAV transduction in primary human hepatocytes. We first characterized 3(5) and 3(5) Loop1R, which both have AAV3b's VP1 and VP2 unique regions and either a wt-AAV5 VP3 (3(5)) or a mutated AAV5 VP3 with a G257R mutation (3(5) Loop1R). Huh7 cells were transduced with sc-GFP vectors packaged by AAV5, 3(5), and 3(5) Loop1R at a MOI of 1e5vg per cell and co-infected with 5000 vg/cell of wt-Ad5 to accelerate the process of transgene expression. Imaging of GFP expression in infected Huh7 cells revealed that 3(5) was substantially better at transducing Huh7 cells versus wt-AAV5 (Figure 25A). Swapping the AAV3b VP1/VP2 domains onto AAV5 increased infectivity in Huh7 cells roughly 22-fold (Figure 25B and 25C). Adding the Loop1R mutation further enhanced transduction, leading to a 350-fold increase over AAV5 and a 16-fold increase over 3(5) (Figure 25A-C). However, low yields and titers during production of the 3(5) Loop1R capsid prevented further characterization of the capsid as it was difficult to produce enough virus for future experiments. Interestingly, the yield issue only occurred with the 3(5) Loop1R capsid, and not with 3(5), indicating that the Loop1R mutation was unstable when combined with AAV3b VP1 and VP2 (data not shown). This issue was not found in either the AAV8 or AAV9 chimeric capsids.

Huh7 cells were then transduced with sc-GFP vectors packaged by AAV5, 8(5), 8(5) Loop1R, 9(5), and 9(5) Loop1R. Swapping AAV8 and AAV9 VP1/VP2 unique domains on to AAV5 resulted in similar trends regarding increases in transduction when compared to the

AAV3b chimeric variants (Figure 26A). The AAV8 VP1/VP2 swap alone (8(5)) increased infectivity in Huh7 cells by roughly 55-fold, with AAV9 VP1/VP2 swap (9(5)) increasing infectivity by 50-fold (Figure 26B and 26C). There was no significant difference between 8(5) and 9(5), indicating that the activity of those domains in Huh7 cells was similar (Fig 26B). After the addition of the Loop1R mutation, both 8(5) Loop1R and 9(5) loop1R saw drastic increases in infectivity. Both the 8(5) Loop1R and 9(5) Loop1R capsids increased transduction by roughly 2x fold over 8(5) and 9(5) (Figure 26B). Overall, 9(5) Loop1R was the best performing capsid, but was only slightly better in Huh7 cells when compared to 8(5) Loop1R.

We first tested the 8(5) and 8(5) Loop1R capsids against wt-AAV5 in donor primary human hepatocytes (TRL 4037). Using the same sc-GFP vectors as before, a MOI of 5e5vg was added to the hepatocytes. Ninety-six hours after infection, hepatocytes were taken for GFP imaging and quantification. Imaging of GFP expression in the hepatocytes revealed similar trends, but less markedly differences in the overall increase in infectivity when compared to Huh7 cells (Figure 27A). The 8(5) capsid had 12-fold higher GFP expression compared to wt-AAV5 while 8(5) Loop1R had 31-fold higher GFP expression (Figure 27B and 27C). The overall fold increase between AAV5 and 8(5) and subsequently AAV5 and 8(5) Loop1R was much lower in primary human hepatocytes when compared with Huh7 cells (31x vs 110x). The ~2.5-fold difference between 8(5) and 8(5) Loop1R in hepatocytes was consistent with the 2-fold difference found in Huh7 cells, indicating that the increase provided by the Loop1R mutation was consistent across both cell lines. However, the difference between AAV5 and 8(5) was not consistent (50x in Huh7 vs 12x in hepatocytes) and could potentially be attributed to differences in expression of factors required for endosomal escape. In total, the 8(5) Loop1R capsid was tested in three different sets of primary human hepatocytes (TRL 4037, 4016, 4021) to determine

if the capsid would behave in hepatocytes from different donors. For each set of primary hepatocytes, 8(5) Loop1R significantly enhanced GFP expression when compared to AAV5 (Figures 25B, 25D, and 25E). Across the three sets, 8(5) loop1R increased transduction by an average of 25-fold (Figure 27F). We also compared 8(5) Loop1R to XL32.1, which is an evolved-DNA shuffled AAV capsid that has been validated in both primary human hepatocytes and also non-human primates to be efficient at transducing hepatocytes. The XL32.1 capsid was still significantly better at transducing human hepatocytes when compared to 8(5) Loop1R, indicating that the chimeric capsids likely would need more engineering before being able to compete with the best of the hepatotropic capsids (Figure 27B and 27C).

Next, 9(5) Loop1R was similarly tested in primary human hepatocytes. Surprisingly, 9(5) Loop1R exhibited far greater increases in transduction in primary human hepatocytes when compared to 8(5) Loop1R (Figure 28A). This was observed in two different sets of human hepatocytes (TRL 4021, 4016), in which 9(5) Loop1R provided 3-fold greater GFP expression when compared to 8(5) Loop1R (Figure 28B). The quantification of the difference between 9(5) Loop1R and AAV5 was accomplished using two different quantification methods, a GFP fluorescence assay and a LacZ-activity chemiluminescent assay. Both methods revealed that 9(5) Loop1R had markedly increased infectivity in primary human hepatocytes, with LacZ indicating a larger difference between AAV5 and 9(5) Loop1R (Figures 28C and 28D). Across two sets of primary human hepatocytes, 9(5) Loop1R transduction was on average 70-fold greater than AAV5 transduction for the GFP method, and on average 210-fold with the LacZ method (Figure 28E).

B-galactosidase (LacZ) reporter gene vectors were packaged by four chimeric AAV5 variants, 8(5), 9(5), 8(5) loop1R , and 9(5) loop1R and tested against AAV5 in C57BL/6 mice. A

total of 1×10^{12} vg was intravenously injected into each mouse to test for any alterations in infectivity in mouse liver or lung. Three weeks post injection, the mice were sacrificed, and their livers and lungs were harvested and assessed for LacZ expression through x-gal staining and LacZ activity assays. LacZ staining revealed marked decrease in mouse liver transduction for the Loop1R chimeric variants, suggesting that the combination of the VP1 swap and the Loop1R mutation caused a de-targeting of the mouse liver (Figure 29A). Interestingly, the VP1 swap alone did not seem to alter mouse liver transduction markedly. Significant increases in mouse lung transduction were noted for the Loop1R chimeric variants, with both 8(5) Loop1R and 9(5) Loop1R exhibiting far greater LacZ staining when compared with AAV5 (Figures 29A). The 8(5) loop1R and 9(5) loop1r capsids increased mouse lung transduction by 15-fold and 17-fold, respectively (Figures 29B and 29C).

Assessing Seroreactivity of Chimeric Loop1R AAV5 viruses with pre-existing antibodies in Pooled Human IgGs

We then assessed the seroreactivity of our chimeric Loop1R viruses to IVIG. Seroreactivity was investigated using a neutralizing assay that utilized intravenous immunoglobulin (IVIG) that is pooled from thousands of donors. Curve fitting of the transformed and normalized data from the IVIG neutralization assay allowed for the comparison of seroreactivity between AAV5 and 8(5) Loop1R and 9(5) Loop1R. The IVIG neutralizing assay revealed that the chimeric Loop1R mutants had similar seroreactivities against IVIG compared to AAV5 (Figure 30). There were no significant differences between the fitted curve for AAV5 when compared to those of 8(5) Loop1R and 9(5) Loop1R.

Assessing the Mechanisms Behind VP1/VP2 Swaps

We next investigated the changes in binding and internalization as a result of swapping the AAV9 VP1/2 onto the AAV5 capsid and the inclusion of the Loop1R mutation. We first probed the binding differences between AAV5, 9(5), and 9(5) Loop1R and were surprised to find that both 9(5) and 9(5) Loop1R had significant decreases in binding when compared to AAV5 (Figure 31A). Additionally, the overall amount of virus that was internalized was significantly reduced for both viruses when compared to AAV5 (Figure 31B). However, 9(5) Loop1R significantly increased the amount of internalized virus when compared to 9(5) (Figure 31B). As a result, there was no significant difference between 9(5) Loop1R and AAV5 for the percentage of bound virus that was internalized (Figure 31C). Interestingly, the % of bound virus that was internalized for 9(5) was lower than that of AAV5, even though in transduction assays 9(5) was by far superior to AAV5 (Figure 31C). In general, the results of the internalization assay general did not match the results from the transduction assay, indicating that the “static” conditions of the binding assay and internalization were not sufficient to probe all of the differences between the viruses.

As such, we modified the internalization assay to allow binding rates and receptor turnover to play more of a role. Instead of the system where any unbound virus was washed off, we allowed the unbound virus to remain as part of a more realistic dynamic system where internalization rates and receptor turnover heavily influence the amount of virus. We also increased the amount of time the virus could be internalized from 1 hour to 4 hours. As a result, there was more than a 6-fold difference between 9(5) Loop1R and AAV5 in terms of virus internalized that was not previously seen in the binding and internalization assays (Figure 31D and 31G). Interestingly, the amount of 9(5) virus that was internalized was still far less when

compared to AAV5 (Figure 31D and 31F), indicating that the key to the overall increase in transduction for 9(5) was for a process post receptor internalization, which matched our initial hypothesis that swapping the AAV VP1/VP2 regions on to AAV5 could result in increased endosomal escape or cellular trafficking. In order to probe the differences between the capsids post receptor internalization, we infected Huh7 cells with the viruses and allowed internalization for 4 hours, similar to the internalization assay. We then isolated the nuclei from the cells and extracted total DNA for quantification of nuclear vector copies. The assay revealed that both 9(5) and 9(5) Loop1R had significantly more nuclear vector copies when compared to AAV5 which matched the transduction data well (Figure 31E). In particular, the nuclear vector copy data demonstrated that the fold increase in nuclear copies for both 9(5) and 9(5) Loop1R were far greater than their fold changes in overall internalized virus, indicating significant increases in either endosomal escape or cellular trafficking for the AAV9 VP1/VP2 swapped viruses when compared to AAV5 (Figure 31G).

We observed from the binding assays that the AAV9 VP1/VP2 swap decreased binding to the cell surface, and thus were interested to see whether the VP1/VP2 regions of other serotypes would provide similar changes in binding. We tested binding of chimeric AAV5 variants with the VP1/VP2 of AAV6, AAV8, and AAV9. Interestingly, both AAV8 and AAV9 VP1/VP2 caused similar decreases in binding when compared to wt-AAV5 (Figure 32A). However, 6(5), the chimeric AAV5 variant with AAV6 VP1/VP2, exhibited significant increases in binding relative to AAV5 (Figure 32B). This data suggests that the VP1/VP2 could potentially have domains that are involved with binding different factors and is corroborated with data from previous studies that showed a mutation in the AAV5 VP1/VP2 region could also enhance binding to the cell surface. Interestingly, 8(5) Loop1R bound to the cell surface much less

compared to 9(5) Loop1R even though 8(5) and 9(5) showed similar decreases in binding relative to AAV5(Figure 32C). No differences were found in the amount of virus internalized (Figure 32D). The difference in binding could partially explain the differences between 8(5) Loop1R and 9(5) Loop1R in transduction of Huh7 cells and human hepatocytes.

The alterations to binding due to the presence of different AAV VP1/VP2 domains was unexpected, and we decided to further investigate the role the VP1/VP2 common region plays in infection for our chimeric AAV capsids. We modified 6(5) into two different variants by replacing certain amino acids in the AAV6 VP1/VP2 with wt-AAV5 sequences; one with 15 amino acids replaced of the AAV6 VP2 near the VP3 start codon (6(5) 15AA) and the other with 40 amino acids replaced (6(5) 40AA) (Figure 33A). Production of 6(5), 6(5) 15AA, and 6(5) 40AA viruses revealed that higher yields were obtainable from the 6(5) 15AA and 6(5) 40AA capsids when compared to 6(5) (Figure 33C). Interestingly, when these three viruses were tested on Huh7 cells, dramatic decreases in infectivity were observed for 6(5) 15AA and 6(5) 40AA when compared to 6(5) (Figure 33B). The GFP expression observed from 6(5) 15AA was much stronger when compared to 6(5) 40AA. Binding assays revealed that both 6(5) 15AA and 6(5) 40AA had significantly decreased binding to Huh7 cells when compared to 6(5) but were no different from each other (Figure 33D, Left Panel). Internalization assays further revealed that the 6(5) 15AA and 6(5) 40AA viruses had deficiencies in internalization when compared with 6(5) (Figure 33D, Center Panel). Similar to the transduction results, 6(5) 40AA internalized significantly less versus 6(5) 15AA, leading to a significant difference in the percentage of bound virus that was internalized between the two viruses (Figure 33D, Right Panel). Overall, the replacement of AAV6VP1/VP2 amino acids with wt-AAV5 caused a decrease in binding ability, but more importantly resulted in lower percentages of the virus with the ability to

internalize. This data further suggests that there may be a binding domain in the VP1/VP2 common region, but additionally that the VP1/VP2 has domains that are also important with internalization as well.

4.5 Discussion

Studies on factors that are critical for AAV entry consistently characterize AAV5 as an outlier, likely due to its highly divergent sequence compared to other AAV serotypes. AAV5 differs greatly from other serotypes particularly in factors influencing internalization and subsequent endosomal escape. AAV5 interacts with AAVR via VR-II and VR-IV in contrast to VR-I and VR-III for other AAV serotypes, indicating an evolutionary difference in receptor engagement for internalization.⁸⁸ Additionally, AAV5 is the only serotype that can internalize independently of clathrin-coated vesicles.⁸⁴ The most significant difference may be AAV5's ability to facilitate endosomal escape independently of GPR108; it was found to escape the endosome through some other unknown pathway.⁹² Most AAV serotypes are thought to interact with GPR108 via highly conserved residues in the VP1u region. However, sequence alignments revealed that the AAV5 VP1u sequence is divergent from other serotypes (Figure 24), which could suggest that differences in phospholipase activity or GPR108 engagement are leading to the low infectivity of AAV5 when compared to other commonly used serotypes. Due to these differences in the VP1u, we believed that swapping the entire VP1/VP2 unique and common regions of AAV5 to that of other serotypes could enhance the ability of AAV5 to escape the endosomal and traffic to the nucleus. This could potentially synergize with our Loop1R mutants, that we had previously described as having increased binding and internalization. Swapping the VP1/2 of AAV3b, AAV6, AAV8, and AAV9 on to wt-AAV5 all revealed substantial increases in infectivity in Huh7 cells. Interestingly, the same study that discovered GPR108 tested an

AAV5 capsid with the VP1u region of AAV2 and found that this virus was able to utilize GPR108 but did not observe any substantial increases in infectivity. This indicates that the VP2 portion is critical to the increase in transduction that we observed from our chimeric AAV5 viruses, and without that section our viruses may not have been as effective, as was observed in the aforementioned study. The VP2 protein is particularly interesting as some studies have suggested that it is not essential for transduction. An AAV2 capsid with only VP1 and VP3 proteins was shown to have similar transduction profiles when compared to wt-AAV2, suggesting that the VP2 protein itself was not needed.⁴⁵ However, the sequences seem to certainly be very important as our study has shown, but the exact role of VP2 in the overall scheme of AAV transduction is not understood.

Addition of the Loop1R mutation to the VP1 swapped mutants did indeed further increase infectivity in liver cells as originally theorized. However, not every serotype's VP1 was stable with the AAV5 Loop1R mutation. The yield of the chimeric variants with the AAV3b and AAV6 VP1 swaps and Loop1R mutations were significantly lower indicating the viral capsids were unable to assemble and package DNA as well. The yield of 3(5) Loop1R was roughly 10-fold lower compared to 3(5) and 6(5) Loop1R was roughly 100-fold lower than 6(5) (data not shown). It appeared that the AAV6 VP1 could not tolerate the Loop1 mutation, which was striking as their locations in the capsid structure is were fairly far apart and no previous interactions had been discovered between the VP1 and Loop1. In fact, the Loop1R mutation also did not work when mutated into the wt-AAV6 capsid, indicating that the problem did not involve the sequences of AAV5. It is unclear why the Loop1R mutation does not work with the AAV6 VP1/2 unique and common sequences. The Loop1R mutation had little effect on yield when combined with the AAV8 and AAV9 VP1/VP2. This raises the question on why AAV8 and

AAV9 can tolerate the mutation, but AAV3 and AAV6 cannot, as the sequences of the VP1 for each serotype aside from AAV4 and AAV5 are very extremely similar.

Transduction-wise, the two mutations, the Loop1R and the VP1 swap, were not multiplicatively synergistic together in increasing transduction for either 8(5) Loop1R or 9(5) Loop1R. In Huh7 cells, it seemed that dominant mutation was the altered VP1 swap, which provided roughly a 50-fold increase in infectivity over wt-AAV5 whereas the Loop1R mutation only provided a 7-8 fold increase in infectivity. Combination of the two only resulted in an overall 2-fold increase in infectivity, which was lower than what we expected. Different results played out in primary human hepatocytes, with the AAV8 and AAV9 VP1/VP2 only increasing infectivity by 10-fold, a large decrease in comparison to the results from Huh7 cells. This difference in infectivity provided by the VP1 swaps could be due to differences in GPR108 expression in Huh7 cells versus primary human hepatocytes. If Huh7 cells have a higher innate expression of GPR108 compared to human hepatocytes, it could lead to more efficient endosomal escape of the virus, leading to the large difference in transduction efficiency between the two cell lines for 8(5) and 9(5). Differences in receptor binding leading to different amounts of viral accumulation in the endosome could also contribute to the observed difference. 8(5) Loop1R had an overall average of a 2.5-fold increase in infectivity over 8(5) in hepatocytes, which was very similar to the 2-fold increase observed in Huh7 cells. However, 9(5) Loop1R unexpectedly performed better than 8(5) Loop1R in primary hepatocytes, resulting in a transduction increase of over 3-fold versus 8(5) Loop1R in two separate human hepatocyte donors. This was particularly surprising because 9(5) Loop1R was only marginally better than 8(5) Loop1R at transducing Huh7 cells. Subsequent binding assays comparing 9(5) Loop1R and 8(5) Loop1R revealed that 9(5) Loop1R had higher binding to the cell surface, which could be a

potential explanation as to why 9(5) Loop1R is better than 8(5) Loop1R. It is plausible that the receptor in which 9(5) Loop1R has increased binding to has higher expression on human hepatocytes. However, that likely is not the entire story as we did not test whether the AAV9 VP1 conferred enhanced ability to escape the endosome or cellular trafficking compared to the AAV8 VP1. Further studies into the differences in functionality between each serotype's VP1/VP2 would be needed in order to understand why some VP1/VP2 regions behave differently in different cells.

Contrary to our expectations, we found that the addition of the AAV9 VP1 swap decreased binding to the cell surface with and without the Loop1R mutation. However, there was no difference in binding between 9(5) and 9(5) Loop1R, which was interesting as we previously established that the Loop1R mutation was able to significantly confer greater binding compared to the wt-AAV5 VP3. It is plausible that the decrease in binding caused by the AAV9 VP1 could overrule the binding increase of the Loop1R mutation, leading to a net negative in binding. This is particularly interesting as no known binding domains that have been characterized in the VP1 unique and VP1/VP2 common regions thus far. The swapping of other serotype's VP1/VP2 segments such as AAV6 and AAV8 also resulted in changes in binding, where the AAV6 VP1/VP2 conferred an increase in binding and the AAV8 VP1/VP2 decreased binding similar to the AAV9 VP1/VP2. The increase and decrease of binding depending on the serotype highly suggests that a variable binding domain is located in the VP1/VP2 segment, most likely near the junction between the VP2/VP3 which would be near the five-fold axis of symmetry. This region has not been resolved by x-ray crystallography, and it is unknown if it lies on the exterior or interior of the capsid. Our data would suggest that this region is near or on the surface of the capsid due to its ability to affect binding. A previously characterized Q179R mutation in the

VP1/VP2 common region of AAV5 also increased binding to the cell surface, adding further evidence to our theory that some portion of the VP1/VP2 common region near the VP2/VP3 junction is near the surface of the capsid.

We decided to investigate which section of the VP1/VP2 common region was necessary for the increase in binding affinity to the cell surface. We engineered 6(5) 15AA and 40AA, which have portions of the wt-AAV5 sequence in the VP1/VP2 common that end at the VP3 start codon. Binding assays revealed both 6(5) 15AA and 6(5) 40AA had similar decreases in binding compared to 6(5), which indicated that there certainly was an important domain for binding near the VP2/VP3 junction. There was no difference between the 40AA and 15AA versions, which indicated that the domain was at least partially located within the last 15 amino acids of the VP1/VP2 common region. It is also possible that this domain extends into the N terminus of the VP3. This domain may not necessarily be the only domain affecting binding as 6(5) 15AA and 40AA were still better at binding compared to wt-AAV5. It is possible that there are other domains in the VP1/VP2 common region that affect binding. The seroreactivity data comparing 8(5) Loop1R and 9(5) Loop1R also corroborate our theory that a portion of the VP1/VP2 common region is exposed outside the capsid. Previous experiments showed that AAV5 with the Loop1R mutation was slightly less seroreactive compared to wt-AAV5. However, with the inclusion of the VP1 swaps for both AAV8 and AAV9, the resulting chimeric capsids are no different in seroreactivity versus wt-AAV5, potentially indicating that portions of the AAV8 and AAV9 VP1/VP2 common region are on the surface. However, we also cannot rule out the possibility that the swapped VP1/VP2 regions are causing a conformational change in the AAV5 capsid structure that alters binding with one or more of its receptors, leading to the observed changes in binding for each chimeric capsid. The increase in yield after replacing 15

and 40 amino acids in the AAV6 VP2 could be an indication that the full AAV6 VP1/VP2 decreases the stability of the capsid, which could also have implications in the conformational changes that the AAV5 capsid goes through for successful infection. Alterations in the structure of the capsid and its ability to bind multiple receptors could facilitate increases or decreases in cell adhesion if the AAV capsid can or cannot conform to allow binding of one or more receptors.

We did not expect internalization also to be significantly affected by the VP1 swap, as at the time of designing the capsids there was only information on the role of the VP1u in endosomal escape. Overall, the AAV9 VP1 dramatically decreased the internalization of the virus, which is seemingly inconsistent with the results of transduction studies in which 9(5) was 50-fold better vs AAV5. Even the addition of the Loop1R mutation, which supposedly increases both binding and internalization, did little to change the amount of internalized virus. Interestingly, experiments that determined the specific regions within the 6(5) capsid that are important for the altered binding also revealed importance of these regions for internalization. The 6(5) 15AA capsid had significantly decreased internalized virus compared to 6(5). Increasing the amount of replaced amino acids to 40 further decreased the internalized virus even compared to 15AA, suggesting that the 40 amino acids before the VP3 start codon in the VP1 and VP2 proteins were essential for internalization. Again, it is unclear if the replacement of the AAV6 sequences directly impacted internalization, or whether it prevented a conformational change occurring to the capsid to facilitate entry. However, this data is consistent with previous results from other groups in which an AAV5 capsid with the AAV2 VP1u domain did not show enhanced infectivity compared to wt-AAV5. Their capsid did not have the AAV2 VP1/VP2 common region sequences which could be the reason no difference was observed in their study.

The difference in internalization should not be attributed to differences in extrusion of the VP1u as this process theoretically should have no effect on entry of the virus.

We were able to confirm that swapping the AAV9 VP1/VP2 onto wt-AAV5 likely enhanced transduction through an increase in either endosomal escape or trafficking to the nucleus. A substantial increase in the fold change of nuclear localized virus versus internalized virus suggested that even though the AAV9 VP1 decreased the amount of virus that internalized, the total amount that was able to escape the endosome and localize to the nucleus increased, hence resulting in the overall net gain in transduction. The decrease in binding also provides another opportunity to engineer the 9(5) Loop1R capsid. Rational engineering methods or directed evolution can be utilized to further increase the binding of the 9(5) Loop1R capsid in order to further enhance transduction in the liver. Specifically targeting the VP2/VP3 region could also prove to be an effective strategy in enhancing the 9(5) Loop1R capsid. However, due to its likely position on the surface, careful selection of the sequences must be applied to evade increases in seroreactivity of the capsid.

In summary, we developed a chimeric AAV5 capsid with significantly increased liver transduction versus AAV5 by swapping in VP1/VP2 region of other AAV serotype and complementing it with the Loop1R mutation. The engineered capsid had decreased binding in comparison to AAV5, but significantly enhanced internalization and endosomal escape. This resulted in a capsid with a greater than 80-fold increase in transduction over AAV5, but similar seroreactivities, rendering it an ideal candidate capsid for liver gene therapy. This capsid has the potential to enhance existing liver gene therapies but requires more careful characterization in appropriate animal models such as non-human primates.

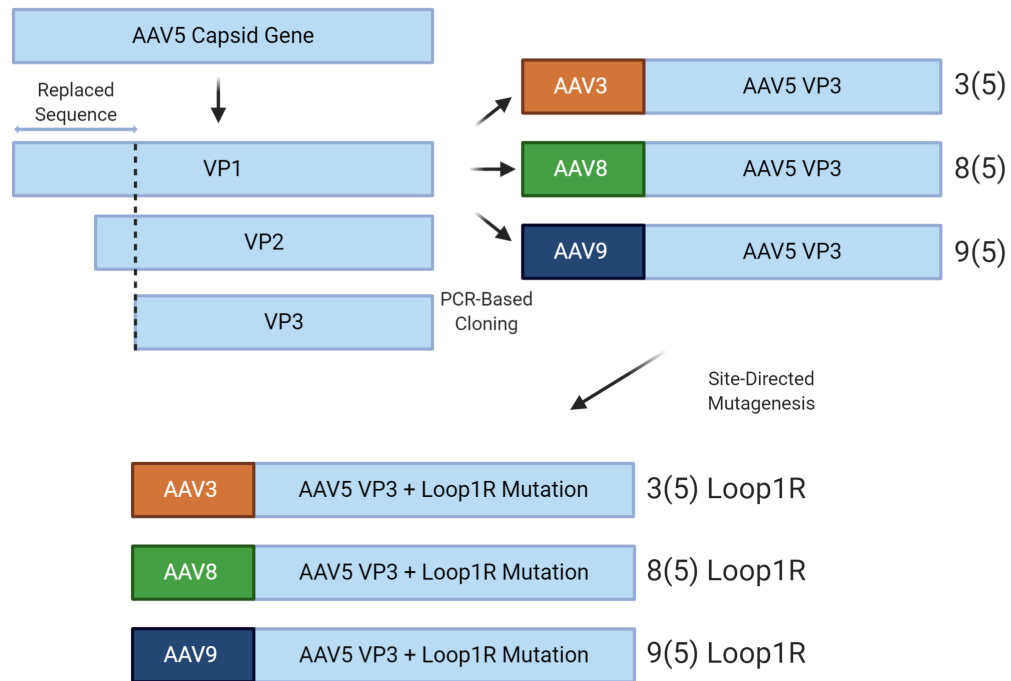


Figure 23. Diagram of Swapping the AAV5 VP1/VP2 unique regions

Process of constructing 3(5) Loop1R, 8(5) Loop1R, and 9(5) Loop1R. The VP1/VP2 common regions and the VP1 unique region on WT-AAV5 were replaced with the equivalent amino acid sequence from AAV3, AAV8, and AAV9. The Loop1R mutation was added by site directed mutagenesis. Figure made with Biorender.

AAV1	53	LGPFNGLDKGEPVNAADAAALEHDKAYDQQLKAGDNPYLRYN
AAV6	53	LGPFNGLDKGEPVNAADAAALEHDKAYDQQLKAGDNPYLRYN
AAV2	53	LGPFNGLDKGEPVNEADAAALEHDKAYDRQLD ^S GDNPYLKYN
AAV3	53	LGP ^G FNGLDKGEPVNEADAAALEHDKAYDQQLKAGDNPYLKYN
AAV3B	53	LGP ^G FNGLDKGEPVNEADAAALEHDKAYDQQLKAGDNPYLKYN
AAV7	53	LGPFNGLDKGEPVNAADAAALEHDKAYDQQLKAGDNPYLRYN
AAV8	53	LGPFNGLDKGEPVNAADAAALEHDKAYDQQL ^Q AGDNPYLRYN
AAV4	52	LGP ^G FNGLDKGEPVNAADAAALEHDKAYDQQLKAGDNPYLKYN
AAV5	52	LGP ^G FNGLD ^R GEPVNR ^A DEVA ^R EHDI ^S YNE ^Q LEAGDNPYLKYN
AAV9	53	LGP ^G FNGLDKGEPVNAADAAALEHDKAYDQQLKAGDNPYLKYN

AAV Phospholipase A2 Domain

Figure 24: Alignment of Phospholipase A2 Domain for AAV Serotypes 1-9

Amino acid sequence of domain related to phospholipase A2 was aligned for each serotype using XAlign. Yellow indicates amino acid is the same for every variant. Green indicates that one or more serotypes has a differing amino acid that is similar to the blue highlighted amino acids. The white highlight indicates that the serotype has a differing amino acid that are non-similar compared to the blue highlighted amino acids from the other serotypes. Alignment of AAV5 versus other serotypes reveals marked divergence from other AAV serotypes in the PLA2 domain.

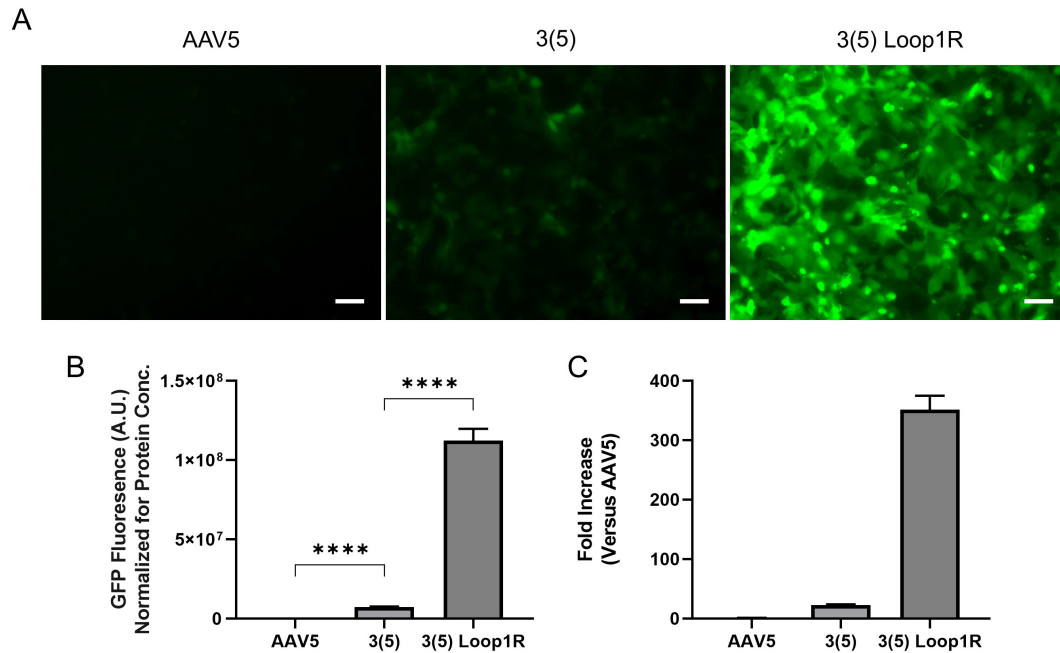


Figure 25: AAV5 versus 3(5) and 3(5) Loop1R in Huh7 Cells

(A) Fluorescent imaging of Huh7 cells transduced with self-complementary GFP vectors with AAV5, 3(5), 3(5) Loop1R. Huh7 cells were transduced at a MOI of 1e5 vg/cell. Images were taken 96 hours after infection. Expression of GFP (green) indicates transduced cells. 10x magnification. Scale Bar: 100um. (B) Comparison of normalized GFP expression in Huh7 cells. Data are shown as mean values \pm SD. ****p<0.0001. ns = no significance (C) Fold increase in infectivity over wt-AAV5. Data are shown as mean values \pm SD.

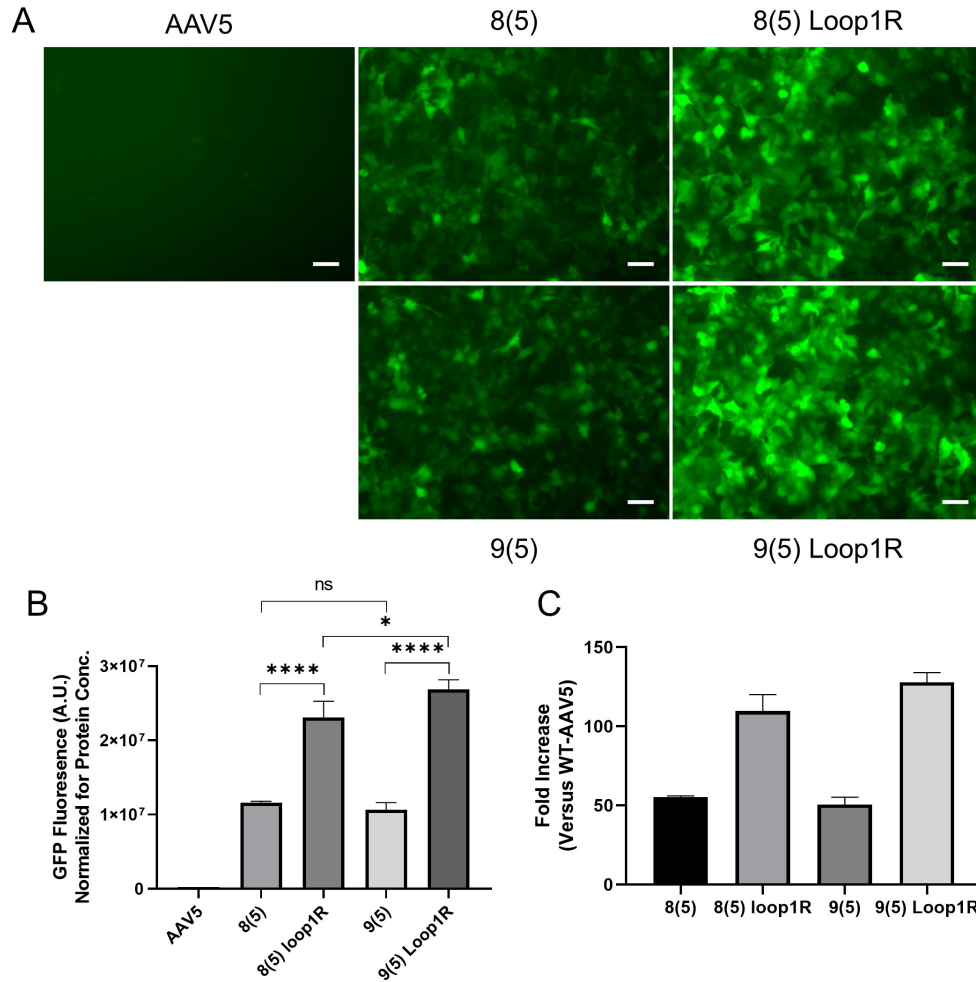


Figure 26: 9(5) Loop1R vs 8(5) Loop1R in Huh7 Cells

(A) Fluorescent imaging of Huh7 cells transduced with self-complementary GFP vectors with AAV5, 8(5), 9(5), 8(5) Loop1R, and 9(5) Loop1R. Huh7 cells were transduced at a MOI of $1e5$ vg/cell. Images were taken 96 hours after infection. Expression of GFP (green) indicates transduced cells. 10x magnification. Scale Bar: 100 μ m. (B) Comparison of normalized GFP expression in Huh7 cells. Data are shown as mean values \pm SD. * $p < 0.05$; **** $p < 0.0001$. ns = no significance (C) Fold increase in infectivity over wt-AAV5. Data are shown as mean values \pm SD.

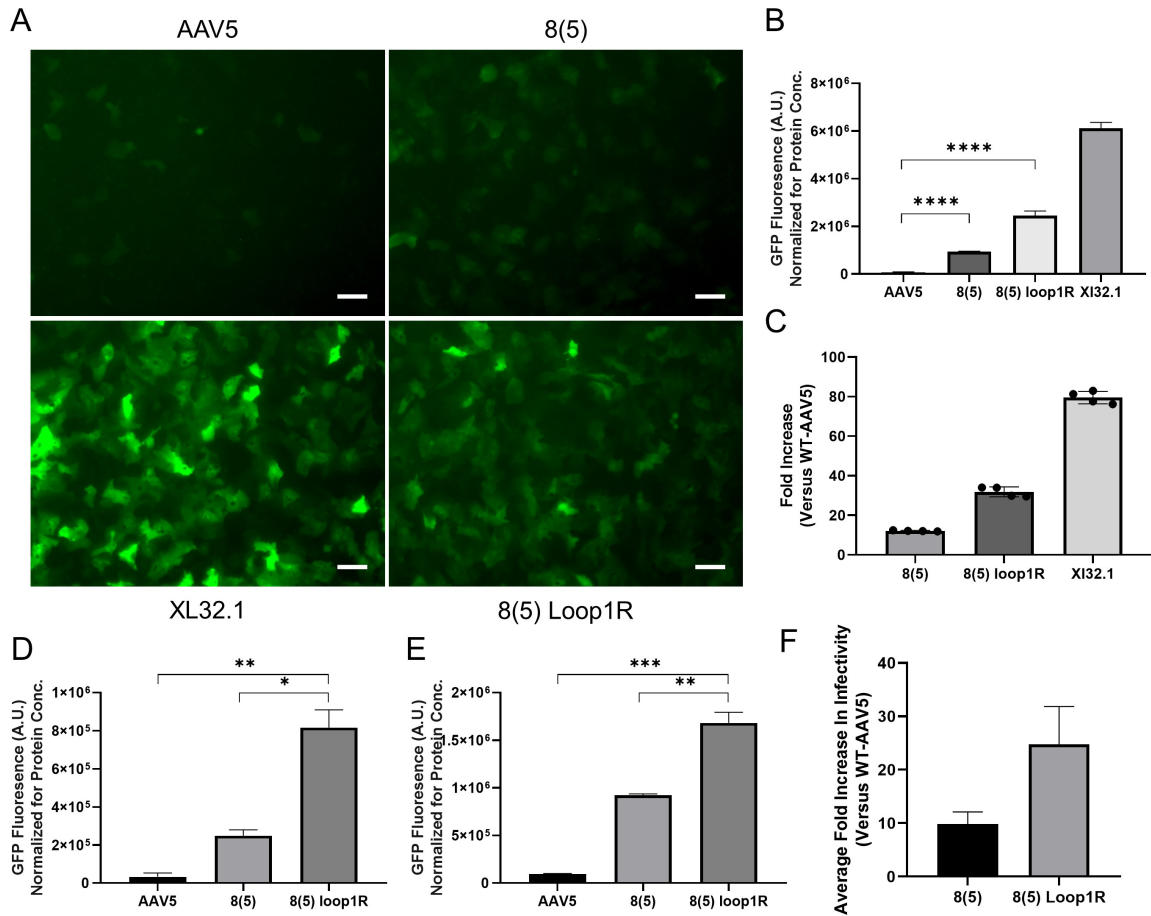


Figure 27: 8(5) Loop1R Primary Human Hepatocyte Transduction

(A) Fluorescent imaging of primary human hepatocytes (TRL 4037) transduced with self-complementary GFP vectors with AAV5, 8(5), 9(5), 8(5) Loop1R, and 9(5) Loop1R. Hepatocytes were transduced at a MOI of 5e5 vg/cell. Images were taken 96 hours after infection. Expression of GFP (green) indicates transduced cells. 10x magnification. Scale Bar: 100μm. (B) Comparison of normalized GFP expression in primary human hepatocytes (TRL 4037). Data are shown as mean values ± SD. ****p<0.0001. (C) Fold increase in infectivity over wt-AAV5 for TRL 4037. Data are shown as mean values ± SD. (D) Comparison of normalized GFP expression in primary human hepatocytes (TRL 4016). Data are shown as mean values ± SD. *p<0.05; **p<0.01. (E) Comparison of normalized GFP expression in primary human hepatocytes (TRL 4021). Data are shown as mean values ± SD. **p<0.01; ***p<0.001.

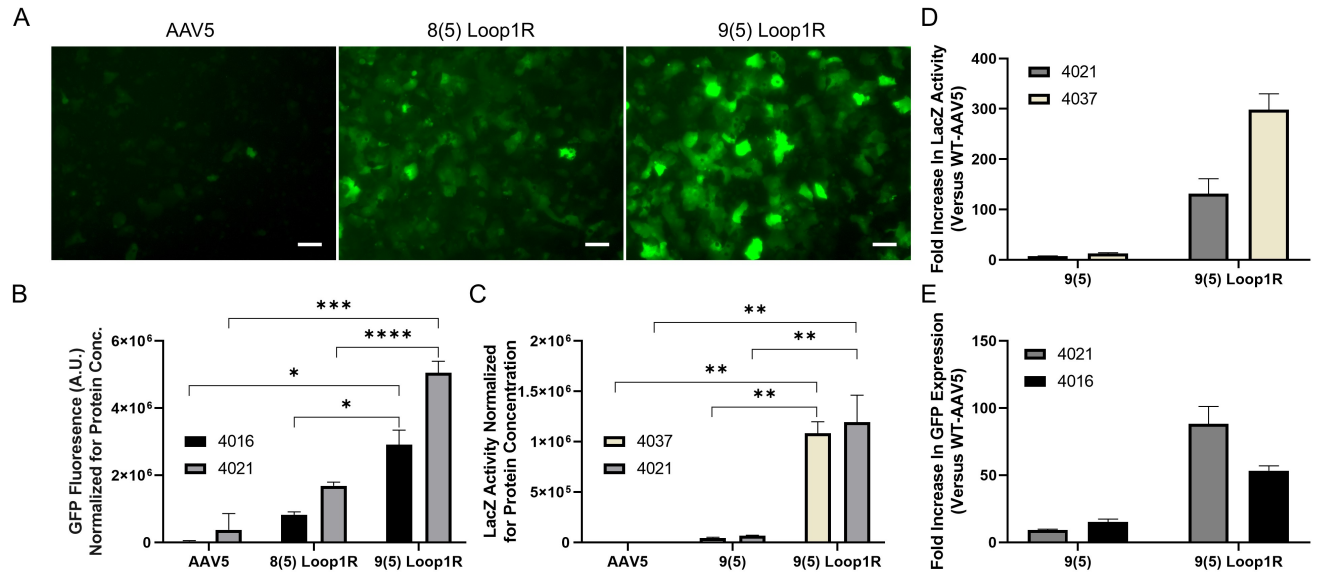


Figure 28: 9(5) Loop1R Primary Human Hepatocyte Transduction

(A) Fluorescent imaging of primary human hepatocytes (TRL 4021) transduced with self-complementary GFP vectors with AAV5, 8(5) Loop1R, and 9(5) Loop1R. Hepatocytes were transduced at a MOI of 5e5 vg/cell. Images were taken 96 hours after infection. Expression of GFP (green) indicates transduced cells. 10x magnification. Scale Bar: 100µm. (B) Comparison of normalized GFP expression in primary human hepatocytes 4016 (Black) and 4021 (Grey). Data are shown as mean values ± SD. *p<0.05; ****p<0.0001. (C) Comparison of normalized LacZ activity in primary human hepatocytes 4037 (Tan) and 4021 (Grey). Data are shown as mean values ± SD. **p<0.01. (D) Fold increase in LacZ activity in primary human hepatocytes 4021 (Grey) and 4037 (Tan). Data are shown as mean values ± SD. (E) Fold increase in GFP expression in primary human hepatocytes 4021 (Grey) and 4016 (Black). Data are shown as mean values ± SD.

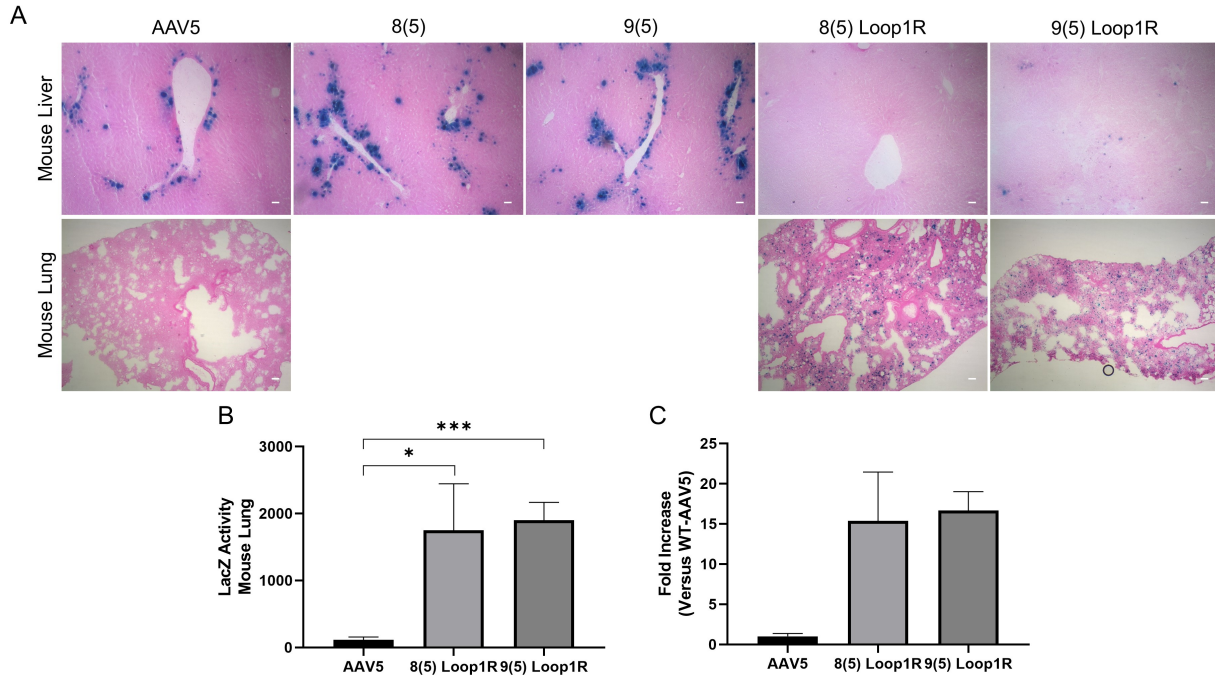


Figure 29: Comparison of Gene Transfer Efficiency in C57/BL6 Mice between 8(5) Loop1R and 9(5) Loop1R

(A) Upper panels are LacZ staining of 10-micron sections of mouse liver transduced by AAV5-CB-LacZnls, 8(5)-CB-LacZnls, 9(5)-CB-LacZnls, 8(5) Loop1R-CB-LacZnls, and 9(5) Loop1R-CB-LacZnls. Lower panels are LacZ staining of 10-micron sections of mouse lung transduced by AAV5-CB-LacZnls, 8(5) Loop1R-CB-LacZnls, and 9(5) Loop1R-CB-LacZnls. Transduced cells are stained blue. Scale bar = 200um. (B) Quantification of LacZ activity in homogenized mouse lung tissue. Data are shown as mean values \pm SD. * $p < 0.05$. *** $p < 0.001$. (C) Fold increase in mouse lung infectivity of 8(5) Loop1R and 9(5) Loop1R vs wt-AAV5. Data are shown as mean values \pm SD.

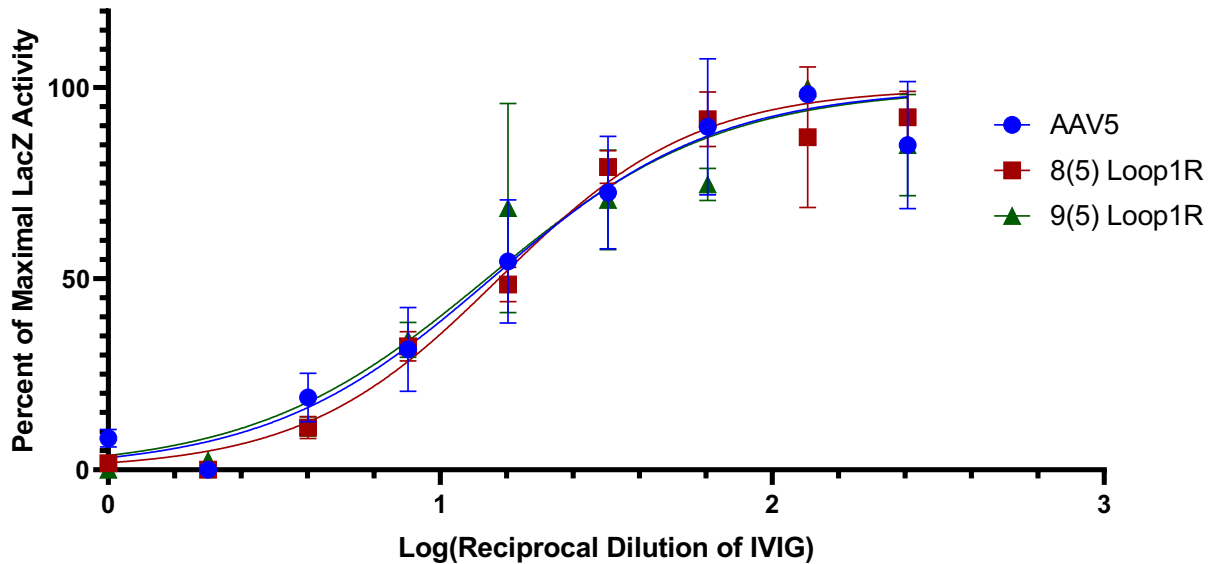


Figure 30: Seroreactivity of 8(5) Loop1R and 9(5) Loop1R

AAV Neutralization Assay using pooled human immunoglobulins from thousands of donors (IVIG Carimune NF, ZLB Behring) to assess seroreactivity. 8(5) Loop1R and 9(5) Loop1R were compared to AAV5 in their ability to resist neutralization by IVIG. Each capsid serotype containing ss-LacZnlS was incubated with reciprocal dilutions of IVIG and added to Huh7 cells. After 72 hours, the LacZ activity for each reciprocal dilution was quantified and compared to LacZ activity of an infection control without the presence of IVIG. The percentage of max LacZ activity at each reciprocal dilution for each virus was used to generate curves that represented the seroreactivity of each virus. Graphpad Prism 8 was used to curve fit the data. Serotypes with curves further to the right indicate less IVIG is needed to neutralize the virus. Serotypes with curves further to the left indicate more IVIG is needed to neutralize the virus. Plotted data points are shown as mean values \pm SD.

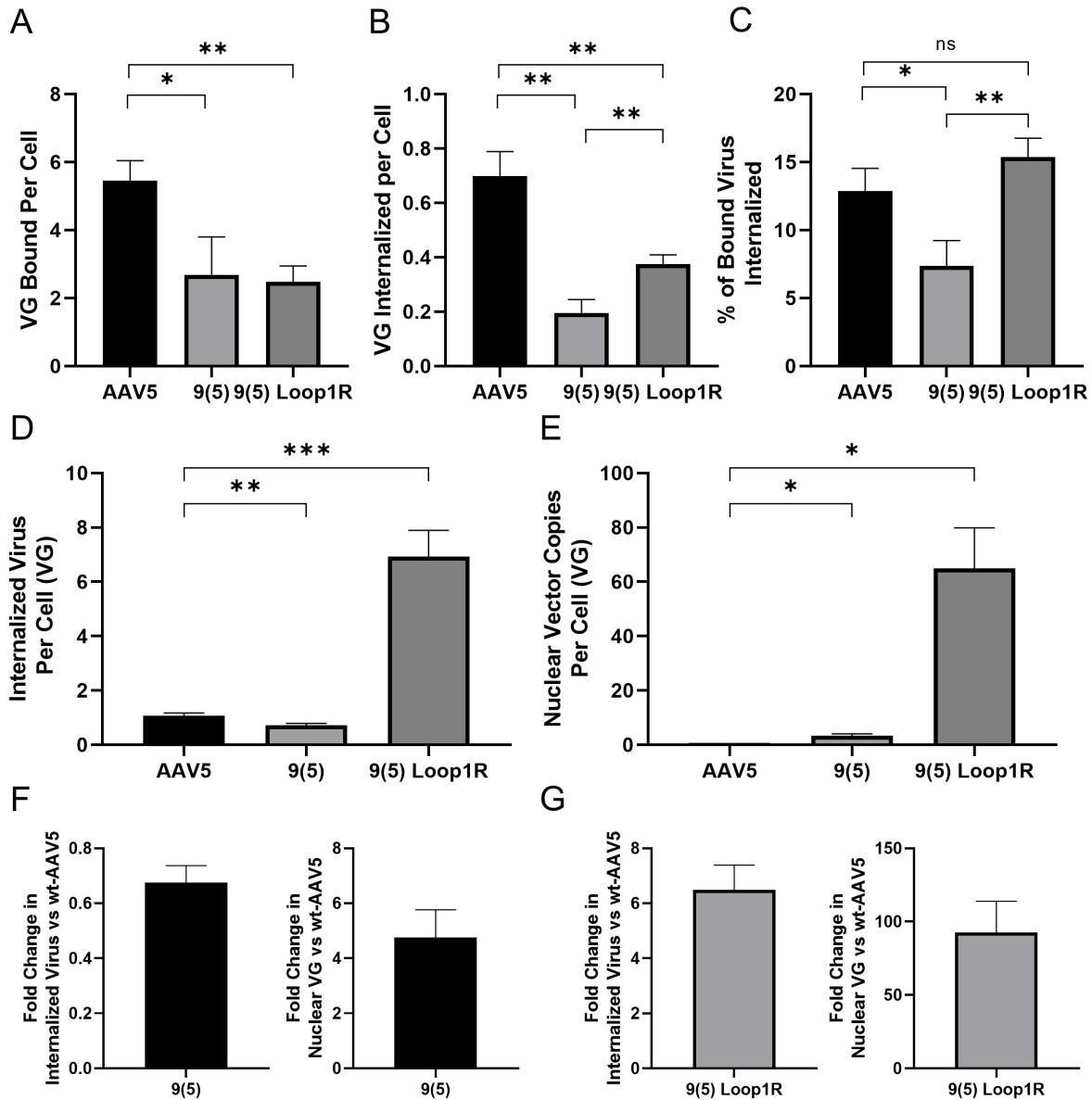


Figure 31: Comparison of Binding, Internalization, and Nuclear Localization for AAV5, 9(5) and 9(5) Loop1R

(A) Binding assay comparing binding of capsid to Huh7 cell surface between AAV5, 9(5), and 9(5) Loop1R. Data shown are mean values \pm SD. * p <0.05. ** p <0.01. (B) Internalization assay comparing amount of internalized virus in Huh7 cells between AAV5, 9(5), and 9(5) Loop1R. Data shown are mean values \pm SD. ** p <0.01; (C) Percentage of bound viral genomes that are internalized comparison between AAV5, 9(5), and 9(5) Loop1R. Data shown are mean values \pm SD. * p <0.05; ** p <0.01, ns = no significance. (D) Modified internalization assay comparing amount of internalized virus in Huh7 cells between AAV5, 9(5), and 9(5) Loop1R. Data shown are mean values \pm SD. ** p <0.01. *** p <0.001. (E) Nuclear vector copy assay comparing amount of vector copies in the nucleus between AAV5, 9(5), and 9(5) Loop1R. Data shown are mean values \pm SD. * p <0.05. (F) Fold change in internalized (left panel) and nuclear (right panel) vector copies for 9(5) versus wt-AAV5. Data shown are mean values \pm SD. (G) Fold change in internalized (left panel) and nuclear (right panel) vector copies for 9(5) Loop1R versus wt-AAV5. Data shown are mean values \pm SD.

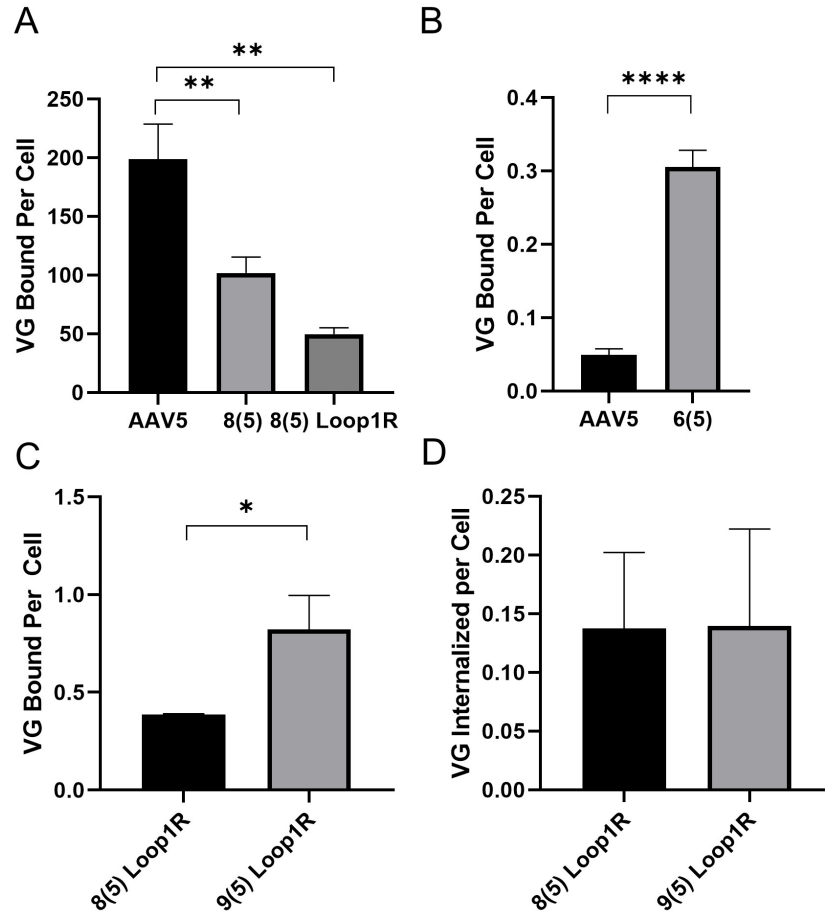


Figure 32: Effects of Different AAV VP1/VP2 Regions on Binding in Chimeric AAV5 Viruses

(A) Binding assay comparing binding of capsid to Huh7 cell surface between AAV5, 8(5), and 8(5) Loop1R. Data shown are mean values \pm SD. ** $p < 0.01$. (B) Binding assay comparing binding of capsid to Huh7 cell surface between AAV5 and 6(5). Data shown are mean values \pm SD. **** $p < 0.0001$. (C) Binding assay comparing binding of capsid to Huh7 cell surface between 8(5) Loop1R and 9(5) Loop1R. Data shown are mean values \pm SD. * $p < 0.05$. (D) Internalization assay comparing amount of internalized virus between 8(5) Loop1R and 9(5) Loop1R. Data shown are mean values \pm SD.

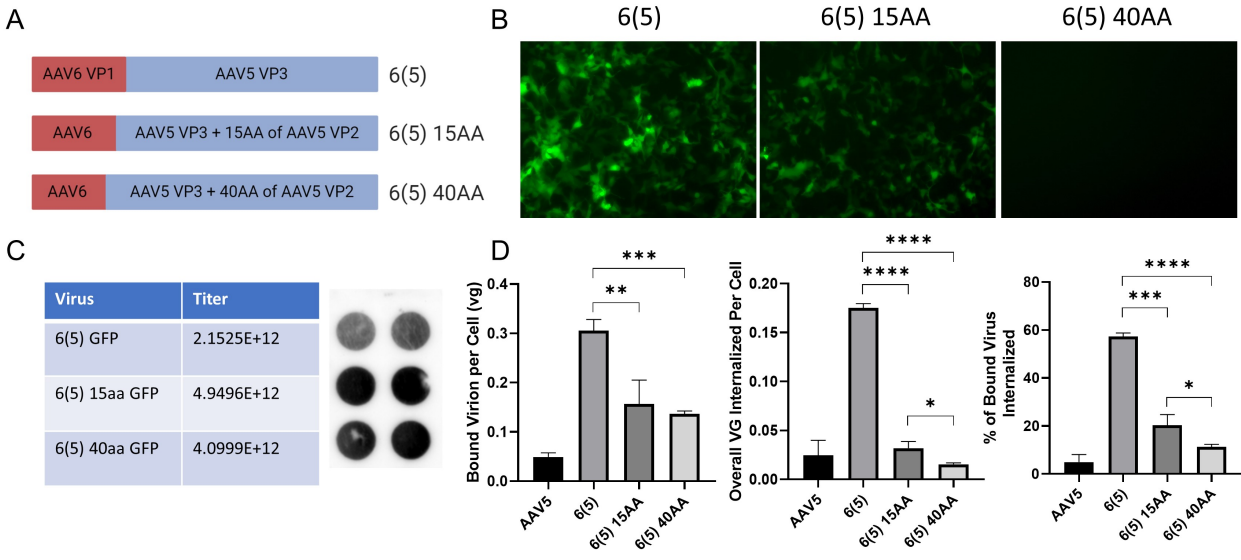


Figure 33: Probing the VP2/VP3 Junction of 6(5)

(A) Diagram depicting 6(5), 6(5) 15AA, and 6(5) 40AA. For 6(5) 15AA, the 15 amino acid AAV6 sequence ending at the AAV5 VP3 start codon of 6(5) was replaced with the 15 amino acid sequence from AAV5. For 6(5) 40AA, the 40 amino acid AAV6 sequence ending at the AAV5 VP3 start codon of 6(5) was replaced with the 40 amino acid sequence from AAV5. (B) Transduction study in Huh7 cells comparing 6(5), 6(5) 15AA, and 6(5) 40AA. Transduced cells are expressing GFP(Green). (C) Titer of the three viruses using DNA dotblot. (D) Binding (left panel), internalized virus (center panel), and percentage of bound virion (right panel) assays comparing 6(5), 6(5) 15AA, and 6(5) 40AA.

CHAPTER 5

SYNOPSIS AND FUTURE DIRECTIONS

As AAV-based gene therapy continues to grow, it has become apparent that the AAV capsid is the most critical part of the therapy. The capsid governs immunogenicity, tropism, and yield, all which must be balanced in order to fully realize the potential of AAV-based gene therapy. However, most of the capsids that are used in clinical trials have deficiencies in one or more areas that render them suboptimal for treating diseases. In particular, the AAV5 capsid elicits the mildest immune response out of any capsid but lacks strong tropism to any organs of interest. As such, this thesis was focused on engineering and evolving AAV5 for increased liver tropism while maintaining AAV5's favorable immunological properties. We successfully generated a diverse library of AAV5 mutants using random mutagenesis which was screened on Huh7 cells to isolate mutants with increased liver cell transduction. After seven rounds of selection, five screened mutants were found to be significantly better at transducing Huh7 cells compared to wt-AAV5. Analysis of the mutations revealed the one mutation, the Loop1R mutation, was positively selected for during the screening process. The Loop1R mutation contributed to increased infectivity by increasing binding and internalization. Further rational engineering of the Loop1R mutant using the VP1/VP2 region from other serotypes resulted in chimeric AAV5 variants with substantially greater transduction in primary human hepatocytes. The AAV8 and AAV9 VP1/VP2 were revealed to decrease binding, but significantly enhanced nuclear localization of the virus, suggesting that the chimeric AAV5 variants were able to more

efficiently escape the endosome and traffic to the nucleus compared to wt-AAV5. These viruses also had increased infectivity in a mouse lung, indicating their potential in treating diseases. Seroreactivity assays revealed that all the evolved and engineered AAV5 mutants retained similar seroreactivity compared to wt-AAV5. Future studies involving testing of donated human serum for neutralizing antibodies against our variants would be of interest. However, the conclusions from our data suggest we were successful in generating an AAV5 variant that has an increase in transduction capabilities and elicit a mild immune response similar to wt-AAV5. Additionally, through our studies, we have possibly discovered the presence of a domain in the VP1/VP2 common region that is heavily involved with binding and internalization. Mutations and sequence swaps in this location of the AAV5 revealed marked differences in binding, suggesting that there was domain that was affecting binding of the virus. Further studies partially isolated the domain to the last 15 amino acids of the VP1/VP2 common region and indicated that this stretch of amino acids were surface exposed.

Further studies validating these capsids in an appropriate animal model are required. While we did test the capsids in a mouse model, we have previously noted that transduction in mouse hepatocytes do not translate well to transduction in human hepatocytes. Therefore, a model more closely resembling the human liver is needed. While a humanized liver mouse model may be appealing, the drawbacks of using these models outweighs the benefits. In a sense, the structure of the “humanized liver” does accurately resemble that of a human due to the method in which the mouse model is generated. Additionally, the variability of remaining mouse hepatocytes raises the degree of difficulty in analyzing the transduction properties in human liver cells.¹⁹² Ultimately, we believe that testing our capsids in a non-human primate model is the best

method of verifying if the liver transduction increase yield by our chimeric AAV5 capsids would translate well to humans.

Additionally, through our mechanistic studies, we have found that our capsids still have more room to be improved, particularly in the areas of yield and infectivity. From our VP2 studies, we found that that amino acid sequence near the VP3 start codon could be heavily involved in binding and internalization. Targeted engineering of this particular region using random mutagenesis for either the 9(5) Loop1R or 8(5) Loop1R capsids could further enhance transduction. Additionally, simple amino acid sequence swaps could result in an increase in yield, as seen with the 6(5) 15AA and 40AA capsids. One deficiency that 9(5) Loop1R and 8(5) Loop1R have in comparison to AAV5 is a decrease in binding. One potential solution is to apply random peptide insertions to different loops of the chimeric variants to screen for chimeric variants with increased binding to receptors that have synergistic effects with the Loop1R mutation. This method could make up for the decrease in binding that the AAV8 and AAV9 VP1/VP2 confer and could further enhance transduction due to an increase in bound viral particles. This would lead to a subsequent increase in the number of viral particles internalized and hopefully localized to the nucleus due to enhanced endosomal escape conferred by the VP1 swaps. The peptide insertion method could also have a drastic effect on seroreactivity by breaking up antigenic domains that neutralizing antibodies bind. This could further decrease the seroreactivity of the viruses, allowing more patients to receive a therapy based on these capsids. Additionally, another round of random mutagenesis could be enough to increase binding. The 8(5) Loop1R and 9(5) Loop1R capsids already have tropism to the liver, so small incremental increases could be advantageous over significant changes that peptide insertions yield.

Understanding the function of the VP1/VP2 common region is critical to further understanding of the AAV virus. Current methods of engineering the AAV capsid are primarily focused on modifying domains that are involved with receptor binding. However, this method typically cannot affect events that occur post endocytosis. The VP2 has previously been characterized as nonessential for AAV transduction, as AAV2 capsids consisting of only VP1 and VP3 units were found to have similar transduction efficiency as wt-AAV2.⁴⁵ However, our data suggests that the VP2 is essential for both binding and internalization, indicating that there is a domain that may be readily evolvable. This domain can potentially serve as another site for modification that can enhance transduction in a multitude of ways that is not necessarily reliant on receptor binding. Only further investigation into the VP2 will properly confirm if the sequence directly binds to a receptor or affects the conformational changes in the capsid.

Finally, 8(5) Loop1R and 9(5) Loop1R are interesting vectors to consider for lung gene therapy as they have significant expression in the lungs when compared to AAV5, which is a commonly used for lung transduction. However, judging from the transduction studies in mice, these two vectors may need additional mutations to properly target cell types in the lung. Currently, we believe that these two chimeric AAV5 capsids are targeting endothelial cells in the lungs which typically are not the cell types targeted for lung-based gene therapy. Combinations of previously characterized AAV5 mutations with our chimeric variants may further enhance the lung transduction. Additionally, applying different routes of administration such as aerosolized delivery of AAV may enhance transduction of the proper cell types. Thus, the potential uses of our chimeric capsids for lung and liver-based gene therapies in appropriate animal models is of great interest as we believe our capsids may be of great use in furthering AAV-based gene therapy.

REFERENCES

1. Anderson, WF (1992). Human gene therapy. *Science* **256**: 808-813.
2. McLachlin, JR, Cornetta, K, Eglitis, MA, and Anderson, WF (1990). Retroviral-mediated gene transfer. *Prog Nucleic Acid Res Mol Biol* **38**: 91-135.
3. Robbins, PD, Tahara, H, and Ghivizzani, SC (1998). Viral vectors for gene therapy. *Trends Biotechnol* **16**: 35-40.
4. Boulaiz, H, Marchal, JA, Prados, J, Melguizo, C, and Aranega, A (2005). Non-viral and viral vectors for gene therapy. *Cell Mol Biol (Noisy-le-grand)* **51**: 3-22.
5. Perez Ruiz de Garibay, A (2016). Endocytosis in gene therapy with non-viral vectors. *Wien Med Wochenschr* **166**: 227-235.
6. Montini, E, Cesana, D, Schmidt, M, Sanvito, F, Bartholomae, CC, Ranzani, M, *et al.* (2009). The genotoxic potential of retroviral vectors is strongly modulated by vector design and integration site selection in a mouse model of HSC gene therapy. *J Clin Invest* **119**: 964-975.
7. Schirmbeck, R, Reimann, J, Kochanek, S, and Kreppel, F (2008). The immunogenicity of adenovirus vectors limits the multispecificity of CD8 T-cell responses to vector-encoded transgenic antigens. *Mol Ther* **16**: 1609-1616.
8. Einerhand, MP, Antoniou, M, Zolotukhin, S, Muzyczka, N, Berns, KI, Grosveld, F, *et al.* (1995). Regulated high-level human beta-globin gene expression in erythroid cells following recombinant adeno-associated virus-mediated gene transfer. *Gene Ther* **2**: 336-343.
9. LaFace, D, Hermonat, P, Wakeland, E, and Peck, A (1988). Gene transfer into hematopoietic progenitor cells mediated by an adeno-associated virus vector. *Virology* **162**: 483-486.
10. Atchison, RW, Casto, BC, and Hammon, WM (1966). Electron microscopy of adenovirus-associated virus (AAV) in cell cultures. *Virology* **29**: 353-357.
11. Mingozzi, F, and High, KA (2017). Overcoming the Host Immune Response to Adeno-Associated Virus Gene Delivery Vectors: The Race Between Clearance, Tolerance, Neutralization, and Escape. *Annu Rev Virol* **4**: 511-534.
12. Srivastava, A (2016). In vivo tissue-tropism of adeno-associated viral vectors. *Curr Opin Virol* **21**: 75-80.
13. Ginn, SL, Amaya, AK, Alexander, IE, Edelstein, M, and Abedi, MR (2018). Gene therapy clinical trials worldwide to 2017: An update. *J Gene Med* **20**: e3015.

14. Keeler, AM, and Flotte, TR (2019). Recombinant Adeno-Associated Virus Gene Therapy in Light of Luxturna (and Zolgensma and Glybera): Where Are We, and How Did We Get Here? *Annu Rev Virol* **6**: 601-621.
15. Yla-Herttuala, S (2012). Endgame: glybera finally recommended for approval as the first gene therapy drug in the European union. *Mol Ther* **20**: 1831-1832.
16. (2018). Voretigene neparvovec-rzyl (Luxturna) for inherited retinal dystrophy. *Med Lett Drugs Ther* **60**: 53-55.
17. (2019). Zolgensma - one-time gene therapy for spinal muscular atrophy. *Med Lett Drugs Ther* **61**: 113-114.
18. Pfizer Inc. (2018). PFIZER'S NEW PHASE 1B RESULTS OF GENE THERAPY IN AMBULATORY BOYS WITH DUCHENNE MUSCULAR DYSTROPHY (DMD) SUPPORT ADVANCEMENT INTO PIVOTAL PHASE 3 STUDY <https://investors.pfizer.com/investor-news/press-release-details/2020/Pfizers-New-Phase-1b-Results-of-Gene-Therapy-in-Ambulatory-Boys-with-Duchenne-Muscular-Dystrophy-DMD-Support-Advancement-into-Pivotal-Phase-3-Study/default.aspx>.
19. George, LA, Sullivan, SK, Giermasz, A, Rasko, JEJ, Samelson-Jones, BJ, Ducore, J, *et al.* (2017). Hemophilia B Gene Therapy with a High-Specific-Activity Factor IX Variant. *N Engl J Med* **377**: 2215-2227.
20. Rangarajan, S, Walsh, L, Lester, W, Perry, D, Madan, B, Laffan, M, *et al.* (2017). AAV5-Factor VIII Gene Transfer in Severe Hemophilia A. *N Engl J Med* **377**: 2519-2530.
21. Naso, MF, Tomkowicz, B, Perry, WL, 3rd, and Strohl, WR (2017). Adeno-Associated Virus (AAV) as a Vector for Gene Therapy. *BioDrugs* **31**: 317-334.
22. Li, C, and Samulski, RJ (2020). Engineering adeno-associated virus vectors for gene therapy. *Nat Rev Genet* **21**: 255-272.
23. Fitzpatrick, Z, Leborgne, C, Barbon, E, Masat, E, Ronzitti, G, van Wittenberghe, L, *et al.* (2018). Influence of Pre-existing Anti-capsid Neutralizing and Binding Antibodies on AAV Vector Transduction. *Mol Ther Methods Clin Dev* **9**: 119-129.
24. Nathwani, AC, Tuddenham, EG, Rangarajan, S, Rosales, C, McIntosh, J, Linch, DC, *et al.* (2011). Adenovirus-associated virus vector-mediated gene transfer in hemophilia B. *N Engl J Med* **365**: 2357-2365.
25. Clement, N, and Grieger, JC (2016). Manufacturing of recombinant adeno-associated viral vectors for clinical trials. *Mol Ther Methods Clin Dev* **3**: 16002.

26. Srivastava, A, Lusby, EW, and Berns, KI (1983). Nucleotide sequence and organization of the adeno-associated virus 2 genome. *J Virol* **45**: 555-564.
27. Xiao, X, Xiao, W, Li, J, and Samulski, RJ (1997). A novel 165-base-pair terminal repeat sequence is the sole cis requirement for the adeno-associated virus life cycle. *J Virol* **71**: 941-948.
28. Wang, XS, Qing, K, Ponnazhagan, S, and Srivastava, A (1997). Adeno-associated virus type 2 DNA replication in vivo: mutation analyses of the D sequence in viral inverted terminal repeats. *J Virol* **71**: 3077-3082.
29. Duan, D, Sharma, P, Yang, J, Yue, Y, Dudus, L, Zhang, Y, *et al.* (1998). Circular intermediates of recombinant adeno-associated virus have defined structural characteristics responsible for long-term episomal persistence in muscle tissue. *J Virol* **72**: 8568-8577.
30. Flotte, TR, Afione, SA, Solow, R, Drumm, ML, Markakis, D, Guggino, WB, *et al.* (1993). Expression of the cystic fibrosis transmembrane conductance regulator from a novel adeno-associated virus promoter. *J Biol Chem* **268**: 3781-3790.
31. Collaco, RF, Kalman-Maltese, V, Smith, AD, Dignam, JD, and Trempe, JP (2003). A biochemical characterization of the adeno-associated virus Rep40 helicase. *J Biol Chem* **278**: 34011-34017.
32. Smith, RH, and Kotin, RM (2000). An adeno-associated virus (AAV) initiator protein, Rep78, catalyzes the cleavage and ligation of single-stranded AAV ori DNA. *J Virol* **74**: 3122-3129.
33. Ward, P, Urcelay, E, Kotin, R, Safer, B, and Berns, KI (1994). Adeno-associated virus DNA replication in vitro: activation by a maltose binding protein/Rep 68 fusion protein. *J Virol* **68**: 6029-6037.
34. McCarty, DM, Ni, TH, and Muzyczka, N (1992). Analysis of mutations in adeno-associated virus Rep protein in vivo and in vitro. *J Virol* **66**: 4050-4057.
35. Im, DS, and Muzyczka, N (1992). Partial purification of adeno-associated virus Rep78, Rep52, and Rep40 and their biochemical characterization. *J Virol* **66**: 1119-1128.
36. Weitzman, MD, Kyostio, SR, Kotin, RM, and Owens, RA (1994). Adeno-associated virus (AAV) Rep proteins mediate complex formation between AAV DNA and its integration site in human DNA. *Proc Natl Acad Sci U S A* **91**: 5808-5812.
37. Dubielzig, R, King, JA, Weger, S, Kern, A, and Kleinschmidt, JA (1999). Adeno-associated virus type 2 protein interactions: formation of pre-encapsidation complexes. *J Virol* **73**: 8989-8998.

38. Enemark, EJ, and Joshua-Tor, L (2006). Mechanism of DNA translocation in a replicative hexameric helicase. *Nature* **442**: 270-275.
39. Pereira, DJ, McCarty, DM, and Muzyczka, N (1997). The adeno-associated virus (AAV) Rep protein acts as both a repressor and an activator to regulate AAV transcription during a productive infection. *J Virol* **71**: 1079-1088.
40. Muralidhar, S, Becerra, SP, and Rose, JA (1994). Site-directed mutagenesis of adeno-associated virus type 2 structural protein initiation codons: effects on regulation of synthesis and biological activity. *J Virol* **68**: 170-176.
41. Becerra, SP, Koczot, F, Fabisch, P, and Rose, JA (1988). Synthesis of adeno-associated virus structural proteins requires both alternative mRNA splicing and alternative initiations from a single transcript. *J Virol* **62**: 2745-2754.
42. Weger, S, Wistuba, A, Grimm, D, and Kleinschmidt, JA (1997). Control of adeno-associated virus type 2 cap gene expression: relative influence of helper virus, terminal repeats, and Rep proteins. *J Virol* **71**: 8437-8447.
43. Kurian, JJ, Lakshmanan, R, Chmely, WM, Hull, JA, Yu, JC, Bennett, A, *et al.* (2019). Adeno-Associated Virus VP1u Exhibits Protease Activity. *Viruses* **11**.
44. Venkatakrisnan, B, Yarbrough, J, Domsic, J, Bennett, A, Bothner, B, Kozyreva, OG, *et al.* (2013). Structure and dynamics of adeno-associated virus serotype 1 VP1-unique N-terminal domain and its role in capsid trafficking. *J Virol* **87**: 4974-4984.
45. Warrington, KH, Jr., Gorbatyuk, OS, Harrison, JK, Opie, SR, Zolotukhin, S, and Muzyczka, N (2004). Adeno-associated virus type 2 VP2 capsid protein is nonessential and can tolerate large peptide insertions at its N terminus. *J Virol* **78**: 6595-6609.
46. Sonntag, F, Kother, K, Schmidt, K, Weghofer, M, Raupp, C, Nieto, K, *et al.* (2011). The assembly-activating protein promotes capsid assembly of different adeno-associated virus serotypes. *J Virol* **85**: 12686-12697.
47. Ogden, PJ, Kelsic, ED, Sinai, S, and Church, GM (2019). Comprehensive AAV capsid fitness landscape reveals a viral gene and enables machine-guided design. *Science* **366**: 1139-1143.
48. Moore, AR, Dong, B, Chen, L, and Xiao, W (2015). Vaccinia virus as a subhelper for AAV replication and packaging. *Mol Ther Methods Clin Dev* **2**: 15044.
49. Ogston, P, Raj, K, and Beard, P (2000). Productive replication of adeno-associated virus can occur in human papillomavirus type 16 (HPV-16) episome-containing keratinocytes and is augmented by the HPV-16 E2 protein. *J Virol* **74**: 3494-3504.

50. Xiao, X, Li, J, and Samulski, RJ (1998). Production of high-titer recombinant adeno-associated virus vectors in the absence of helper adenovirus. *J Virol* **72**: 2224-2232.
51. Weindler, FW, and Heilbronn, R (1991). A subset of herpes simplex virus replication genes provides helper functions for productive adeno-associated virus replication. *J Virol* **65**: 2476-2483.
52. Mouw, MB, and Pintel, DJ (2000). Adeno-associated virus RNAs appear in a temporal order and their splicing is stimulated during coinfection with adenovirus. *J Virol* **74**: 9878-9888.
53. Winter, K, von Kietzell, K, Heilbronn, R, Pozzuto, T, Fechner, H, and Weger, S (2012). Roles of E4orf6 and VA I RNA in adenovirus-mediated stimulation of human parvovirus B19 DNA replication and structural gene expression. *J Virol* **86**: 5099-5109.
54. DiMattia, MA, Nam, HJ, Van Vliet, K, Mitchell, M, Bennett, A, Gurda, BL, *et al.* (2012). Structural insight into the unique properties of adeno-associated virus serotype 9. *J Virol* **86**: 6947-6958.
55. Ng, R, Govindasamy, L, Gurda, BL, McKenna, R, Kozyreva, OG, Samulski, RJ, *et al.* (2010). Structural characterization of the dual glycan binding adeno-associated virus serotype 6. *J Virol* **84**: 12945-12957.
56. Lerch, TF, Xie, Q, and Chapman, MS (2010). The structure of adeno-associated virus serotype 3B (AAV-3B): insights into receptor binding and immune evasion. *Virology* **403**: 26-36.
57. Nam, HJ, Lane, MD, Padron, E, Gurda, B, McKenna, R, Kohlbrenner, E, *et al.* (2007). Structure of adeno-associated virus serotype 8, a gene therapy vector. *J Virol* **81**: 12260-12271.
58. Govindasamy, L, Padron, E, McKenna, R, Muzyczka, N, Kaludov, N, Chiorini, JA, *et al.* (2006). Structurally mapping the diverse phenotype of adeno-associated virus serotype 4. *J Virol* **80**: 11556-11570.
59. Walters, RW, Agbandje-McKenna, M, Bowman, VD, Moninger, TO, Olson, NH, Seiler, M, *et al.* (2004). Structure of adeno-associated virus serotype 5. *J Virol* **78**: 3361-3371.
60. Xie, Q, Bu, W, Bhatia, S, Hare, J, Somasundaram, T, Azzi, A, *et al.* (2002). The atomic structure of adeno-associated virus (AAV-2), a vector for human gene therapy. *Proc Natl Acad Sci U S A* **99**: 10405-10410.
61. Lochrie, MA, Tatsuno, GP, Christie, B, McDonnell, JW, Zhou, S, Surosky, R, *et al.* (2006). Mutations on the external surfaces of adeno-associated virus type 2 capsids that affect transduction and neutralization. *J Virol* **80**: 821-834.

62. Raupp, C, Naumer, M, Muller, OJ, Gurda, BL, Agbandje-McKenna, M, and Kleinschmidt, JA (2012). The threefold protrusions of adeno-associated virus type 8 are involved in cell surface targeting as well as postattachment processing. *J Virol* **86**: 9396-9408.
63. Tseng, YS, and Agbandje-McKenna, M (2014). Mapping the AAV Capsid Host Antibody Response toward the Development of Second Generation Gene Delivery Vectors. *Front Immunol* **5**: 9.
64. Bleker, S, Sonntag, F, and Kleinschmidt, JA (2005). Mutational analysis of narrow pores at the fivefold symmetry axes of adeno-associated virus type 2 capsids reveals a dual role in genome packaging and activation of phospholipase A2 activity. *J Virol* **79**: 2528-2540.
65. Kronenberg, S, Bottcher, B, von der Lieth, CW, Bleker, S, and Kleinschmidt, JA (2005). A conformational change in the adeno-associated virus type 2 capsid leads to the exposure of hidden VP1 N termini. *J Virol* **79**: 5296-5303.
66. Tenney, RM, Bell, CL, and Wilson, JM (2014). AAV8 capsid variable regions at the two-fold symmetry axis contribute to high liver transduction by mediating nuclear entry and capsid uncoating. *Virology* **454-455**: 227-236.
67. Bartlett, JS, Wilcher, R, and Samulski, RJ (2000). Infectious entry pathway of adeno-associated virus and adeno-associated virus vectors. *J Virol* **74**: 2777-2785.
68. Levy, HC, Bowman, VD, Govindasamy, L, McKenna, R, Nash, K, Warrington, K, *et al.* (2009). Heparin binding induces conformational changes in Adeno-associated virus serotype 2. *J Struct Biol* **165**: 146-156.
69. Huang, LY, Patel, A, Ng, R, Miller, EB, Halder, S, McKenna, R, *et al.* (2016). Characterization of the Adeno-Associated Virus 1 and 6 Sialic Acid Binding Site. *J Virol* **90**: 5219-5230.
70. Kaludov, N, Brown, KE, Walters, RW, Zabner, J, and Chiorini, JA (2001). Adeno-associated virus serotype 4 (AAV4) and AAV5 both require sialic acid binding for hemagglutination and efficient transduction but differ in sialic acid linkage specificity. *J Virol* **75**: 6884-6893.
71. Arnett, AL, Beutler, LR, Quintana, A, Allen, J, Finn, E, Palmiter, RD, *et al.* (2013). Heparin-binding correlates with increased efficiency of AAV1- and AAV6-mediated transduction of striated muscle, but negatively impacts CNS transduction. *Gene Ther* **20**: 497-503.
72. Lerch, TF, and Chapman, MS (2012). Identification of the heparin binding site on adeno-associated virus serotype 3B (AAV-3B). *Virology* **423**: 6-13.

73. Shen, S, Bryant, KD, Brown, SM, Randell, SH, and Asokan, A (2011). Terminal N-linked galactose is the primary receptor for adeno-associated virus 9. *J Biol Chem* **286**: 13532-13540.
74. Bell, CL, Gurda, BL, Van Vliet, K, Agbandje-McKenna, M, and Wilson, JM (2012). Identification of the galactose binding domain of the adeno-associated virus serotype 9 capsid. *J Virol* **86**: 7326-7333.
75. Kashiwakura, Y, Tamayose, K, Iwabuchi, K, Hirai, Y, Shimada, T, Matsumoto, K, *et al.* (2005). Hepatocyte growth factor receptor is a coreceptor for adeno-associated virus type 2 infection. *J Virol* **79**: 609-614.
76. Qing, K, Mah, C, Hansen, J, Zhou, S, Dwarki, V, and Srivastava, A (1999). Human fibroblast growth factor receptor 1 is a co-receptor for infection by adeno-associated virus 2. *Nat Med* **5**: 71-77.
77. Akache, B, Grimm, D, Pandey, K, Yant, SR, Xu, H, and Kay, MA (2006). The 37/67-kilodalton laminin receptor is a receptor for adeno-associated virus serotypes 8, 2, 3, and 9. *J Virol* **80**: 9831-9836.
78. Asokan, A, Hamra, JB, Govindasamy, L, Agbandje-McKenna, M, and Samulski, RJ (2006). Adeno-associated virus type 2 contains an integrin alpha5beta1 binding domain essential for viral cell entry. *J Virol* **80**: 8961-8969.
79. Ling, C, Lu, Y, Kalsi, JK, Jayandharan, GR, Li, B, Ma, W, *et al.* (2010). Human hepatocyte growth factor receptor is a cellular coreceptor for adeno-associated virus serotype 3. *Hum Gene Ther* **21**: 1741-1747.
80. Di Pasquale, G, Davidson, BL, Stein, CS, Martins, I, Scudiero, D, Monks, A, *et al.* (2003). Identification of PDGFR as a receptor for AAV-5 transduction. *Nat Med* **9**: 1306-1312.
81. Weller, ML, Amornphimoltham, P, Schmidt, M, Wilson, PA, Gutkind, JS, and Chiorini, JA (2010). Epidermal growth factor receptor is a co-receptor for adeno-associated virus serotype 6. *Nat Med* **16**: 662-664.
82. Nonnenmacher, M, and Weber, T (2011). Adeno-associated virus 2 infection requires endocytosis through the CLIC/GEEC pathway. *Cell Host Microbe* **10**: 563-576.
83. Duan, D, Li, Q, Kao, AW, Yue, Y, Pessin, JE, and Engelhardt, JF (1999). Dynamin is required for recombinant adeno-associated virus type 2 infection. *J Virol* **73**: 10371-10376.
84. Bantel-Schaal, U, Braspenning-Wesch, I, and Kartenbeck, J (2009). Adeno-associated virus type 5 exploits two different entry pathways in human embryo fibroblasts. *J Gen Virol* **90**: 317-322.

85. Dudek, AM, Pillay, S, Puschnik, AS, Nagamine, CM, Cheng, F, Qiu, J, *et al.* (2018). An Alternate Route for Adeno-associated Virus (AAV) Entry Independent of AAV Receptor. *J Virol* **92**.
86. Meyer, NL, Hu, G, Davulcu, O, Xie, Q, Noble, AJ, Yoshioka, C, *et al.* (2019). Structure of the gene therapy vector, adeno-associated virus with its cell receptor, AAVR. *Elife* **8**.
87. Zhang, R, Cao, L, Cui, M, Sun, Z, Hu, M, Zhang, R, *et al.* (2019). Adeno-associated virus 2 bound to its cellular receptor AAVR. *Nat Microbiol* **4**: 675-682.
88. Zhang, R, Xu, G, Cao, L, Sun, Z, He, Y, Cui, M, *et al.* (2019). Divergent engagements between adeno-associated viruses with their cellular receptor AAVR. *Nat Commun* **10**: 3760.
89. Summerford, C, Johnson, JS, and Samulski, RJ (2016). AAVR: A Multi-Serotype Receptor for AAV. *Mol Ther* **24**: 663-666.
90. Pillay, S, Zou, W, Cheng, F, Puschnik, AS, Meyer, NL, Ganaie, SS, *et al.* (2017). Adeno-associated Virus (AAV) Serotypes Have Distinctive Interactions with Domains of the Cellular AAV Receptor. *J Virol* **91**.
91. Ding, W, Zhang, LN, Yeaman, C, and Engelhardt, JF (2006). rAAV2 traffics through both the late and the recycling endosomes in a dose-dependent fashion. *Mol Ther* **13**: 671-682.
92. Dudek, AM, Zabaleta, N, Zinn, E, Pillay, S, Zengel, J, Porter, C, *et al.* (2020). GPR108 Is a Highly Conserved AAV Entry Factor. *Mol Ther* **28**: 367-381.
93. Kelkar, S, De, BP, Gao, G, Wilson, JM, Crystal, RG, and Leopold, PL (2006). A common mechanism for cytoplasmic dynein-dependent microtubule binding shared among adeno-associated virus and adenovirus serotypes. *J Virol* **80**: 7781-7785.
94. Hirosue, S, Senn, K, Clement, N, Nonnenmacher, M, Gigout, L, Linden, RM, *et al.* (2007). Effect of inhibition of dynein function and microtubule-altering drugs on AAV2 transduction. *Virology* **367**: 10-18.
95. Zhao, W, Zhong, L, Wu, J, Chen, L, Qing, K, Weigel-Kelley, KA, *et al.* (2006). Role of cellular FKBP52 protein in intracellular trafficking of recombinant adeno-associated virus 2 vectors. *Virology* **353**: 283-293.
96. Popa-Wagner, R, Sonntag, F, Schmidt, K, King, J, and Kleinschmidt, JA (2012). Nuclear translocation of adeno-associated virus type 2 capsid proteins for virion assembly. *J Gen Virol* **93**: 1887-1898.

97. Sanlioglu, S, Benson, PK, Yang, J, Atkinson, EM, Reynolds, T, and Engelhardt, JF (2000). Endocytosis and nuclear trafficking of adeno-associated virus type 2 are controlled by rac1 and phosphatidylinositol-3 kinase activation. *J Virol* **74**: 9184-9196.
98. Nicolson, SC, and Samulski, RJ (2014). Recombinant adeno-associated virus utilizes host cell nuclear import machinery to enter the nucleus. *J Virol* **88**: 4132-4144.
99. Sonntag, F, Bleker, S, Leuchs, B, Fischer, R, and Kleinschmidt, JA (2006). Adeno-associated virus type 2 capsids with externalized VP1/VP2 trafficking domains are generated prior to passage through the cytoplasm and are maintained until uncoating occurs in the nucleus. *J Virol* **80**: 11040-11054.
100. McCarty, DM, Monahan, PE, and Samulski, RJ (2001). Self-complementary recombinant adeno-associated virus (scAAV) vectors promote efficient transduction independently of DNA synthesis. *Gene Ther* **8**: 1248-1254.
101. Sun, L, Li, J, and Xiao, X (2000). Overcoming adeno-associated virus vector size limitation through viral DNA heterodimerization. *Nat Med* **6**: 599-602.
102. Hirsch, ML, Wolf, SJ, and Samulski, RJ (2016). Delivering Transgenic DNA Exceeding the Carrying Capacity of AAV Vectors. *Methods Mol Biol* **1382**: 21-39.
103. Pryadkina, M, Lostal, W, Bourg, N, Charton, K, Roudaut, C, Hirsch, ML, *et al.* (2015). A comparison of AAV strategies distinguishes overlapping vectors for efficient systemic delivery of the 6.2 kb Dysferlin coding sequence. *Mol Ther Methods Clin Dev* **2**: 15009.
104. Harding, TC, Koprivnikar, KE, Tu, GH, Zayek, N, Lew, S, Subramanian, A, *et al.* (2004). Intravenous administration of an AAV-2 vector for the expression of factor IX in mice and a dog model of hemophilia B. *Gene Ther* **11**: 204-213.
105. Vandenberghe, LH, Bell, P, Maguire, AM, Cearley, CN, Xiao, R, Calcedo, R, *et al.* (2011). Dosage thresholds for AAV2 and AAV8 photoreceptor gene therapy in monkey. *Sci Transl Med* **3**: 88ra54.
106. Xu, R, Janson, CG, Mastakov, M, Lawlor, P, Young, D, Mouravlev, A, *et al.* (2001). Quantitative comparison of expression with adeno-associated virus (AAV-2) brain-specific gene cassettes. *Gene Ther* **8**: 1323-1332.
107. Riaz, M, Raz, Y, Moloney, EB, van Putten, M, Krom, YD, van der Maarel, SM, *et al.* (2015). Differential myofiber-type transduction preference of adeno-associated virus serotypes 6 and 9. *Skelet Muscle* **5**: 37.
108. Hauck, B, and Xiao, W (2003). Characterization of tissue tropism determinants of adeno-associated virus type 1. *J Virol* **77**: 2768-2774.

109. Wang, L, Wang, H, Bell, P, McCarter, RJ, He, J, Calcedo, R, *et al.* (2010). Systematic evaluation of AAV vectors for liver directed gene transfer in murine models. *Mol Ther* **18**: 118-125.
110. Ling, C, Wang, Y, Zhang, Y, Ejjigani, A, Yin, Z, Lu, Y, *et al.* (2014). Selective in vivo targeting of human liver tumors by optimized AAV3 vectors in a murine xenograft model. *Hum Gene Ther* **25**: 1023-1034.
111. Gruntman, AM, Mueller, C, Flotte, TR, and Gao, G (2012). Gene transfer in the lung using recombinant adeno-associated virus. *Curr Protoc Microbiol* **Chapter 14**: Unit14D 12.
112. Wiley, LA, Burnight, ER, Kaalberg, EE, Jiao, C, Riker, MJ, Halder, JA, *et al.* (2018). Assessment of Adeno-Associated Virus Serotype Tropism in Human Retinal Explants. *Hum Gene Ther* **29**: 424-436.
113. Alisky, JM, Hughes, SM, Sauter, SL, Jolly, D, Dubensky, TW, Jr., Staber, PD, *et al.* (2000). Transduction of murine cerebellar neurons with recombinant FIV and AAV5 vectors. *Neuroreport* **11**: 2669-2673.
114. Nathwani, AC, Gray, JT, McIntosh, J, Ng, CY, Zhou, J, Spence, Y, *et al.* (2007). Safe and efficient transduction of the liver after peripheral vein infusion of self-complementary AAV vector results in stable therapeutic expression of human FIX in nonhuman primates. *Blood* **109**: 1414-1421.
115. Louboutin, JP, Wang, L, and Wilson, JM (2005). Gene transfer into skeletal muscle using novel AAV serotypes. *J Gene Med* **7**: 442-451.
116. Wang, Z, Zhu, T, Qiao, C, Zhou, L, Wang, B, Zhang, J, *et al.* (2005). Adeno-associated virus serotype 8 efficiently delivers genes to muscle and heart. *Nat Biotechnol* **23**: 321-328.
117. Wang, L, Calcedo, R, Nichols, TC, Bellinger, DA, Dillow, A, Verma, IM, *et al.* (2005). Sustained correction of disease in naive and AAV2-pretreated hemophilia B dogs: AAV2/8-mediated, liver-directed gene therapy. *Blood* **105**: 3079-3086.
118. Inagaki, K, Fuess, S, Storm, TA, Gibson, GA, McTiernan, CF, Kay, MA, *et al.* (2006). Robust systemic transduction with AAV9 vectors in mice: efficient global cardiac gene transfer superior to that of AAV8. *Mol Ther* **14**: 45-53.
119. Halder, S, Van Vliet, K, Smith, JK, Duong, TT, McKenna, R, Wilson, JM, *et al.* (2015). Structure of neurotropic adeno-associated virus AAVrh.8. *J Struct Biol* **192**: 21-36.
120. Selot, R, Arumugam, S, Mary, B, Cheemadan, S, and Jayandharan, GR (2017). Optimized AAV rh.10 Vectors That Partially Evade Neutralizing Antibodies during Hepatic Gene Transfer. *Front Pharmacol* **8**: 441.

121. Monahan, PE, Samulski, RJ, Tazelaar, J, Xiao, X, Nichols, TC, Bellinger, DA, *et al.* (1998). Direct intramuscular injection with recombinant AAV vectors results in sustained expression in a dog model of hemophilia. *Gene Ther* **5**: 40-49.
122. Wang, B, Li, J, and Xiao, X (2000). Adeno-associated virus vector carrying human minidystrophin genes effectively ameliorates muscular dystrophy in mdx mouse model. *Proc Natl Acad Sci U S A* **97**: 13714-13719.
123. Manno, CS, Pierce, GF, Arruda, VR, Glader, B, Ragni, M, Rasko, JJ, *et al.* (2006). Successful transduction of liver in hemophilia by AAV-Factor IX and limitations imposed by the host immune response. *Nat Med* **12**: 342-347.
124. Latz, E, Visintin, A, Espevik, T, and Golenbock, DT (2004). Mechanisms of TLR9 activation. *J Endotoxin Res* **10**: 406-412.
125. Zhu, J, Huang, X, and Yang, Y (2009). The TLR9-MyD88 pathway is critical for adaptive immune responses to adeno-associated virus gene therapy vectors in mice. *J Clin Invest* **119**: 2388-2398.
126. Suzuki, M, Bertin, TK, Rogers, GL, Cela, RG, Zolotukhin, I, Palmer, DJ, *et al.* (2013). Differential type I interferon-dependent transgene silencing of helper-dependent adenoviral vs. adeno-associated viral vectors in vivo. *Mol Ther* **21**: 796-805.
127. Faust, SM, Bell, P, Cutler, BJ, Ashley, SN, Zhu, Y, Rabinowitz, JE, *et al.* (2013). CpG-depleted adeno-associated virus vectors evade immune detection. *J Clin Invest* **123**: 2994-3001.
128. Martino, AT, Suzuki, M, Markusic, DM, Zolotukhin, I, Ryals, RC, Moghimi, B, *et al.* (2011). The genome of self-complementary adeno-associated viral vectors increases Toll-like receptor 9-dependent innate immune responses in the liver. *Blood* **117**: 6459-6468.
129. Vollmer, J, Weeratna, RD, Jurk, M, Samulowitz, U, McCluskie, MJ, Payette, P, *et al.* (2004). Oligodeoxynucleotides lacking CpG dinucleotides mediate Toll-like receptor 9 dependent T helper type 2 biased immune stimulation. *Immunology* **113**: 212-223.
130. Hosel, M, Broxtermann, M, Janicki, H, Esser, K, Arzberger, S, Hartmann, P, *et al.* (2012). Toll-like receptor 2-mediated innate immune response in human nonparenchymal liver cells toward adeno-associated viral vectors. *Hepatology* **55**: 287-297.
131. High, KA, and Aubourg, P (2011). rAAV human trial experience. *Methods Mol Biol* **807**: 429-457.
132. Cao, O, Dobrzynski, E, Wang, L, Nayak, S, Mingle, B, Terhorst, C, *et al.* (2007). Induction and role of regulatory CD4⁺CD25⁺ T cells in tolerance to the transgene product following hepatic in vivo gene transfer. *Blood* **110**: 1132-1140.

133. Markusic, DM, Hoffman, BE, Perrin, GQ, Nayak, S, Wang, X, LoDuca, PA, *et al.* (2013). Effective gene therapy for haemophilic mice with pathogenic factor IX antibodies. *EMBO Mol Med* **5**: 1698-1709.
134. Keeler, GD, Markusic, DM, and Hoffman, BE (2019). Liver induced transgene tolerance with AAV vectors. *Cell Immunol* **342**: 103728.
135. Herzog, RW (2019). Complexity of immune responses to AAV transgene products - Example of factor IX. *Cell Immunol* **342**: 103658.
136. Mingozi, F, and High, KA (2013). Immune responses to AAV vectors: overcoming barriers to successful gene therapy. *Blood* **122**: 23-36.
137. Mendell, JR, Campbell, K, Rodino-Klapac, L, Sahenk, Z, Shilling, C, Lewis, S, *et al.* (2010). Dystrophin immunity in Duchenne's muscular dystrophy. *N Engl J Med* **363**: 1429-1437.
138. Flotte, TR, Trapnell, BC, Humphries, M, Carey, B, Calcedo, R, Rouhani, F, *et al.* (2011). Phase 2 clinical trial of a recombinant adeno-associated viral vector expressing alpha1-antitrypsin: interim results. *Hum Gene Ther* **22**: 1239-1247.
139. Wang, Z, Storb, R, Halbert, CL, Banks, GB, Butts, TM, Finn, EE, *et al.* (2012). Successful regional delivery and long-term expression of a dystrophin gene in canine muscular dystrophy: a preclinical model for human therapies. *Mol Ther* **20**: 1501-1507.
140. Brown, BD, Venneri, MA, Zingale, A, Sergi Sergi, L, and Naldini, L (2006). Endogenous microRNA regulation suppresses transgene expression in hematopoietic lineages and enables stable gene transfer. *Nat Med* **12**: 585-591.
141. Haurigot, V, Mingozi, F, Buchlis, G, Hui, DJ, Chen, Y, Basner-Tschakarjan, E, *et al.* (2010). Safety of AAV factor IX peripheral transvenular gene delivery to muscle in hemophilia B dogs. *Mol Ther* **18**: 1318-1329.
142. Colella, P, Sellier, P, Costa Verdera, H, Puzzo, F, van Wittenberghe, L, Guerchet, N, *et al.* (2019). AAV Gene Transfer with Tandem Promoter Design Prevents Anti-transgene Immunity and Provides Persistent Efficacy in Neonate Pompe Mice. *Mol Ther Methods Clin Dev* **12**: 85-101.
143. Rabinowitz, J, Chan, YK, and Samulski, RJ (2019). Adeno-associated Virus (AAV) versus Immune Response. *Viruses* **11**.
144. Ertl, HCJ, and High, KA (2017). Impact of AAV Capsid-Specific T-Cell Responses on Design and Outcome of Clinical Gene Transfer Trials with Recombinant Adeno-Associated Viral Vectors: An Evolving Controversy. *Hum Gene Ther* **28**: 328-337.

145. Mingozi, F, Maus, MV, Hui, DJ, Sabatino, DE, Murphy, SL, Rasko, JE, *et al.* (2007). CD8(+) T-cell responses to adeno-associated virus capsid in humans. *Nat Med* **13**: 419-422.
146. Mingozi, F, and High, KA (2011). Therapeutic in vivo gene transfer for genetic disease using AAV: progress and challenges. *Nat Rev Genet* **12**: 341-355.
147. Mingozi, F (2018). AAV Immunogenicity: A Matter of Sensitivity. *Mol Ther* **26**: 2335-2336.
148. Kuranda, K, Jean-Alphonse, P, Leborgne, C, Hardet, R, Collaud, F, Marmier, S, *et al.* (2018). Exposure to wild-type AAV drives distinct capsid immunity profiles in humans. *J Clin Invest* **128**: 5267-5279.
149. Calcedo, R, Morizono, H, Wang, L, McCarter, R, He, J, Jones, D, *et al.* (2011). Adeno-associated virus antibody profiles in newborns, children, and adolescents. *Clin Vaccine Immunol* **18**: 1586-1588.
150. Boutin, S, Monteilhet, V, Veron, P, Leborgne, C, Benveniste, O, Montus, MF, *et al.* (2010). Prevalence of serum IgG and neutralizing factors against adeno-associated virus (AAV) types 1, 2, 5, 6, 8, and 9 in the healthy population: implications for gene therapy using AAV vectors. *Hum Gene Ther* **21**: 704-712.
151. Stanford, S, Pink, R, Creagh, D, Clark, A, Lowe, G, Curry, N, *et al.* (2019). Adenovirus-associated antibodies in UK cohort of hemophilia patients: A seroprevalence study of the presence of adenovirus-associated virus vector-serotypes AAV5 and AAV8 neutralizing activity and antibodies in patients with hemophilia A. *Res Pract Thromb Haemost* **3**: 261-267.
152. Halbert, CL, Miller, AD, McNamara, S, Emerson, J, Gibson, RL, Ramsey, B, *et al.* (2006). Prevalence of neutralizing antibodies against adeno-associated virus (AAV) types 2, 5, and 6 in cystic fibrosis and normal populations: Implications for gene therapy using AAV vectors. *Hum Gene Ther* **17**: 440-447.
153. Ling, C, Wang, Y, Feng, YL, Zhang, YN, Li, J, Hu, XR, *et al.* (2015). Prevalence of neutralizing antibodies against liver-tropic adeno-associated virus serotype vectors in 100 healthy Chinese and its potential relation to body constitutions. *J Integr Med* **13**: 341-346.
154. Mingozi, F, Anguela, XM, Pavani, G, Chen, Y, Davidson, RJ, Hui, DJ, *et al.* (2013). Overcoming preexisting humoral immunity to AAV using capsid decoys. *Sci Transl Med* **5**: 194ra192.
155. Meliani, A, Boisgerault, F, Hardet, R, Marmier, S, Collaud, F, Ronzitti, G, *et al.* (2018). Antigen-selective modulation of AAV immunogenicity with tolerogenic rapamycin nanoparticles enables successful vector re-administration. *Nat Commun* **9**: 4098.

156. Paulk, NK, Pekrun, K, Zhu, E, Nygaard, S, Li, B, Xu, J, *et al.* (2018). Bioengineered AAV Capsids with Combined High Human Liver Transduction In Vivo and Unique Humoral Seroreactivity. *Mol Ther* **26**: 289-303.
157. Barnes, C, Scheideler, O, and Schaffer, D (2019). Engineering the AAV capsid to evade immune responses. *Curr Opin Biotechnol* **60**: 99-103.
158. Wang, D, Tai, PWL, and Gao, G (2019). Adeno-associated virus vector as a platform for gene therapy delivery. *Nat Rev Drug Discov* **18**: 358-378.
159. Gray, SJ, Blake, BL, Criswell, HE, Nicolson, SC, Samulski, RJ, McCown, TJ, *et al.* (2010). Directed evolution of a novel adeno-associated virus (AAV) vector that crosses the seizure-compromised blood-brain barrier (BBB). *Mol Ther* **18**: 570-578.
160. Marsch, S, Huber, A, Hallek, M, Buning, H, and Perabo, L (2010). A novel directed evolution method to enhance cell-type specificity of adeno-associated virus vectors. *Comb Chem High Throughput Screen* **13**: 807-812.
161. Paulk, NK, Pekrun, K, Charville, GW, Maguire-Nguyen, K, Wosczyzna, MN, Xu, J, *et al.* (2018). Bioengineered Viral Platform for Intramuscular Passive Vaccine Delivery to Human Skeletal Muscle. *Mol Ther Methods Clin Dev* **10**: 144-155.
162. Smith, JK, and Agbandje-McKenna, M (2018). Creating an arsenal of Adeno-associated virus (AAV) gene delivery stealth vehicles. *PLoS Pathog* **14**: e1006929.
163. Ojala, DS, Sun, S, Santiago-Ortiz, JL, Shapiro, MG, Romero, PA, and Schaffer, DV (2018). In Vivo Selection of a Computationally Designed SCHEMA AAV Library Yields a Novel Variant for Infection of Adult Neural Stem Cells in the SVZ. *Mol Ther* **26**: 304-319.
164. Asokan, A, and Samulski, RJ (2006). AAV does the shuffle. *Nat Biotechnol* **24**: 158-160.
165. Perabo, L, Endell, J, King, S, Lux, K, Goldnau, D, Hallek, M, *et al.* (2006). Combinatorial engineering of a gene therapy vector: directed evolution of adeno-associated virus. *J Gene Med* **8**: 155-162.
166. Muller, OJ, Kaul, F, Weitzman, MD, Pasqualini, R, Arap, W, Kleinschmidt, JA, *et al.* (2003). Random peptide libraries displayed on adeno-associated virus to select for targeted gene therapy vectors. *Nat Biotechnol* **21**: 1040-1046.
167. Schaffer, DV, and Maheshri, N (2004). Directed evolution of AAV mutants for enhanced gene delivery. *Conf Proc IEEE Eng Med Biol Soc* **2004**: 3520-3523.

168. Li, W, Asokan, A, Wu, Z, Van Dyke, T, DiPrimio, N, Johnson, JS, *et al.* (2008). Engineering and Selection of Shuffled AAV Genomes: A New Strategy for Producing Targeted Biological Nanoparticles. *Mol Ther* **16**: 1252-1260.
169. Koerber, JT, Jang, JH, and Schaffer, DV (2008). DNA shuffling of adeno-associated virus yields functionally diverse viral progeny. *Mol Ther* **16**: 1703-1709.
170. Yang, L, Jiang, J, Drouin, LM, Agbandje-McKenna, M, Chen, C, Qiao, C, *et al.* (2009). A myocardium tropic adeno-associated virus (AAV) evolved by DNA shuffling and in vivo selection. *Proc Natl Acad Sci U S A* **106**: 3946-3951.
171. Pekrun, K, De Alencastro, G, Luo, QJ, Liu, J, Kim, Y, Nygaard, S, *et al.* (2019). Using a barcoded AAV capsid library to select for clinically relevant gene therapy vectors. *JCI Insight* **4**.
172. Vercauteren, K, Hoffman, BE, Zolotukhin, I, Keeler, GD, Xiao, JW, Basner-Tschakarjan, E, *et al.* (2016). Superior In vivo Transduction of Human Hepatocytes Using Engineered AAV3 Capsid. *Mol Ther* **24**: 1042-1049.
173. Lisowski, L, Dane, AP, Chu, K, Zhang, Y, Cunningham, SC, Wilson, EM, *et al.* (2014). Selection and evaluation of clinically relevant AAV variants in a xenograft liver model. *Nature* **506**: 382-386.
174. Perocheau, DP, Cunningham, S, Lee, J, Antinao Diaz, J, Waddington, SN, Gilmour, K, *et al.* (2019). Age-Related Seroprevalence of Antibodies Against AAV-LK03 in a UK Population Cohort. *Hum Gene Ther* **30**: 79-87.
175. Buning, H, and Srivastava, A (2019). Capsid Modifications for Targeting and Improving the Efficacy of AAV Vectors. *Mol Ther Methods Clin Dev* **12**: 248-265.
176. Deverman, BE, Pravdo, PL, Simpson, BP, Kumar, SR, Chan, KY, Banerjee, A, *et al.* (2016). Cre-dependent selection yields AAV variants for widespread gene transfer to the adult brain. *Nat Biotechnol* **34**: 204-209.
177. Hordeaux, J, Wang, Q, Katz, N, Buza, EL, Bell, P, and Wilson, JM (2018). The Neurotropic Properties of AAV-PHP.B Are Limited to C57BL/6J Mice. *Mol Ther* **26**: 664-668.
178. Matsuzaki, Y, Tanaka, M, Hakoda, S, Masuda, T, Miyata, R, Konno, A, *et al.* (2019). Neurotropic Properties of AAV-PHP.B Are Shared among Diverse Inbred Strains of Mice. *Mol Ther* **27**: 700-704.
179. Huang, Q, Chan, KY, Tobey, IG, Chan, YA, Poterba, T, Boutros, CL, *et al.* (2019). Delivering genes across the blood-brain barrier: LY6A, a novel cellular receptor for AAV-PHP.B capsids. *PLoS One* **14**: e0225206.

180. Pasi, KJ, Rangarajan, S, Mitchell, N, Lester, W, Symington, E, Madan, B, *et al.* (2020). Multiyear Follow-up of AAV5-hFVIII-SQ Gene Therapy for Hemophilia A. *N Engl J Med* **382**: 29-40.
181. Colella, P, Ronzitti, G, and Mingozi, F (2018). Emerging Issues in AAV-Mediated In Vivo Gene Therapy. *Mol Ther Methods Clin Dev* **8**: 87-104.
182. Doshi, BS, and Arruda, VR (2018). Gene therapy for hemophilia: what does the future hold? *Ther Adv Hematol* **9**: 273-293.
183. Kattenhorn, LM, Tipper, CH, Stoica, L, Geraghty, DS, Wright, TL, Clark, KR, *et al.* (2016). Adeno-Associated Virus Gene Therapy for Liver Disease. *Hum Gene Ther* **27**: 947-961.
184. Calcedo, R, and Wilson, JM (2016). AAV Natural Infection Induces Broad Cross-Neutralizing Antibody Responses to Multiple AAV Serotypes in Chimpanzees. *Hum Gene Ther Clin Dev* **27**: 79-82.
185. Majowicz, A, Nijmeijer, B, Lampen, MH, Spronck, L, de Haan, M, Petry, H, *et al.* (2019). Therapeutic hFIX Activity Achieved after Single AAV5-hFIX Treatment in Hemophilia B Patients and NHPs with Pre-existing Anti-AAV5 NABs. *Mol Ther Methods Clin Dev* **14**: 27-36.
186. Zhao, H, Giver, L, Shao, Z, Affholter, JA, and Arnold, FH (1998). Molecular evolution by staggered extension process (StEP) in vitro recombination. *Nat Biotechnol* **16**: 258-261.
187. Maheshri, N, Koerber, JT, Kaspar, BK, and Schaffer, DV (2006). Directed evolution of adeno-associated virus yields enhanced gene delivery vectors. *Nat Biotechnol* **24**: 198-204.
188. Arad, U (1998). Modified Hirt procedure for rapid purification of extrachromosomal DNA from mammalian cells. *Biotechniques* **24**: 760-762.
189. Li, S, Ling, C, Zhong, L, Li, M, Su, Q, He, R, *et al.* (2015). Efficient and Targeted Transduction of Nonhuman Primate Liver With Systemically Delivered Optimized AAV3B Vectors. *Mol Ther* **23**: 1867-1876.
190. Braet, F, and Wisse, E (2002). Structural and functional aspects of liver sinusoidal endothelial cell fenestrae: a review. *Comp Hepatol* **1**: 1.
191. Zincarelli, C, Soltys, S, Rengo, G, and Rabinowitz, JE (2008). Analysis of AAV serotypes 1-9 mediated gene expression and tropism in mice after systemic injection. *Mol Ther* **16**: 1073-1080.

192. Grompe, M, and Strom, S (2013). Mice with human livers. *Gastroenterology* **145**: 1209-1214.
193. Afione, S, DiMattia, MA, Halder, S, Di Pasquale, G, Agbandje-McKenna, M, and Chiorini, JA (2015). Identification and mutagenesis of the adeno-associated virus 5 sialic acid binding region. *J Virol* **89**: 1660-1672.
194. Packer, MS, and Liu, DR (2015). Methods for the directed evolution of proteins. *Nat Rev Genet* **16**: 379-394.
195. Thomas, CE, Storm, TA, Huang, Z, and Kay, MA (2004). Rapid uncoating of vector genomes is the key to efficient liver transduction with pseudotyped adeno-associated virus vectors. *J Virol* **78**: 3110-3122.
196. Bennett, A, Patel, S, Mietzsch, M, Jose, A, Lins-Austin, B, Yu, JC, *et al.* (2017). Thermal Stability as a Determinant of AAV Serotype Identity. *Mol Ther Methods Clin Dev* **6**: 171-182.
197. Excoffon, KJ, Koerber, JT, Dickey, DD, Murtha, M, Keshavjee, S, Kaspar, BK, *et al.* (2009). Directed evolution of adeno-associated virus to an infectious respiratory virus. *Proc Natl Acad Sci U S A* **106**: 3865-3870.
198. Dickey, DD, Excoffon, KJ, Koerber, JT, Bergen, J, Steines, B, Klesney-Tait, J, *et al.* (2011). Enhanced sialic acid-dependent endocytosis explains the increased efficiency of infection of airway epithelia by a novel adeno-associated virus. *J Virol* **85**: 9023-9030.